THE UNIVERSITY OF CHICAGO

FEATURE-LEVEL EFFECTS IN OBJECT-SUBSTITUTION MASKING OF COLOR AND TILT

A DISSERTATION SUBMITTED TO

THE FACULTY OF THE DIVISION OF THE SOCIAL SCIENCES

IN CANDIDACY FOR THE DEGREE OF

DOCTOR OF PHILOSOPHY

DEPARTMENT OF PSYCHOLOGY

BY

RYAN MATTHEW LANGE

CHICAGO, ILLINOIS

AUGUST 2022

TABLE OF CONTENTS

LIST OF FIGURES

LIST OF TABLES

ACKNOWLEDGMENTS

I thank my family for their unwavering support in my long journey. You've talked me through countless frustrations and setbacks, and believed in me when I had difficulty believing in myself. You gave me the resources and strength to make this happen.

I'm grateful to my past mentors: Dr. John Watt at the University of North Dakota School of Medicine, and Drs. Delwin Lindsey and Angela Brown at the Ohio State University College of Optometry. You have inspired and sharpened my thinking more than I could describe. I'm also grateful to Dr. Michael Earley at the Ohio State University College of Optometry, who moved heaven and earth to help me turn a major roadblock into a new path.

My friends at the University of Chicago have kept me standing through thick and thin, and have always been there to bounce ideas off of. I'd like to especially thank Caleb and JP; you've been the most reliable, engaged, and kind friends a person could ask for.

Finally and most importantly, I thank my lab for supporting and challenging me throughout my time here. Every one of you have made me a better scientist and a better person. Prof. Steven Shevell, you've helped me keep my thinking grounded and clear, and your mentorship has been invaluable. You've kept me on the path through crises of confidence and showed more patience than I could've asked for. Jae, Emily, thank you so much for the laughs we've shared, the wisdom you've dispensed, and the innumerable hours you put into the keeping the lab running. Sunny, Andy, thanks for always helping me keep smiling. Linda, your work has been instrumental in making my experiments happen. And finally, Nick, you showed more interest in people than anyone I've ever met. Your memory reminds me daily of the importance of being kind—regardless of what I'm going through. Rest in peace Nick, you are missed.

ABSTRACT

Visual perception requires the construction of "neural representations," patterns of neuronal activity that represent the things we see. The most well-understood component of this construction is the feedforward hierarchical processing pathway, in which neural signals, starting at the eyes, are serially processed to form more integrated and specific representations at successive levels of the visual hierarchy. There is, however, growing evidence that feedback signals from higher to lower levels of the visual hierarchy moderate the quality of neural representations, and may even dictate whether those representations can be perceived.

Object-substitution masking (OSM) is a visual "masking" technique used to investigate how neural representations become available to conscious awareness. It is thought to disrupt "reentrant processing," a form of feedback signaling thought to be required for visual awareness. By disrupting this reentrant processing, OSM is thought to prevent confirmation and conscious awareness of the initial neural representations of briefly presented stimuli. Theories of OSM have traditionally appealed to disruptions of "object-level" neural representations; however, there is evidence for "feature-level" effects in OSM, along with theoretical grounds for predicting that reentrant processing may operate on both object-level and feature-level neural representations.

The experiments of this dissertation were performed to test for and investigate feature-level contributions to OSM for the features of tilt, color, and lightness. Stimuli were designed to selectively activate specific types of feature-processing neurons, and parameterized to isolate feature-level contributions to OSM. Experiments 1A-1C established OSM for tilt and color, and showed that masking of these two features can be dissociated. Experiments 2A-2D confirmed this masking using single-feature report. These experiments did not show any effects of

similarity between targets and their masking flankers on masking, regardless of whether that similarity was of a task-relevant or a task-irrelevant feature.

Finally, Experiments 3A-3C showed masking of targets defined by a single color or luminance feature. These experiments also showed evidence that the color or luminance axis and identity of the target and flankers affected degree of masking, with greater masking of and by some types of targets and flankers than others. This pattern of results is not as would be predicted by previous models of the role of flanker-target similarity in OSM. Instead, they are consistent with a feature-level contribution to OSM that is mediated by neurons that process specific feature signals, such as cone-opponent L/(L+M) and S/(L+M) color signals and (L+M) luminance signals. Furthermore, the efficacy of masking for target color or luminance features aligns with the transmission speeds of low-level feature-processing neurons for those features: Specifically, color or luminance representations processed by faster-signaling neurons are masked more effectively than those processed by slower-signaling neurons. From these patterns of results, a new model of OSM is developed. This new model suggests feature-level contributions to OSM based on relative signal-transmission speeds of low-level feature-processing pathways for those features.

CHAPTER 1

INTRODUCTION

1.1 Object-substitution masking links neural feedback to visual awareness

Object-substitution masking (OSM) is a "visual backward masking" paradigm, in which simultaneous onset and delayed offset of nearby flankers reduces the ability to recall a target in a briefly presented target-and-distractor array; this loss of awareness is referred to as "masking" (Bischof & Di Lollo, 1995; Di Lollo et al., 1993; Enns & Di Lollo, 1997). Visual backward masking paradigms are useful tools in visual and perceptual research, as they can be used to relate qualities of visual awareness to properties of the visual input and neural processing. In such experiments, a host of stimulus and task parameters can be manipulated, and changes in measured visual awareness can be linked to these manipulations. Information-theoretic models and analyses can then be used to make inferences about how neural signals representing the stimuli are processed. Other forms of visual backward masking have long been used to study the neural information processing required for conscious awareness of stimuli; traditionally, these theories have explained masking in terms of inhibition of neural processing of the target by neural processing of the mask, via feedforward and lateral inhibition by low-level neural feature-processing units (Alpern, 1953; Bachmann & Allik, 1976; Breitmeyer & Ganz, 1976; Di Lollo, 1980; Kahneman, 1968).

The properties of OSM, however, cannot be accounted for with theories based solely on these low-level processes. The dynamics of the target and masking stimuli, the need for divided attention in most OSM paradigms, and the role of object-segmentation cues in "releasing" objects from masking are all said to point to the disruption of higher-level, "object-based" neural

processing in OSM (Di Lollo et al., 2000; Enns & Di Lollo, 1997; Gellatly et al., 2006; Goodhew et al., 2015; Moore & Lleras, 2005). (See Table 1-1, later in this Introduction, for a comparison of models of visual backward masking).

Established theories of OSM posit that it disrupts "reentrant processing" between feedforward and feedback neural signals. This reentrant processing is thought to enable "perceptual hypothesis testing," the confirmation of visual object identity between stimulus-driven feedforward signals and representation-driven feedback signals, which is thought to be required for visual awareness (Di Lollo et al., 2000; Goodhew, 2017; Lleras & Moore, 2003). In some cases, multiple cycles of "iterative" reentrant processing are thought to be required for full awareness of an object; any or multiple of these cycles may be disrupted by OSM (Di Lollo, 2010, 2018). These theories of disrupted reentrant processing in OSM are in turn informed by broader theories of the roles of feedback signaling in perception (Bullier, 2001; Fahrenfort et al., 2008; Harth et al., 1987; Lamme, 2000).

Sophisticated models have been developed to relate disruption of reentrant processing in OSM to object-level neural processing. Such models have generally related OSM to neural "object tokens" (Treisman, 1988) or "object files" (Kahneman et al., 1992), and their creation and individuation (Goodhew et al., 2014, 2015; Guest et al., 2011; Lleras & Moore, 2003; Moore & Lleras, 2005). Some have argued that OSM specifically disrupts binding together of different feature-type representations in these object files or tokens (Bouvier & Treisman, 2010; Koivisto & Silvanto, 2011). However, the dominant model is that OSM disrupts proper temporal segmentation of object representations of the target and masking flankers; thus, the original representation of the target-plus-flankers is either "replaced by" or "updated to" a new representation—that of the flankers only—when the flankers' offset is delayed (Goodhew, 2017;

Guest et al., 2011; Kahan & Enns, 2010; Moore & Lleras, 2005). Critical to many of these studies' models of how OSM affects temporal object segmentation is the effect of flanker-target similarity in masking; flanker-target differences in features such as motion, color, luminance, tilt, or spatial frequency all tend to reduce masking in various OSM paradigms (Gellatly et al., 2006; Goodhew et al., 2015; Lleras & Moore, 2003; Luiga & Bachmann, 2008; Moore & Lleras, 2005),

While there is extensive scholarship around the role of object-level neural processing in OSM, feature-level contributions to OSM have received little attention. This is despite evidence of feature-level masking—and feature-level similarity effects on such masking—from several studies (Gellatly et al., 2006; Goodhew et al., 2015; Harris et al., 2016). This represents a gap not only in understanding of OSM itself, but also in attempts to synthesize OSM with broader theories of the function of feedback processing in visual perception (Di Lollo et al., 2000; Di Lollo, 2010). In the realm of neurobiology, there is ample evidence and theory that feedback processing specifically affects feature-level neural representations. Physiological studies have shown that neural feedback can influence feature selectivity of neurons in various low-level visual regions, including V2, V1, and even LGN; this allows tuning of feature selectivity based on the spatial and temporal context, likely enhancing detection and discrimination (Shmuel et al., 2005; Sillito et al., 1994; Wang et al., 2018). Based on these findings, numerous theories have been formulated to relate feedback signaling to feature processing and perception (Bullier, 2001; Harth et al., 1987; Lamme, 2000; Schwabe et al., 2006).

The paucity of studies and theory on feature-level effects in OSM, despite evidence of such effects in prior OSM studies and extensive evidence and theory for feedback modification of low-level neural feature processing, forms the motivation for this dissertation.

1.2 Overview of this dissertation

1.2.1 General overview

The experiments reported here were conducted to test for and characterize feature-level contributions to object-substitution masking (OSM). They use OSM paradigms incorporating targets, distractors, and flankers defined in color, luminance, and tilt, all defined with respect to selectivity and sensitivity of low-level feature processing neurons (Johnson et al., 2008).

Chapters 2-4 detail the rationales, predictions, methods, results, and conclusions of three sets of experiments, each designed to test a set of hypotheses related to feature-level masking and similarity effects in OSM. Experimental designs parameterize flanker-target similarity for color, luminance, and/or tilt features to test for similarity effects on masking; the patterns of similarity effects are related to predictions from "feature-similarity" and "object-similarity" models of similarity effects in OSM (Gellatly et al., 2006; Goodhew et al., 2015; Moore & Lleras, 2005).

Chapter 5 synthesizes results and conclusions from the three sets of experiments to propose a model of OSM that incorporates both object-level and feature-level contributions, reflecting a multitude of potential "points of failure" in the iterative reentrant processing required for detailed conscious perception of an object and its features (Di Lollo, 2010). It relates masking of various objects and features to the properties of low-level feature-processing neurons and the function of feedback processing in feature tuning. Finally, this model is related to broader theories of visual perception and the role of neural feedback.

1.2.2 Overview of literature review

The remainder of this Introduction is organized as a literature review for topics relevant to the motivation, design, and hypotheses of the experiments: First, the general paradigm for object-substitution masking (OSM) is introduced. OSM is contrasted with other forms of visual

backward masking, and the arguments for why OSM represents a "special case" of backward masking, which requires a reentrant-process theory, are reviewed.

Next, properties of feedforward and feedback processing of visual features are reviewed, with a focus on neural representations of surface color, lightness, and form in areas V1 and V2. Properties of feature and object processing in the ventral and dorsal visual streams are summarized, and findings and theories on the role of neural feedback in perceptual organization and visual awareness are introduced. Then, theories about how OSM disrupts neural processing of object representations are discussed, including overviews of "object files," feature integration, and temporal object segmentation.

Finally, evidence of feature-level masking in prior OSM studies is reviewed, and a set of hypotheses about feature-level components in OSM are proposed. The experiments performed to test these hypotheses, which form Chapters 2-4 of this dissertation, are introduced in brief.

1.3 Literature Review

1.3.1 Object-substitution masking (OSM): Paradigm and theory

Object-substitution masking (OSM) is a visual backward masking technique in which a briefly presented target stimulus in an array of similar distractor stimuli is "masked" by the simultaneous onset and delayed offset of sparse, non-overlapping flankers (usually four small dots near the corners of the target). The observer's task is to report some attribute of the target (Di Lollo et al., 1993). The flankers usually also cue which of the stimuli in the array is the target, though a separate cue can also be used (Enns & Di Lollo, 1997; Neill et al., 2002). When the flankers offset at the same time as the target-and-distractor array (usually 10-50 ms after onset), recall performance is quite high, usually between 70% and 100%. However, when the flankers' offset is delayed by 90 ms or more, recall performance becomes considerably less

accurate, in some cases falling to chance (Di Lollo et al., 2000; Moore & Lleras, 2005; Gellatly et al. 2006). These two offset-timing conditions, in which the flankers can offset either simultaneously with the target-and-distractor array or after a delay, are henceforth referred to as "offset-simultaneous" (or "offset-same") and "offset-delayed" conditions. See Figure 1-1 for illustration of the sequence of events and response accuracy for a typical OSM experiment.

Object-substitution masking has shown several notable differences from previously described forms of visual masking which can be explained by feedback processing, but not traditional feed-forward models (Di Lollo et al., 2000). The two traditional forms of backward masking are *pattern masking* and *metacontrast masking*. In pattern masking, a mask stimulus that spatially overlaps the target stimulus is shown before, during, or after display of the target stimulus; this mask stimulus may be a shape or random light and dark areas (Kahneman, 1968; Sperling, 1964). In metacontrast masking the contours of the mask stimulus do not spatially overlap those of the target stimulus, rather providing a near "outline" of them (Alpern, 1953). Masking occurs only if the mask onsets after the target (Kahneman, 1968). The interval between the offset of the target and onset of the mask is known as the interstimulus interval (ISI) (Kahneman, 1968), while the interval between the onset of the target and onset of the mask is called the stimulus-onset asynchrony (SOA) (Kulli, 1967). In metacontrast masking, the SOA, rather than the ISI, is the determining factor in degree of masking, with stimulus-onset asynchronies of 100-150 ms producing the strongest masking (Bachmann & Allik, 1976; Kahneman, 1967). In pattern masking, positive, negative, or zero SOAs may induce masking (Kahneman, 1968).

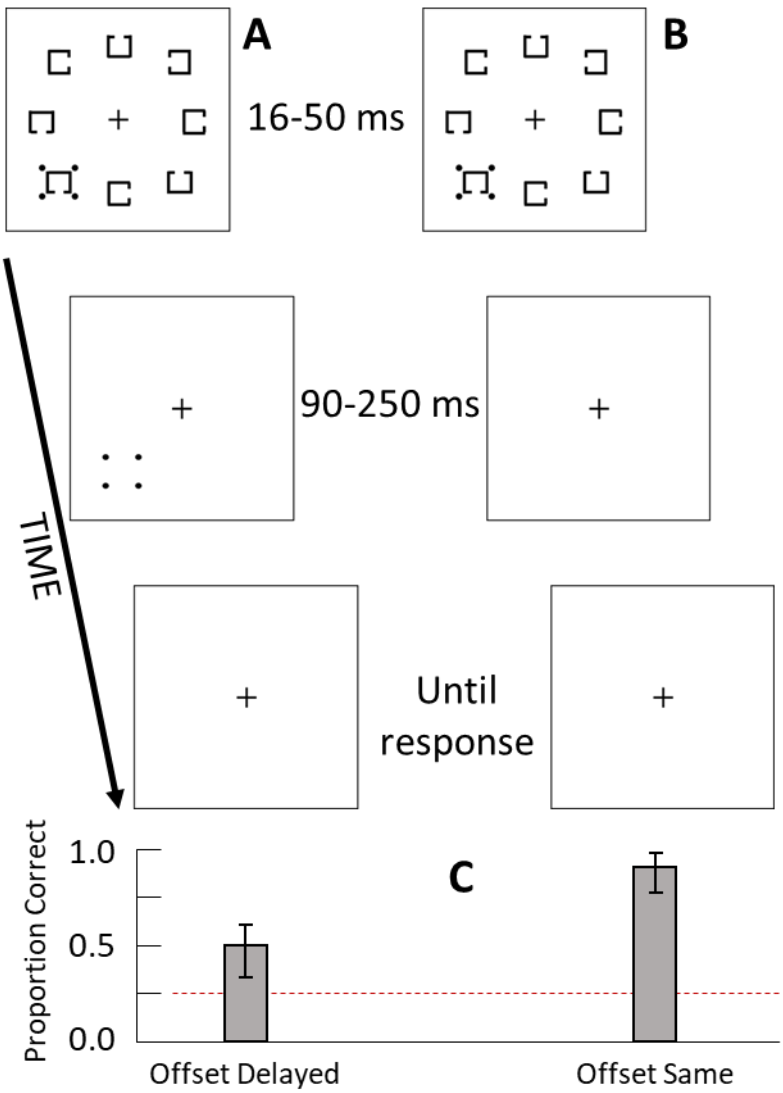

Figure 1-1. Example stimuli and results for object-substitution masking. a) "Offset-delayed" trial sequence. b) "Offset-same" trial sequence. Top frames: "target-plus-flanker" display period. Middle frames: "flanker-only" or blank display period. Bottom frames: Blank display shown while waiting for response. Subject indicates whether the gap in the target "C" was pointed left, right, up, or down. c) Average correct recall for offset-simultaneous and offset-delayed trial types. Red dotted line indicates chance performance for 4-alternative forced response task.

Traditional explanations for both pattern and metacontrast masking have appealed to strictly feedforward processes. "Masking by integration" proposes that the signal for the mask is added to the signal for the target in a process of temporal integration, rendering the resulting percept unintelligible (Di Lollo, 1980; Kahneman, 1968). "Masking by interruption" models suggest that processing of the mask disrupts processing of the target before the target can be

represented in consciousness (Michaels & Turvey, 1979). Finally, “masking by inhibitory contour interaction” appeals to onset and offset transients inhibiting sustained processing of targets (Breitmeyer & Ganz, 1976).

While these feedforward models of masking work well to relate stimulus properties, neural function, and perceptual effects in pattern and metacontrast masking paradigms, the neural mechanisms they propose cannot be used to explain masking in OSM paradigms. Both temporal and spatial attributes of OSM paradigms are incompatible with these feedforward models. Most obviously, in OSM there is no SOA, which is critical to the “interruption” and “inhibitory contour interaction” models. Secondly, OSM flankers need not have contours that overlap the target as in pattern masking, ruling out “masking by integration” (Di Lollo et al, 2000). The time course for OSM rules out transients necessary for the “inhibitory contour interaction” model: If the flanker onset transient were a factor, it would be as much a factor in “flanker offset simultaneous” trials as in “flanker offset delayed” trials, as flankers’ onset in both conditions is simultaneous with the target’s onset. Instead, masking occurs only in “flanker offset delayed” trials. Likewise, the flanker offset transient could play only a small role: OSM is robust even when the flankers are displayed until subject response, a condition in which any flanker offset transient is rendered irrelevant (Di Lollo et al., 2000). OSM is also highly sensitive to attention: In nearly all paradigms, the presence of distractors is necessary for OSM to occur (Di Lollo et al., 1997). While other forms of masking may be enhanced by distractors, they show strong effects for even a single target displayed at fixation (Di Lollo et al., 2000). See Table 1-1 for comparisons of the various models of visual masking, with treatment of experimental factors.

		Model of masking (Theoretically compatible masking protocols)			
		Integration (Pattern masking)	Interruption (Metacontrast masking)	Contour interactions (Metacontrast masking)	Feedforward-feedback interactions (OSM)
Experimental manipulation and effects	Stimulus-onset asynchrony (SOA)	(-), 0, or (+)	(+)	(+)	0
	Contour overlap	Necessary	Not necessary	Not necessary	Not necessary
	Distractors or divided attention	No effect	Medium effect, not necessary	Medium effect, not necessary	Strong effect, necessary

Table 1-1. Comparison of models of visual backward masking. For SOA, (-) indicates that mask onset precedes target onset, 0 indicates they are simultaneous, and (+) indicates that mask onset occurs after target onset.

To reconcile these discrepancies of OSM with feedforward models of masking, Di Lollo and colleagues proposed a model of visual function incorporating feedback signals which they termed "reentrant processing:" As in traditional feedforward models of vision, neural feature representations are built up throughout the ascending visual pathway, with "simple" features like edge orientations and surface colors represented in highly localized fashion by neurons in low levels of visual processing, and more complex features built up at higher levels, represented by neurons with increasingly large receptive fields and invariant responses. To solve the problem of simultaneously representing *what* something is (something low-level cells cannot do) and *where* it is (something for which high-level cells' large receptive fields are poorly optimized), recurrent

projections from high visual levels feed back onto neurons at low visual levels. At these synapses, a form of "perceptual hypothesis testing" is performed, in which activity of the feed-forward signal is compared to the "perceptual hypothesis" relayed by the feedback signal. If these signals match, that representation is consolidated into a conscious percept of an object; if not, the new feedforward signal either "substitutes for" or "updates" the representation of the object (Enns & Di Lollo, 1997; Goodhew, 2017; Kahan & Enns, 2010).

While these theories of OSM make sophisticated and generally-accurate predictions about the object-level outcomes of OSM, they fail to account for apparent "feature-level" masking; that is, the independent masking of objects' individual features, such as color and tilt (Gellatly et al., 2006; Harris et al., 2016). If there is a feature-level component to OSM, it may involve different levels of iterative reentrant processing than the object-level component (Di Lollo, 2010; Gellatly et al., 2006). The neural underpinnings of visual feature processing, particularly of surface color and luminance and of color- and/or luminance-defined tilt, are well characterized (Hubel & Wiesel, 1968; Johnson et al., 2008; Sincich & Horton, 2005). Additionally, context-specific neural feedback has been shown to modify feature processing of feature selectivity for numerous types of low-level feature-processing cells (Sillito et al., 1994; Wang et al., 2018); in several cases, these feedback effects have been shown to correlate with feature-axis selectivity of both the higher-level and lower-level neural populations that are linked (Marques et al., 2018; Shmuel et al., 2005). The experiments in this dissertation were designed to test for disruption of specific feedforward-feedback interactions, based on the properties of low-level visual feature processing and its modification by feedback signals.

1.3.2 Feedforward processing of feature and object representations

The first region of neocortex devoted to visual processing is primary visual cortex, or V1. It receives feedforward input from three primary cell types in the lateral geniculate nucleus (LGN) of the thalamus: magnocellular "M" neurons, parvocellular "P" neurons, and koniocellular "K" neurons (Casagrande et al., 2007; Ding & Casagrande, 1997; Lachica & Casagrande, 1992); these in turn receive input from numerous classes of retinal ganglion cells with varying chromatic, luminance, spatial, and temporal receptive field properties (Boycott & Dowling, 1969; Boynton, 1986; Cao et al., 2010; Dacey & Lee, 1994; Kolb & Dekorver, 1991; Martin et al., 1997, 2011; Patterson et al., 2019, 2019; Sanes & Masland, 2015). The V1 neurons that receive direct input from LGN make extensive interconnections with neurons in other layers in V1, and both first-order and higher-order neurons transmit information about a variety of features including color, luminance, form, motion, and/or binocular disparity (Hubel & Wiesel, 1959, 1962, 1968).

V1 neurons that process color, luminance, form, or some combination of these have three primary receptive field schemes: "non-opponent," "single-opponent," and "double-opponent" (Johnson et al., 2004, 2008). Non-opponent cells are generally selective for oriented luminance edges, though some may have only weak orientation selectivity. Color-sensitive single-opponent cells have roughly ovoid receptive fields with one polarity of cone-opponency, for example "L-cones ON/M-cones OFF" throughout their receptive field (Johnson et al., 2004; Lennie et al., 1990). Double-opponent color-sensitive cells, on the other hand, tend to have oblong receptive fields with side-by-side "ON" and "OFF" regions. For example, a double-opponent color-sensitive cell in V1 might have one oblong "L-cones ON/M-cones OFF" portion of its receptive field paralleled by an adjacent "L-cones OFF/M-cones ON" portion (Johnson et al., 2004, 2008).

Single-opponent cells tend to respond most strongly to low spatial-frequency stimuli, and are selective for chromaticity contrast. Double-opponent cells, on the other hand, respond most selectively to higher spatial-frequency "edge" stimuli, and may be sensitive to edges defined in chromaticity only, or both chromaticity and luminance (Johnson et al., 2008).

Various classes of color, luminance, and form-selective neurons project to area V2, where these features are processed with greater sophistication (Gegenfurtner et al., 1996; Sincich & Horton, 2005). V2 neurons tend to have larger receptive fields and be selective for higher-order form representations than V1 neurons, such as spatially correlated noise or textures (Freeman et al., 2013; Merigan et al., 1993; Ziemba et al., 2016). Both V1 and V2 neurons project to a variety of visual areas, including V3, V4, and MT (Weller & Kaas, 1983; Zeki, 1978; Zeki & Shipp, 1989), which in turn innervate a host of other visual areas in the temporal and parietal lobes. These areas beyond V2 are functionally divided into the ventral "what" and dorsal "where" pathways. Broadly speaking, the ventral pathway processes information about object identity, color, form, shape, and texture, while the dorsal pathway processes information about object location and motion (Mishkin et al., 1983). The dorsal and ventral streams each proceed posterior to anterior, with individual cells' representations becoming increasingly complex, specific and invariant, and receptive fields becoming larger, along each stream (Amano et al., 2009; Rust & DiCarlo, 2010).

In the ventral stream, the first visual area after V2 is area V4. Cells in V4 show strong selectivity for a variety of form features, including size, orientation, spatial frequency, contour, texture, and edge sharpness, with complex receptive fields exhibiting degrees of spatial invariance (Desimone & Schein, 1987; Hanazawa & Komatsu, 2001; Pasupathy & Connor, 1999). V4 also shows selectivity for color (Harada et al., 2009; Lueck et al., 1989; Mckeefry &

Zeki, 1997), and inverse-encoding models of color representations in V4 strongly predict reported color experiences (Kim et al., 2020). Area V4 in turn projects to inferotemporal cortex (IT), which shows form selectivity for texture-like features and for objects including shapes and faces (Desimone et al., 1984; Gross et al., 1972; Sheinberg & Logothetis, 1997; Tsao et al., 2006), in addition to strong color selectivity (Desimone et al., 1984; Harada et al., 2009). The highest levels of processing in the ventral stream include the lateral-occipital complex areas LO1 and LO2. Some subregions of these areas are selective for geometric shapes (Silson et al., 2013) and some play a role in object recognition (Grill-Spector et al., 2001).

In the dorsal stream, neurons in areas such as V5/middle temporal (MT) cortex, V6/dorsomedial cortex, the medial superior temporal area (MST), area 7a, and ventral intraparietal sulcus (VIP) integrate signals from V1 and V2, from each other, and in some cases directly from the thalamus (Warner et al., 2010) to produce responses to location, spatial relations, and motion (including global, local, and self-motion) across large sections of the visual field. (Amano et al., 2009; Andersen et al., 1990; Becker et al., 2013; Britten & Van Wezel, 1998; Field et al., 2020; Siegel, 1998). The transmission of information through the dorsal stream is extremely fast, due to the primary inputs from the low-latency magnocellular pathway (Merigan & Maunsell, 1993) and the presence of direct thalamic input that bypasses V1 and V2 (Warner et al., 2010). Sometimes event-related potentials in area MT can precede those in V1, and initial signaling in areas such as V4 and IT may represent lateral connections from MT rather than feedforward connections from V1 and V2 (Foxe & Simpson, 2002; Schroeder et al., 1998).

These lateral connections between the faster dorsal pathway and slower ventral pathway could be involved in binding the “what” and “where” of visual objects, a long-running concern among adherents of the two-streams model (Mishkin et al., 1983) and among those who study

feature integration (Treisman & Gelade, 1980). Evidence has accumulated for a role of the dorsal pathway in this binding. For example, damage to regions of the parietal lobe can lead to deficits in the ability to localize or integrate features of objects (Cohen & Rafal, 1991; Friedman-Hill et al., 1995; Robertson et al., 1997; Shafritz et al., 2002). However, these feedforward and lateral connections between the dorsal and ventral pathways could only explain certain aspects of binding and localization. Studies around this time found evidence that response properties in V2, V1, and even LGN could be modified over time depending on factors outside their classical receptive fields, or the activity of higher levels of processing. In some cases, these effects were abolished by general anesthesia, indicating a role of conscious processing in the modulation of response properties of neurons thought to operate entirely at a pre-conscious level (Lamme et al., 1998; Sillito et al., 1994; Zipser et al., 1996). A new model of visual perception involving feedback processing was needed to explain these findings.

1.3.3 The role of feedback in feature and object processing

As the characteristics of feedforward processing in the ascending visual hierarchy were being discovered, evidence was mounting for a reverse pathway, equal in scope but initially obscure in function. For each feedforward projection there was a corresponding feedback projection. These feedback projections were initially discovered from areas V3 to V2, V2 to V1, and V1 to LGN and other thalamic nuclei. The thalamic nuclei were also found to receive projections from the brainstem and midbrain reticular formations (Rockland & Pandya, 1979; Singer, 1977; Tigges et al., 1977). Later, extensive feedback connections were found among areas V1, V2, V4, and MT (Shipp & Zeki, 1989a, 1989b; Zeki & Shipp, 1989).

These feedback connections are of varied types, both excitatory and inhibitory. They show particularly complex interactions at the level of the thalamus, where excitatory synapses

may be made onto both excitatory LGN relay neurons and the perigeniculate nucleus neurons that inhibit those same LGN relay neurons; conversely, midbrain formations send inhibitory projections to the perigeniculate neurons and to LGN interneurons, giving them two pathways for *dis*inhibiting LGN relay neurons via inhibition of their inhibitors (Harth et al., 1987). This system of excitation and inhibition was proposed to provide a set of mechanisms whereby visual processing could be gated at the LGN by both higher-level processing and by midbrain formations, which are associated with conscious states such as alertness, drowsiness, and unconsciousness (Harth et al., 1987; Hei et al., 2014).

Based on this system of feedforward and feedback inputs, a model of vision was proposed in which, at each level of processing, a transformation of the visual signal for a feature was passed both upward as driver input to the next level of processing, and downward as a response modifier to optimize the response properties of lower levels for the stimulus. In this "Alopex" algorithm model, both local (feature-specific) and global (feature-nonspecific) feedback signals were proposed to modify processing at each successive step (Harth et al., 1987).

Further evidence of feedback-mediated modulation of visual processing accumulated. Some studies showed changes in selectivity along simple feature axes; for example, V1 feedback was shown to synchronize LGN cell firing in response to drifting gratings (Sillito et al., 1994), while V1 neurons' orientation tuning was shown to change over time in ways consistent with feedback modulation (Ringach et al., 1997). Other experiments showed alterations to low-level neurons' selectivity for more spatially-integrated feature elements, like textures in V1 (Zipser et al., 1996) and naturalistic stimuli in V2 (Ziemba et al., 2018). Finally, some studies showed feedback-associated modification of signaling relevant to object parsing in figure-ground discrimination in V1, V2, and V3 (Hupe et al., 1998; Lamme et al., 1998). In Lamme et al.

(1998), feedback-mediated figure-ground selectivity of V1 neurons was shown to be abolished by anesthesia, while those V1 neurons' classical receptive field properties remained unaffected. These findings were taken to suggest that not only were low-level neurons' response properties modified by feedback, but also that such modification improved sensitivity for contextually relevant information, and that it was tied to conscious state (Lamme et al, 1998). This is consistent with predictions that midbrain formations could influence visual processing via projections to perigeniculate and LGN thalamic regions (Harth et al., 1987; Hei et al., 2014).

Based on this evidence of contextual modulations of response properties by feedback signaling, general models of visual processing and awareness were formulated. These models explicitly centered the role of feedback on a wide range of neural and perceptual phenomena. The most circumscribed of these models relate feedback and lateral connectivity to the receptive field properties of V1 neurons (Angelucci et al., 2002; Schwabe et al., 2006). In these accounts, higher-level neural processing centers send feedback connections to lower-level areas (such as V1); these feedback connections are "highly divergent and convergent," connecting to interneurons throughout both the classical and extra-classical receptive field of their target (Angelucci et al., 2002). They are also purely excitatory in character, and further, synapse solely onto excitatory interneurons. However, due to higher activation-threshold and gain of the inhibitory interneurons these feedback projections excite, such excitatory feedback connections to the classical and extra-classical receptive field can either facilitate or inhibit the receptive field center, depending on other contextual factors (Ichida et al., 2007; Schwabe et al., 2006). Some studies on feedback's role in low-level neurons' receptive field properties have aligned well with the feature-specific feedback prediction of the Alopex theory (Harth et al., 1987). For example, studies of feedback signaling from V2 to V1 (and, in mouse, LM to V1) have shown correlations

between orientation and motion selectivity of the high-level cells and the V1 cells to which they project (Marques et al., 2018; Shmuel et al., 2005).

A related model posits that feedback-mediated interactions between the dorsal and ventral pathways help efficiently bind "what" to "where." In this account, higher dorsal areas such as MT, which receive very fast input from magnocellular neurons, send feedback to areas V1 and V2; this feedback serves to guide receptive-field modification in these areas, which serve as an "active blackboard," integrating the global processing from MT with detailed local processing. This "active blackboard" scheme allows for efficient context modulation in V1 and V2 of signals from slower-signaling parvocellular and koniocellular neurons (Bullier, 2001).

Finally, more general and informal models of feedback processing have posited that it is required for visual awareness, and may be a key component in visual attention. One such model suggests that feedback processing at multiple levels of neural representation, from V1 to portions of the parietal lobe, must all be successful for veridical object perception (Lamme, 2000). Another postulates that iterative feedback processing can explain integration across features, and the simultaneous perception of objects (which are represented invariantly at high processing levels) and their details (which are represented specifically at low neural processing levels) (Di Lollo, 2010). This model has even proposed that visual attention itself is the outcome of dynamical restructuring of visual processing, organized by reentrant processing (Di Lollo, 2018).

These models of feedback's role in visual awareness have influenced theorizing about the neural feedback mechanisms in OSM. Some have linked the disruption of reentrant processing to the disruption of feature integration (Bouvier & Treisman, 2010; Koivisto & Silvanto, 2011). Others, influenced by the "active blackboard" model of Bullier (2001), proposed that OSM may involve disruption of reentrant processing from the dorsal pathway (Boehler et al., 2008), and

that such disruption could alter the normal course of object "segmentation" or "individuation" (Goodhew et al., 2014). Some of these studies have provided additional evidence that OSM disrupts reentrant-processing effects as early as V1 (Boehler et al., 2008; Koivisto & Silvanto, 2011), as predicted by Lamme (2000).

Most theories of OSM have treated it as a disruption of the processing of "object-level" neural representations. While some have suggested OSM may act solely on neural mechanisms that "bind together" features to their appropriate objects (Bouvier & Treisman, 2010), the most dominant models propose that OSM acts upon fully-formed object representations, such as "object files" that robustly represent unique objects over space and time (Kahneman et al., 1992). In these accounts, the initial brief display of the target, distractors, and flankers in an OSM paradigm initiates a standard feedforward signaling cascade, culminating in the creation of a neural object representation for the target-plus-flankers at some high level of the visual hierarchy. The population of neurons that represents this target-plus-flankers object then sends a confirmatory feedback signal to lower visual areas; however, by the time this feedback signal reaches those lower visual areas, the on-screen image has changed to the flankers only (usually the target, flanker, and distractor array is shown for 10-100 ms) (Boehler et al., 2008; Bouvier & Treisman, 2010; Enns & Di Lollo, 1997; Guest et al., 2011; Luiga & Bachmann, 2008; Moore & Lleras, 2005; Woodman & Luck, 2003). The original target-and-flankers neural object representation is therefore thought to be either "replaced by" or "updated to" a new representation of the flankers only (Goodhew et al., 2013; Kahan & Enns, 2010; Lleras & Enns, 2004). The "object-updating" account posits that OSM represents a failure of "temporal object segmentation;" where the target-plus-flankers ought to be assigned a unique object file, it is

instead assigned to the same object file as the subsequent flankers-only stimulus, which is consciously perceived.

That OSM induces improper segmentation of object representations is well supported. One OSM study provided evidence for this by showing that disruption of magnocellular signals, predicted to be involved in fast, feedback-mediated object selection in the "dynamic blackboard" theory (Bullier, 2001), increased masking (Goodhew et al., 2014). Additionally, numerous studies have shown that feature differences between the target and flankers—including color, differential motion, luminance polarity, and spatial frequency—can all reduce masking (Gellatly et al., 2006; Goodhew et al., 2015; Lleras & Moore, 2003; Luiga & Bachmann, 2008; Moore & Lleras, 2005).

Several of these findings could also be interpreted to support masking of individual features, rather than solely of integrated object representations; however, all but two studies cast these similarity effects purely in terms of their possible contributions to object-level individuation. Only in Gellatly et al. (2006) and Huang et al. (2018) were the possibility of a feature-level component of OSM explored in detail. In these studies, masking of color and tilt of a target were shown to be at least partly dissociable, and flankers like their targets were shown to mask them more effectively than flankers unlike their targets. Specifically, flanker-target similarity of the reported feature played the strongest role in determining whether it was masked, whether subjects reported features singly or jointly; flanker-target similarity in the unreported feature did not show any such effect on masking (Gellatly et al., 2006; Huang et al., 2018). This led to speculation that in these paradigms OSM may have independently disrupted the processing of color and orientation, and that masking for each feature was dependent on the flanker-target similarity of that feature specifically. This will be referred to henceforth as the "feature-similarity

model" of flanker-target similarity's effect on masking. Feature-level masking and the feature-similarity model were not suggested to be antithetical to an object-level masking component; rather, it was proposed that OSM could encompass both feature-level and object-level masking, "dependent on experimental conditions" (Gellatly et al., 2006).

However, there has been little follow-up to this finding of feature-level contribution to OSM. One recent study, investigating tilt masking of grayscale Gabors with various types of flankers, showed strong masking of these targets, which are defined by a single feature relevant to low-level visual processing—luminance-defined tilt—and correlated this masking to flanker-target similarity at the level of oriented spatial frequency power. Yet this finding was interpreted entirely in the frameworks of object-level masking and object-level similarity, with little attention given to the potential that it may have reflected feature-level masking of tilt (Goodhew et al., 2015). This interpretation was consistent with that of several previous studies of flanker-target similarity effects in OSM, which had shown that flanker-target dissimilarity in either a task-relevant (Luiga & Bachmann, 2008) or task-irrelevant feature could serve as a cue to object segmentation and thus reduce masking (Lleras & Moore, 2003; Moore & Lleras, 2005). This model, that object-level dissimilarity along either the task-relevant or task-irrelevant feature can decrease masking, is henceforth referred to as the "object-similarity model" of flanker-target similarity's effect on masking.

1.4 Model of OSM, predictions, and introduction to experiments

This dissertation proposes a broad new model of OSM that incorporates both feature-level and object-level masking processes, and tests several hypotheses based on its predictions. This model is based on several key theories and findings about OSM.

1) Feedback from (and possibly to) numerous visual areas is required for complete representation of an object and its features, in line with Enns and Di Lollo's (2000) predictions about the "iterative" nature of reentrant processing and theorizing by Gellatly et al. (2006) and Huang et al. (2018) about the possibility of both feature- and object-level components of OSM. This introduces numerous possible "points of failure" for reentrant processing. Each of these points of failure represents disruption of a feedforward-feedback interaction between two levels of neural processing. Disruption at different points of failure could lead to qualitatively different perceptual outcomes (Gellatly et al., 2006); this could help explain two major discrepancies among OSM studies: 1) Differing accounts of exactly what is masked, whether that is single features, object representations, or the process of feature integration (Bouvier & Treisman, 2010; Gellatly et al., 2006; Moore & Lleras, 2005); and 2) Differing reports of the phenomenal quality of the masked target, ranging from completely absent (Neill et al., 2002; Tata, 2002) to present, but with reduced discriminability (Gellatly et al., 2006).
2) Target display time and number of distractors jointly determine whether masking is primarily feature-level or object-level. Shorter target display times and/or greater numbers of distractors tend to produce more feature-level masking (Gellatly et al., 2006; Goodhew et al., 2015), while longer target display times and/or lower numbers of distractors tend to "spare" the processing of individual features and produce more object-level masking (Bouvier & Treisman, 2010; Koivisto & Silvanto, 2011).
3) Feature-level masking can act independently for different features, such as color, luminance, and edge tilt (Gellatly et al., 2006; Huang et al., 2018).

4) Flanker-target dissimilarity of a task-relevant feature, but not a task-irrelevant one, reduces efficacy of feature-level OSM for that feature (Gellatly et al., 2006). Note that this is proposed to be separate from efficacy of object-level OSM, which has been shown to be reduced by dissimilarity of a task-irrelevant feature (Moore & Lleras, 2005).

Based on these core tenets, the model makes several broad predictions about feature-level contributions to OSM of color. luminance, and tilt in a proposed experimental paradigm:

1) Using a relatively large number of distractors (five distractors and one target) and brief target-and-flanker display times (16.7-50 ms), feature-level masking of color and/or tilt will be observed.
2) The efficacy of feature-level masking for each feature will depend on flanker-target similarity for that feature, but not on flanker-target similarity for the other feature. That is, the "feature-similarity model" will dictate similarity effects for feature-level masking, rather than the "object-similarity model."

Three sets of experiments were performed to replicate previous findings and test eight hypotheses related to the above two questions. The experiments, and the hypotheses they tested, were as follows:

1) Experiment 1 was split into three parts.
    a. Experiment 1A was designed to replicate the findings that i) The single defining feature of a tilted grayscale Gabor, luminance-defined tilt, could be masked with an OSM paradigm; and ii) The degree of this tilt masking was dependent on flanker-target similarity in oriented spatial-frequency power (Goodhew et al., 2015).

b. Experiment 1B was designed to test three sets of questions about masking of color and tilt: i) Could a similar OSM paradigm to Experiment 1A give masking of color and tilt of Gabor targets defined in cone-opponent color and luminance?; ii) Would masking of color and tilt be independent, as predicted by Gellatly et al. (2006)?; and iii) Would flankers identical to the target in color mask color or tilt more effectively than flankers different to the target in color? The feature-similarity model predicts that flanker-target color similarity should only affect color masking, while the object-similarity model predicts that flanker-target color similarity should affect both color and tilt masking.

c. Experiment 1C was designed to test a second hypothesis about flanker color: On average, would flankers modulated in color (and matched to the targets in luminance modulation) mask either color or tilt more effectively than "neutral color" grayscale flankers (matched to the target only in luminance modulation)? This was motivated by a broader version of the feature-similarity model, the "shared-axis model." In the shared-axis model, "similarity" between the flankers and target in a feature is replaced by shared modulation of the same type of low-level feature axis. The prediction is that flankers modulated on the same feature axes as the target will tend to mask that feature more effectively, irrespective of whether the direction of axis modulation is the same for the flankers and target.

2) Experiment 2 introduced flankers that could be "mixed" in a feature dimension to reduce response bias. Subjects reported either target color or tilt singly. Stimuli were tilted Gabors modulated in luminance (lsY *Y*) and, for all targets/distractors and some flankers, color (lsY *l*).

a. Experiments 2A and 2B were designed to test whether flanker-target similarity on the task-relevant feature dimension would affect masking of color or of tilt, using flankers either "mixed" (two with plus (+) modulation and two with minus (–) modulation) or "neutral" (no modulation) in the task-relevant feature.
b. Experiments 2C and 2D were designed to test whether flanker-target similarity on the task-irrelevant feature dimension would affect masking of color or of tilt, using flankers either mixed or opposite in the task-irrelevant feature.

3) Experiment 3 used single-feature Gaussian-like blur stimuli, defined in either of the cone-opponent isoluminant color axes (lsY *l* or *s*) or in the luminance axis (lsY *Y*). It used solely mixed flankers and was divided into three parts. All three parts tested whether such low-level color or luminance feature representations could be masked with OSM, and each part tested whether flanker-target similarity across chromaticity axes would affect degree of masking. These hypotheses were related to the "object-similarity," "feature-similarity," and "shared-axis" models of similarity effects; see the "Rationale" section of Chapter 5 for further details on the hypotheses tested.
   a. Experiment 3A used isoluminant *l* and *s* axes for targets, distractors, and flankers.
   b. Experiment 3B used isoluminant *l* and luminance *Y* axes for targets, distractors, and flankers.
   c. Experiment 3C used isoluminant *s* and luminance *Y* axes for targets, distractors, and flankers.

CHAPTER 2

EXP. 1: OSM FOR TILT AND COLOR

2.1 Rationale

Experiment 1 was divided into three sub-experiments: Exp. 1A attempted to replicate findings from Goodhew et al. (2015) that linked masking efficacy with oriented spatial-frequency similarity between the flankers and target. Exp. 1B tested for masking of color and tilt. Exp. 1C tested whether masking of color and tilt depended on the number of shared axes of modulation between flankers and targets.

Exp. 1A tested whether achromatic, luminance-modulated Gabor flankers and luminance-modulated Gaussian flankers would show significant masking of tilted, luminance-modulated Gabor stimuli. This experiment is a conceptual replication of an experiment in Goodhew et al. (2015), which showed significant tilt masking of Gabor stimuli with Gabor flankers, but not hard-edged or lower-spatial-frequency Gaussian-dot flankers. This difference in masking was attributed to the effect of similarity between the target and flankers. Exp. 1A had two predictions:

1) Tilt would be masked in this paradigm.
2) Masking of tilt would be stronger with similar Gabor flankers than dissimilar Gaussian-dot flankers.

Exp. 1B was performed to establish whether OSM could be used to mask color and tilt of Gabor stimuli modulated in lsY *l* and *Y*, and to determine the effect of flanker-target color relations. This experiment had three predictions, motivated by findings in Gellatly et al. (2006):

1) Color and tilt would be masked in this paradigm.

2) Masking of color and of tilt would be independent.
3) Masking of color, but not of tilt, would correlate with flanker-target color similarity, as predicted by the "feature-similarity model" introduced in Chapter 1.6.

Finally, Exp. 1C tested whether OSM of color and tilt was different when flankers selectively activated one feature axis activated by the target (lsY *Y* only, "grayscale" flankers) or two (lsY *l* and *Y*, "colored" flankers). Exp. 1C predicted that masking of color, but not of tilt, would be stronger with colored than grayscale flankers, consistent with the "shared-axis model" introduced in Chapter 1.6.

2.2 Subjects

Five subjects (three men, mean age 29 years) participated in Exp. 1A-1C. Author RL was one subject; the other four were naïve to the purpose and design of the study. All subjects had normal or corrected-to-normal visual acuity, and all showed normal color vision in Rayleigh matches measured with the Neitz OT-II anomaloscope. Each subject gave informed consent to participate according to the Institutional Review Board protocols for the University of Chicago. One subject completed only Exps. 1A and 1C, as their performance in Exp. 1B was at ceiling. Including color vision pre-testing and four to five sessions of photometry, each subject completed six to eight sessions total, with each session approximately 30-75 minutes.

2.3 Stimuli and Protocol: General

2.3.1 Apparatus

Across all three sets of experiments, stimuli were presented on an NEC MultiSync PA272W LED monitor, driven by an iMac computer with Radeon Pro 560 graphics card. Stimuli were generated and displayed, and data were captured, in MATLAB R2018a (MathWorks, 2022) with the Psychophysics Toolbox (Brainard, 1997; Brainard & Pelli, 2022). Subject responses

were recorded with a Logitech Precision gamepad. Subjects were seated 68.5 cm from the screen, with head position partially fixed with a chinrest. Monitor R, G, and B levels were luminance-equated for each subject prior to experiments with heterochromatic flicker or minimum-motion photometry (Anstis & Cavanagh, 1983; Wagner & Boynton, 1972).

2.3.2 Targets and distractors

The stimuli in each experiment were Gabor gratings, which were tilted either "left" (112.5°) or "right" (67.5°) (Goodhew et al., 2015). Stimulus colors were defined in the lsY color space (Boynton, 1986), with *l* and *s* representing the L/(L+M) and S/(L+M) cone-opponent axes and *Y* representing the luminance axis (expressed in cd/m²). Stimuli were modulated along either the *Y* axis alone, or both the *l* and *Y* axes. The mean luminance was set to Y=12 cd/m², which was also the *Y* value of the gray background. The *s* value for both the stimuli and background was held constant at s=1.0, the neutral point for the S/(L+M) axis and the same *s* value as the background. In all three experiments, the Michelson luminance contrast for Gabor targets, distractors, and flankers was 75%, giving Y_{min}=3 cd/m² and Y_{max}=21 cd/m². For stimuli in which *l* was modulated, l_{min}=0.62 and l_{max}=0.71. For all stimuli l_{mean}=0.665, the neutral point for the L/(L+M) axis and the same *l* value as the background. Stimuli with *l*-modulation were of two types: "red-and-dark" and "green-and-dark." The *l*-modulation for these two types was identical and defined by the same sine-wave and Gaussian envelope function as was used to define the *Y* luminance modulation; the only differences were in their scaling and phase. For red-and-dark stimuli $+l$ was modulated in phase with $+Y$, and for green-and-dark stimuli $-l$ modulated in phase with $+Y$.

Each target or distractor Gabor's Gaussian envelope subtended 1.4° visual angle, and the sinewave for *Y* modulation (and, if applicable, *l* modulation) was centered on 3.0 cycles per

degree. This spatial frequency was chosen over the original 4.0 cycles per degree in Goodhew et al. (2015), as 3.0 cycles per degree corresponds closely to the sensitivity maxima of both color-defined tilt and luminance-defined tilt in V1 double-opponent edge-detecting cells (Johnson et al., 2008). The target and distractors were arrayed with their centers on an imaginary regular hexagon centered on fixation, 9.5° across. In all experiments, one stimulus in this array was cued as the target with four flankers around its four corners. The location of the target in the array, and the features of each distractor, were independently randomized for each trial. The target's features (color and tilt) in each trial were pre-allocated and randomized at the beginning of each experiment. Stimulus specifications follow Goodhew et al. (2015), though their study used achromatic stimuli with Michelson luminance contrast set to 100%. In the present study, Michelson luminance contrast was lowered to 75% to ensure that all stimulus lsY values would translate to RGB tristimulus values within monitor gamut.

In each trial, the target, distractors, and flankers displayed on screen from 16.7 to 50 ms (1 to 3 frames), depending on performance in a practice task, described in Section 2.3.5. Figure 2-1 shows examples of targets and flankers for Exp. 1A-1C, along with examples of the screen layout during "offset-simultaneous" and "offset-delayed" trials.

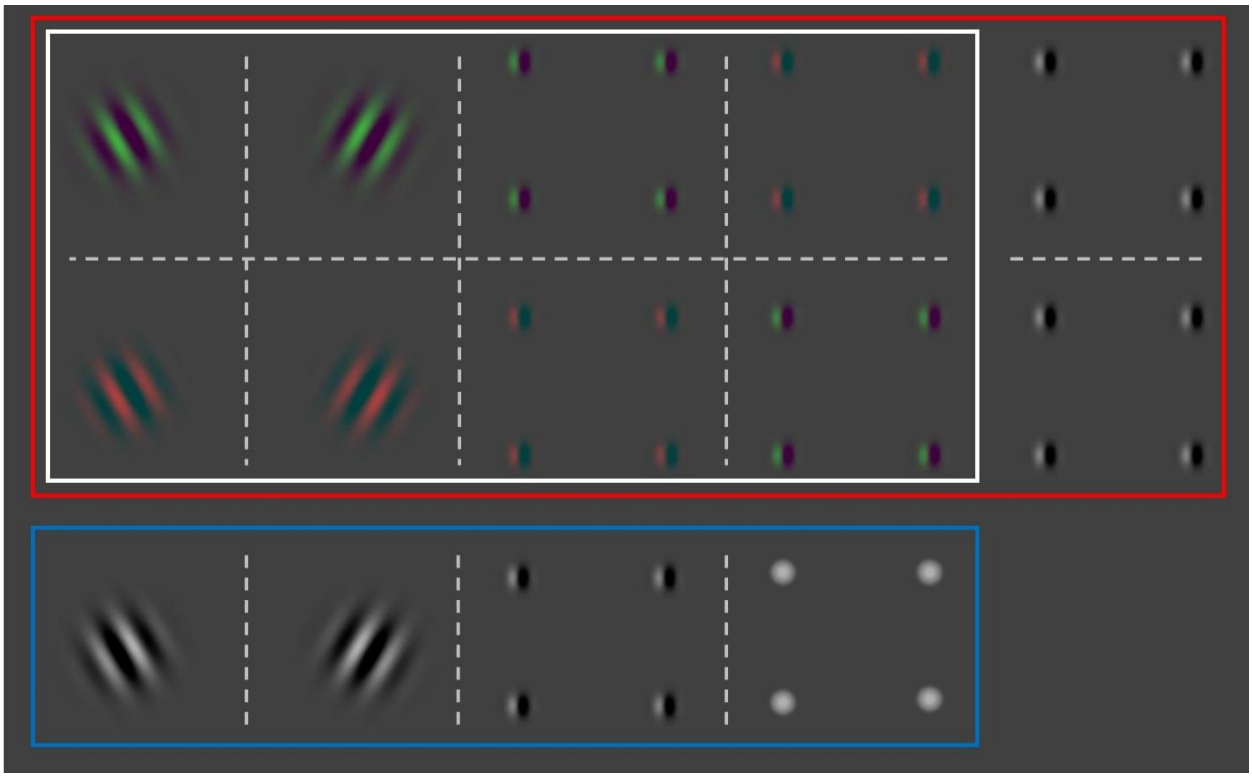

Figure 2-1. Stimuli and flankers used for Experiments 1A–1C. Left two columns: Gabor stimuli. Right columns: four-flanker arrays. BLUE box indicates stimuli and flankers used in Exp. 1A. WHITE box indicates stimuli and flankers used in Exp. 1B. RED box indicates stimuli and flankers used in Exp. 1C.

2.3.3 Flankers

In each trial, one of the six stimulus Gabors was surrounded by four flankers, one at each corner of an imaginary square centered on the target. These flankers each had a Gaussian envelope of 0.5°, and their centers were diagonally separated from the center of the target by 1.34°. The flankers either disappeared at the same time as the target-and-distractor array ("offset-simultaneous"), or 250 ms after ("offset-delayed"). Two to three different types of flankers were used in each experiment; in a single trial, the four flankers were identical. In all three flanker types, *s* was held constant at 1.0. One flanker type, used only in Exp. 1A, was an achromatic Gaussian-increment dot, which had a Gaussian envelope of 0.5° and mean spatial frequency of 1.0 cpd. This dot was modulated only in lsY *Y*, with Y_{min}=12 cd/m² and Y_{max}=21 cd/m². The other

two flanker types were 1.5-cycle Gabors with mean spatial frequency of 3.0 cpd. Both were tilted 90°, with Y_{min}=3 cd/m², Y_{mean}=12 cd/m², and Y_{max}=21 cd/m², as in the targets and distractors. One type, used in Exps. 1A and 1C, was grayscale (modulated only in *Y*), while the other was modulated in *l* and *Y*, with l_{min}=0.62, l_{mean}=0.665, and l_{max}=0.71. As with targets and distractors, "red-and-dark" and "green-and-dark" Gabor flankers had identical *l* modulations, with the phase of *l* modulation simply shifted 90° from the phase of *Y* modulation for the "green-and-dark" flankers. See Figure 2-1 for illustration of the various stimuli and flanker types. See Figure 2-2 for illustration of the trial sequence for "offset-simultaneous" and "offset-delayed" trials.

2.3.4 Blank period, probe array, and response

After both stimuli and flankers had disappeared, there was a blank period in which only the fixation cross was displayed on screen; following this blank period, the fixation cross disappeared and was replaced by a probe array of either four or two Gabor stimuli (depending on session type), with one matching the target (see Figures 2-2 and 2-3). The duration of the blank period was 500 ms for "offset-simultaneous" trials and 250 ms for "offset-delayed" trials, giving 500 ms total between offset of the stimuli and onset of the probe array for both conditions. This was done to equate duration since target offset (DSTO) across the two conditions, since DSTO has been shown to be a more salient factor in masking than time between flanker offset and probe (Goodhew et al., 2012).

At the end of the 500 ms DSTO period, the probe array was displayed until the subject selected the probe they thought matched the target. For Exps. 1B and 1C, in which stimuli were modulated in both *l* and *Y*, the probe array was four Gabors, arrayed in a rectangle around the fixation cross. The two probes above fixation were "red-and-dark" while the two below fixation were "green-and-dark." The two probes left of fixation were tilted left (112.5°) while the two

right of fixation were tilted right (67.5°). Subjects pressed one of four pre-assigned buttons to indicate which probe matched the target. The button-probe mappings were fixed, and mirrored the spatial arrangement of the probe array. This fixed mapping of response button/key to target feature is standard in the OSM literature (Di Lollo et al., 2000; Gellatly et al., 2006; Goodhew et al., 2015; Hirose & Osaka, 2010; Kahan & Lichtman, 2006; Moore & Lleras, 2005). For Exp. 1A, because the stimuli were grayscale, the probe array consisted of only two Gabors, left and right of fixation. The trial sequence described here applies also to Exps. 2-3.

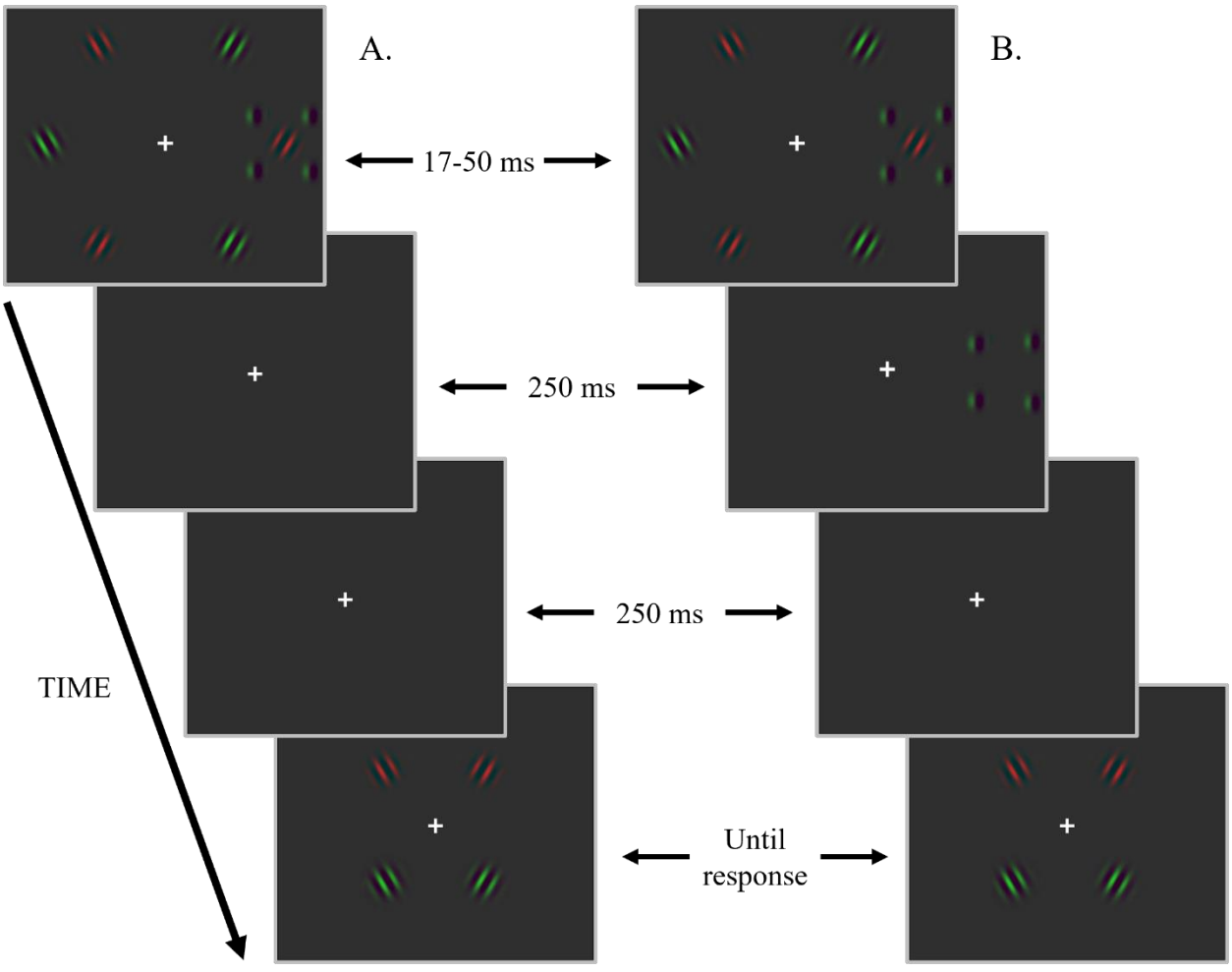

Figure 2-2. Trial sequence for OSM paradigms. a) Sequence for “offset-simultaneous” or “no-masking” trials. b) Sequence for “offset-delayed” or “masking” trials.

2.3.5 Practice task

Prior to each sub-experiment, each subject performed three to four practice blocks to ensure that they understood the task, and to calibrate the duration of target-plus-flanker display to their performance; all practice blocks were excluded from analysis. The first two practice blocks were slowed down and had only one repetition of each trial type. The slowed-down practice blocks had target-plus-flanker durations of 500 and 250 ms and, in "offset-delayed" trials, flanker-only durations of 250 ms. Once a subject could accurately perform the task in these slowed-down blocks, they did one to two blocks with varying full-speed target-plus-flanker durations, with the goal of establishing a correct response rate between 75% and 90% in the "offset-simultaneous" trials. These full-speed blocks had four repetitions of each trial type.

The subject first completed a block with target-plus-flanker duration=33.3 ms (2 frames); if the correct response rate was 75%–90% in this condition, the subject proceeded to the full experiment, with the target-plus-flanker duration set to 33.3 ms. If the correct response rate for "offset-simultaneous" trials was <75%, the subject attempted a block with target-plus-flanker duration=50 ms (3 frames), whereas if correct response rate was >90%, the subject attempted a block with target-plus-flanker duration=16.7 ms (1 frame). If the correct response rate for "offset-simultaneous" trials could not be brought between 75–90%, the subject was excluded from participating in this experiment; this was done to avoid ceiling or floor effects in the following measurements. See Table A-1 in Appendix A Section A.1 for the target-plus-flanker durations used for each subject in Exps. 1A-1C.

2.3.6 Exp. 1A Stimuli and Protocol

In Exp. 1A, stimuli and flankers were modulated in lsY *Y* (luminance, in cd/m²) only. Flankers were either 1.5-cycle Gabor gratings (tilted 90°) or luminance-increment Gaussian dots. After each trial, subjects indicated which of two probes (left-tilt or right-tilt) matched the target. See Figure 2-3 for illustration of stimuli, flankers, and probe array used in Exp. 1A.

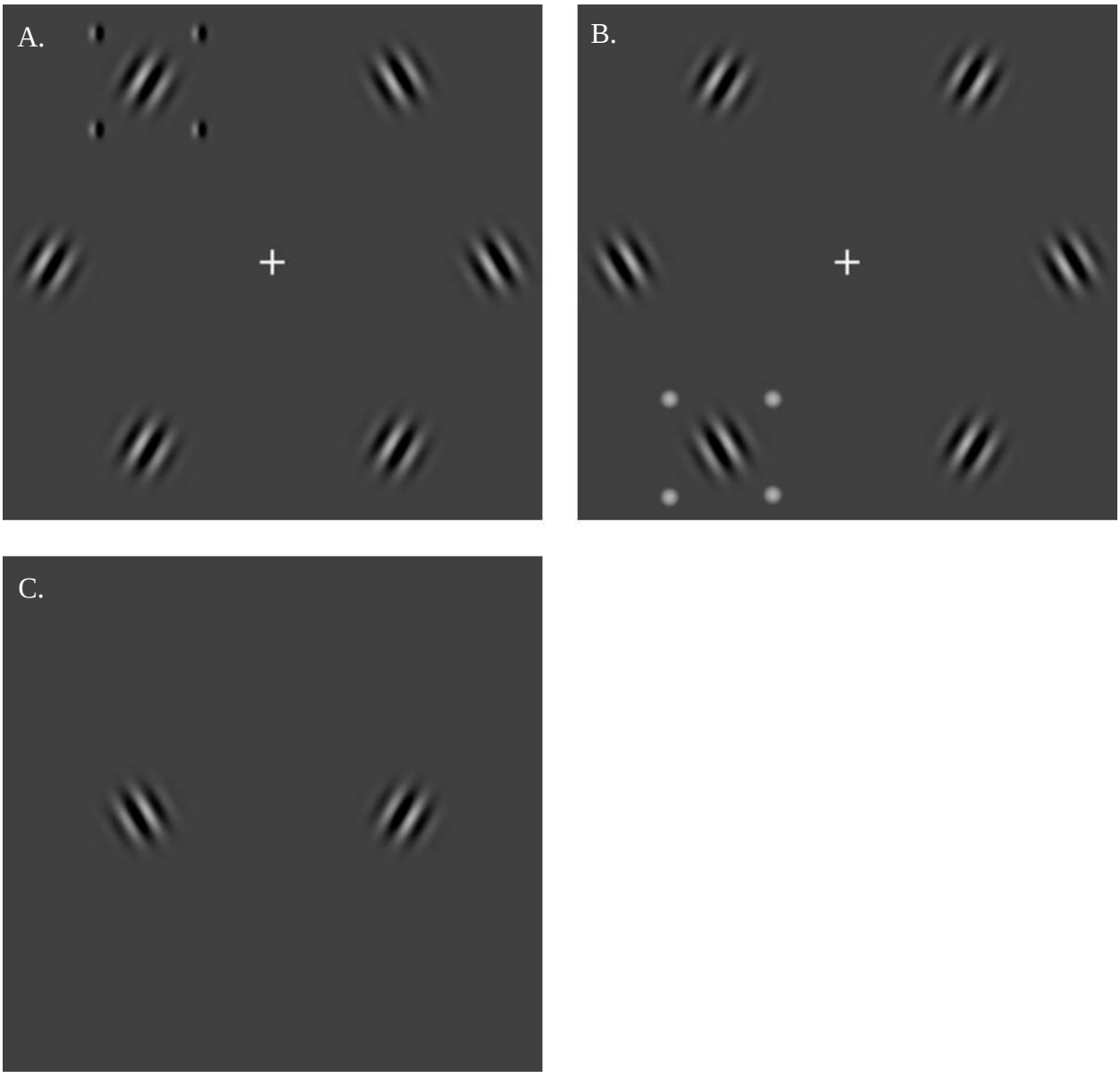

Figure 2-3. Stimuli, flankers, and probe array used in Exp. 1A. a) Example stimulus array with Gabor flankers. b) Example stimulus array with Gaussian-dot flankers. c) Probe array. **Note:** These examples are for demonstration only and do not precisely represent actual stimuli.

In Exp. 1A, each subject completed 40 blocks of eight trials each; each block was a fully counterbalanced 2×2×2 design: 2 levels of target tilt ("left" and "right") × 2 levels of flanker-type ("Gabors" and "Gaussians") × 2 levels of flanker offset ("offset-simultaneous" and "offset-delayed"). The two levels of target tilt were collapsed in the analysis, giving 80 trials per condition in the 2×2 level binomial logistic regression model.

2.3.7 Exp. 1B Stimuli and Protocol

In Exp. 1B, targets, distractors, and flankers were always modulated in lsY *l* and *Y*. Flankers were always 1.5-cycle Gabors oriented vertically. The target and distractors were tilted either left (112.5°) or right (67.5°), while flankers had neutral tilt (90°). Targets, distractors, and flankers could all be either "red-and-dark" (*+l* in phase with *+Y*) or "green-and-dark" (*–l* in phase with *+Y*). Flankers could have either the same color profile as the target ("flankers-same") or the opposite color profile to the target ("flankers-opposite"). See Figure 2-4 for illustration of stimuli, flankers, and probe array in Exp. 1B.

Each subject completed 20 blocks of trials; each block was a fully counterbalanced 2×2×2×2 design: 2 levels of target tilt ("left" and "right") × 2 levels of target color ("red-and-dark" and "green-and-dark") × 2 levels of flanker-target color relation ("flankers-same" and "flankers-opposite") × 2 levels of flanker offset ("offset-simultaneous" and "offset-delayed"). The levels of target tilt and color were collapsed in the analysis, giving 80 trials per condition in the 2×2 level binomial logistic regression model.

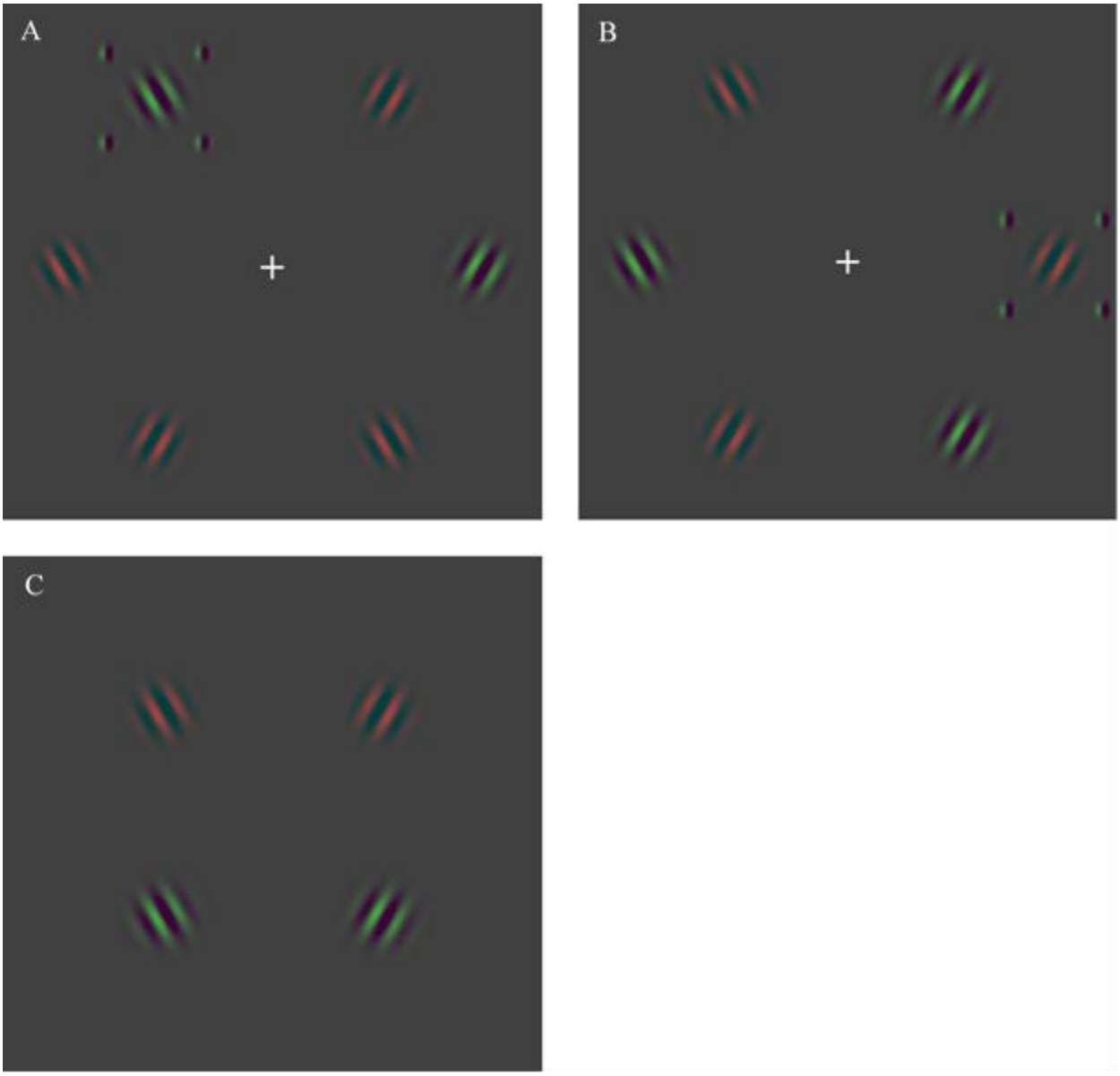

Figure 2-4. Stimuli, flankers, and probe array used in Exp. 1B. a) Example stimuli and flankers for "green-and-dark" target with "flankers-same" color relation. b) Example stimuli and flankers for "red-and-dark" target with "flankers-opposite" color relation. c) Probe array. **Note:** These examples are for demonstration only and do not precisely represent actual stimuli.

2.3.8 Exp. 1C Stimuli and Protocol

In Exp. 1C, targets and distractors were always modulated in lsY *l* and *Y*. Flankers were always 1.5-cycle Gabors oriented vertically. In one-half of trials, targets and distractors were either "red-and-dark" or "green-and-dark," as in Exp. 1B. Flankers could have the same colors as

the target (“flankers-same”) or the opposite colors to the target (“flankers-opposite”). Each of these conditions comprised one-quarter of total trials, and in the primary analysis they were glossed to “flankers colored.” In the-remaining half of trials, flankers were grayscale (“flankers-grayscale.”). See Figure 2-5 for illustration of stimuli, flankers, and probe array in Exp. 1C.

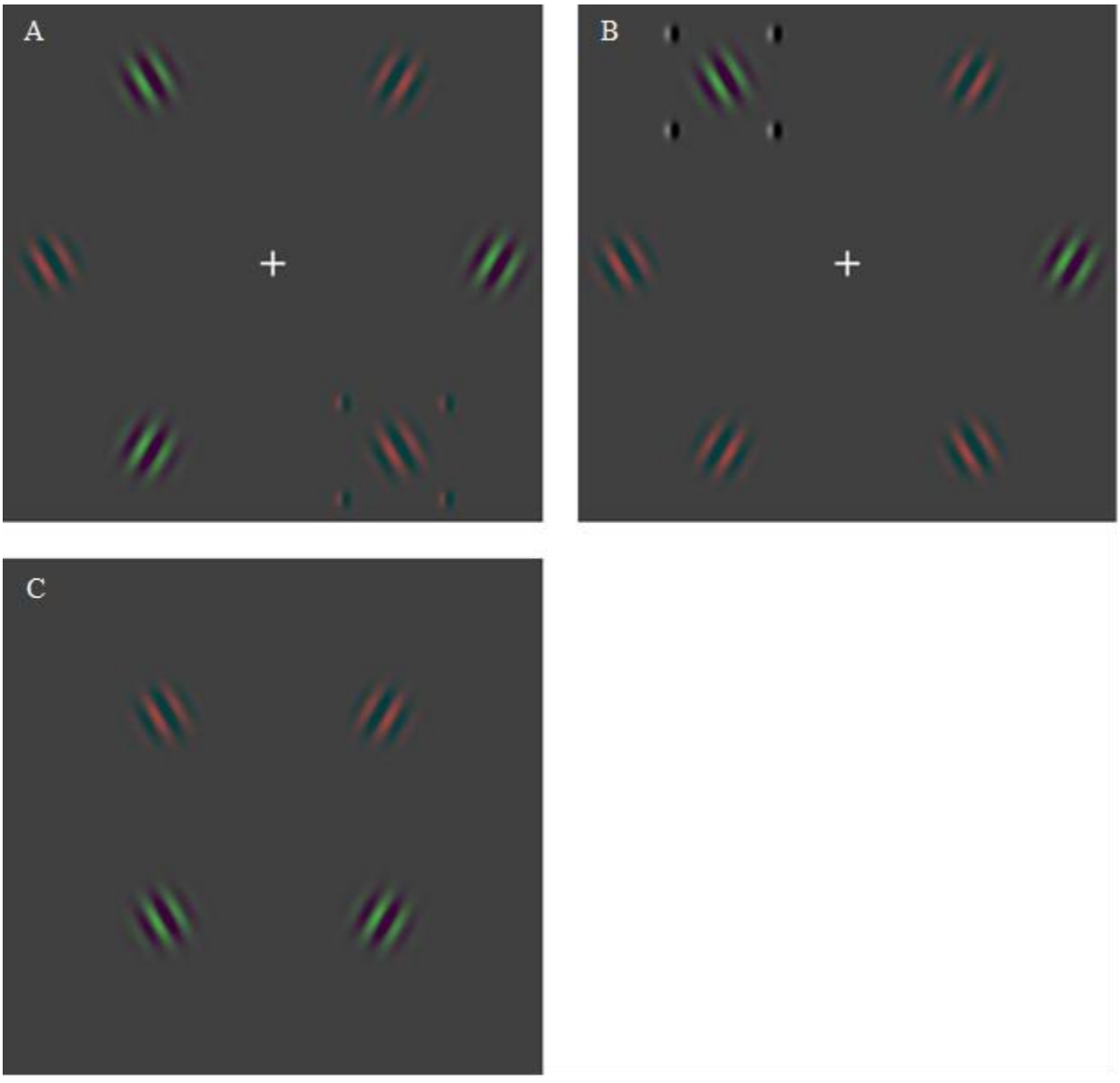

Figure 2-5. Stimuli, flankers, and probe array used in Exp. 1C. a) Example stimulus array with colored flankers. b) Example stimulus array with grayscale flankers. c) Probe array. **Note:** These examples are for demonstration only and do not precisely represent the actual stimuli.

Each subject completed 40 blocks of trials; each block was a fully balanced 2×2×2×2 design: 2 levels of target color ("red-and-dark" and "green-and-dark") × 2 levels of flanker offset ("offset-simultaneous" and "offset-delayed") × 2 levels of flanker color ("flankers colored" and "flankers grayscale") × 2 levels of target color ("target red-and-dark" and "target green-and-dark"). In the primary analysis, the levels of target color were collapsed to give 160 trials per condition in the 2×2 binomial logistic regression model.

2.4 Results

For all three experiments, analyses were within-subjects. Each experiment was analyzed with a 2×2 binomial logistic regression model (`R` function `glm`) with main effects of flanker offset ("masking") and flanker type, and the interaction effect of the two. See Appendix A (Section A.2) for further details of the analyses and models for Exps. 1A-1C.

2.4.1 Exp. 1A Results: Tilt OSM with no significant effect of flanker type

The results for Exp. 1A were as follows: Three of four subjects (S1, S3, S4) showed a significant main effect of flanker offset on tilt recall, such that recall was higher for "offset-simultaneous" than "offset-delayed" trials (logß=1.116–3.285; $p<0.001$ for all). This main effect of flanker offset will hereon be referred to as "tilt masking." One subject (S4) showed a significant main effect of flanker type, such that recall was higher for Gaussian than Gabor flankers (logß=0.838, $p<0.01$). One subject (S2) showed a significant interaction between masking and flanker type, such that tilt masking was stronger with "Gabor" than "Gaussian" flankers. See Figure 2-6 for tilt recall in Exp. 1A, and Table 2-1 for corresponding regression models.

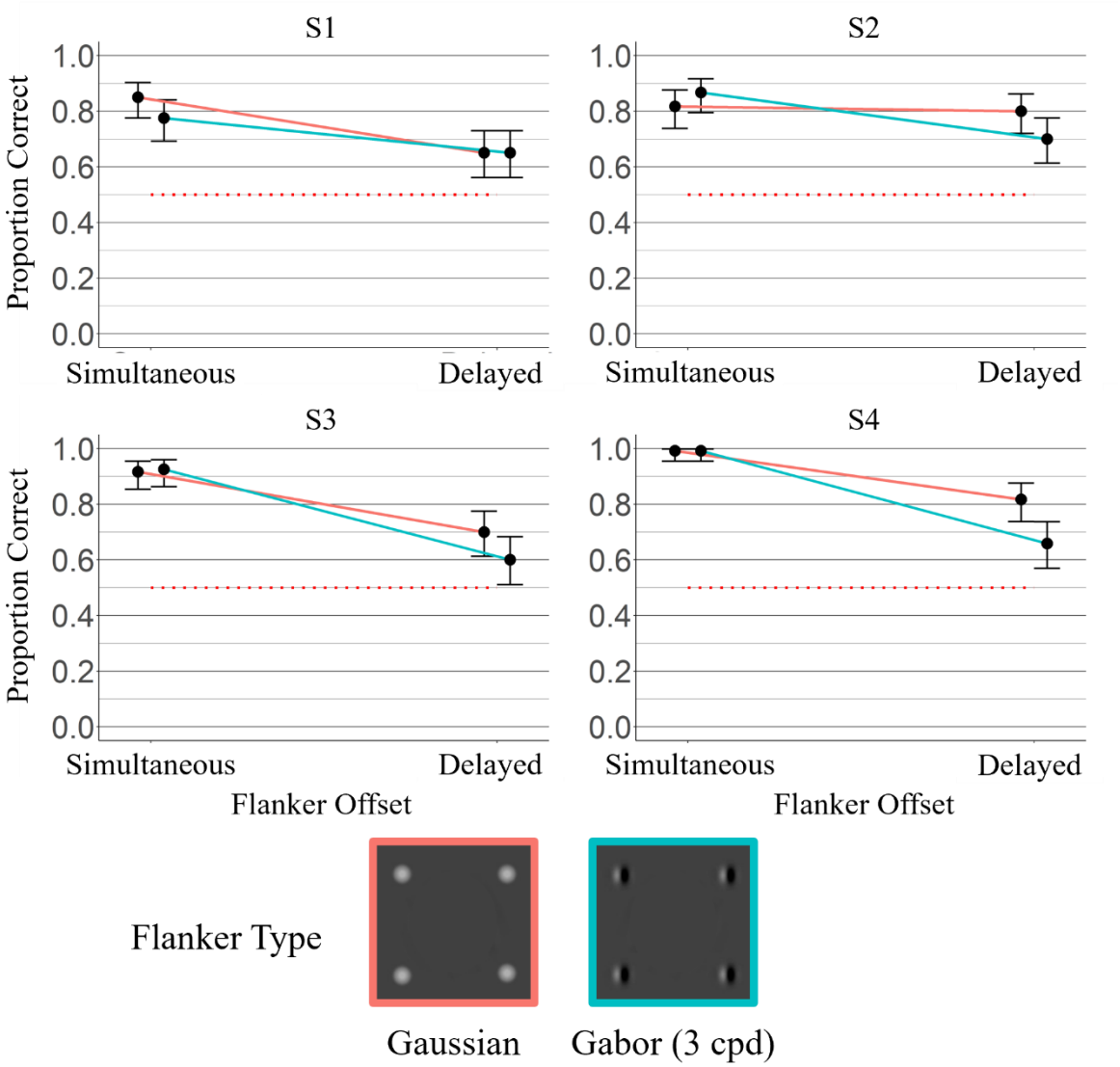

Figure 2-6. Tilt recall in Exp. 1A. Each point represents mean across 120 trials. Error bars represent 95% confidence intervals; red dotted line indicates chance.

Subject	Predictor	Log estimate (SE)	p-value
S1	Flanker offset (Same–Delayed)	1.116 (0.271)	< **0.001**
	Flanker type (Gaussian–Gabor)	0.00 (0.271)	1.000
	Flanker type × Flanker offset	0.489 (0.432)	0.249
S2	Flanker offset (Same–Delayed)	0.108 (0.328)	0.743
	Flanker type (Gaussian–Gabor)	0.539 (0.303)	0.075
	Flanker offset × Flanker type	–0.917 (0.469)	**0.049**
S3	Flanker offset (Same–Delayed)	1.551 (0.386)	< **0.001**
	Flanker type (Gaussian–Gabor)	0.442 (0.273)	0.105
	Flanker offset × Flanker type	–0.556 (0.551)	0.313
S4	Flanker offset (Same–Delayed)	3.285 (1.032)	**0.001**
	Flanker type (Gaussian–Gabor)	0.838 (0.304)	**0.006**
	Flanker type × Flanker offset	–0.838 (1.452)	0.564

Table 2-1. Logistic regression models for Exp. 1A, flanker type effect on tilt recall. Masking was significant for 3/4 subjects. Flanker type was significant for 1 subject. Masking × flanker type interaction was significant for 1 subject, with masking stronger for Gabor flankers than Gaussian flankers.

2.4.2 Exp. 1B Results: Masking of target color and tilt, jointly and singly

Reported here are results for Exp. 1B, in which effects of flanker-target color relation (same versus opposite) were tested for OSM of color and tilt. Recall accuracy figures and binomial logistic regression models are given for 1) overall recall (correct color *and* tilt); 2) color recall (irrespective of tilt); and 3) tilt recall (irrespective of color). These are each reported on a per-subject basis; for each subject, all three measures are derived from the same four-alternative forced choice recall task.

For overall recall, all five subjects showed a significant masking effect. Four of five subjects showed significant main effects of flanker-target color relation, such that overall recall was higher with “flankers same” than “flankers opposite” flanker color condition. Two subjects showed significant interaction effects, such that masking was stronger with “flankers opposite” than “flankers same” flanker color condition. See Figure 2-7. for overall recall in Exp. 1B, and Table 2-2 for corresponding regression models.

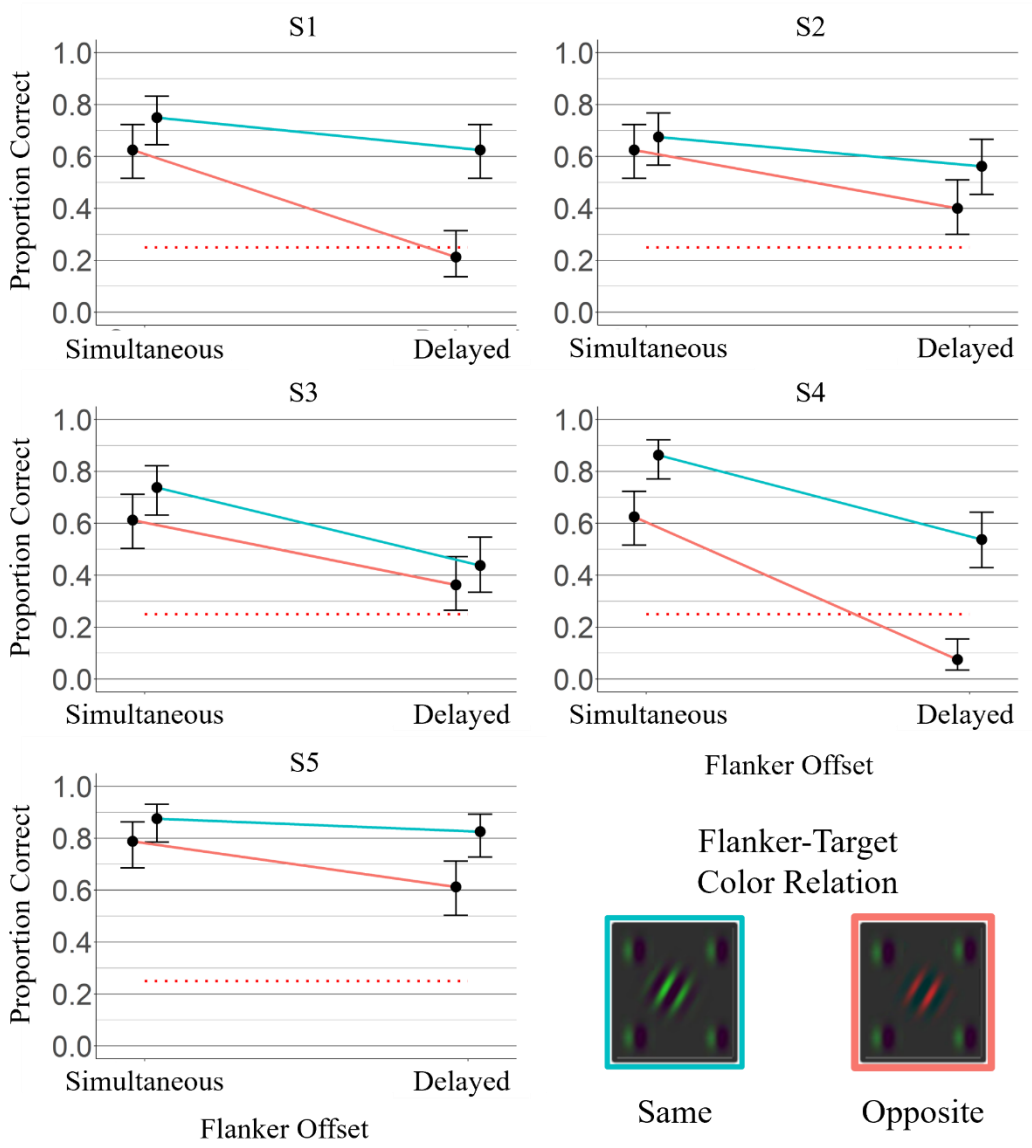

Figure 2-7. Overall recall in Exp. 1B. Each point represents mean across 80 trials. Error bars represent 95% confidence intervals; red dotted line indicates chance.

Subject	Predictor	Log estimate (SE)	p-value
1	Flanker Offset (Simultaneous–Delayed)	1.82 (0.358)	< **0.001**
	Flanker-Target Color Relation (Same–Opposite)	1.82 (0.358)	< **0.001**
	Flanker Offset × Color Relation	-1.23 (0.498)	**0.013**
2	Flanker Offset (Simultaneous–Delayed)	0.657 (0.321)	**0.041**
	Flanker-Target Color Relation (Same–Opposite)	0.915 (0.325)	**0.005**
	Flanker Offset × Color Relation	-0.437 (0.462)	0.344
3	Flanker Offset (Simultaneous–Delayed)	0.313 (0.324)	0.333
	Flanker-Target Color Relation (Same–Opposite)	1.022 (0.327)	**0.002**
	Flanker Offset × Color Relation	0.262 (0.471)	0.578
4	Flanker Offset (Simultaneous–Delayed)	2.66 (0.480)	< **0.001**
	Flanker-Target Color Relation (Same–Opposite)	3.02 (0.483)	< **0.001**
	Flanker Offset × Color Relation	-1.34 (0.624)	**0.032**
5	Flanker Offset (Simultaneous–Delayed)	1.093 (1.093)	**0.003**
	Flanker-Target Color Relation (Same–Opposite)	0.852 (0.357)	**0.017**
	Flanker Offset × Color Relation	-0.457 (0.573)	0.425

Table 2-2. Logistic regression models for overall recall in Exp. 1B. 5/5 subjects showed significant main effects of flanker offset, indicating OSM. 4/5 subjects showed significant main effects of flanker-target color relation, with recall higher when the target and flanker were the same color. 2/5 subjects showed significant interaction effects, such that masking was stronger with flankers the opposite color of the target.

For color recall, four of five subjects showed significant masking, with the fifth showing a non-significant effect in the same direction. All subjects showed significant main effects of flanker-target color relation, such that color recall was higher with “flankers same” than

"flankers opposite" color condition. Two subjects showed significant interaction effects, such that masking was stronger with "flankers opposite" than "flankers same" color. See Figure 2-8 for subjects' color recall in Exp. 1B, and Table 2-3 for corresponding regression models.

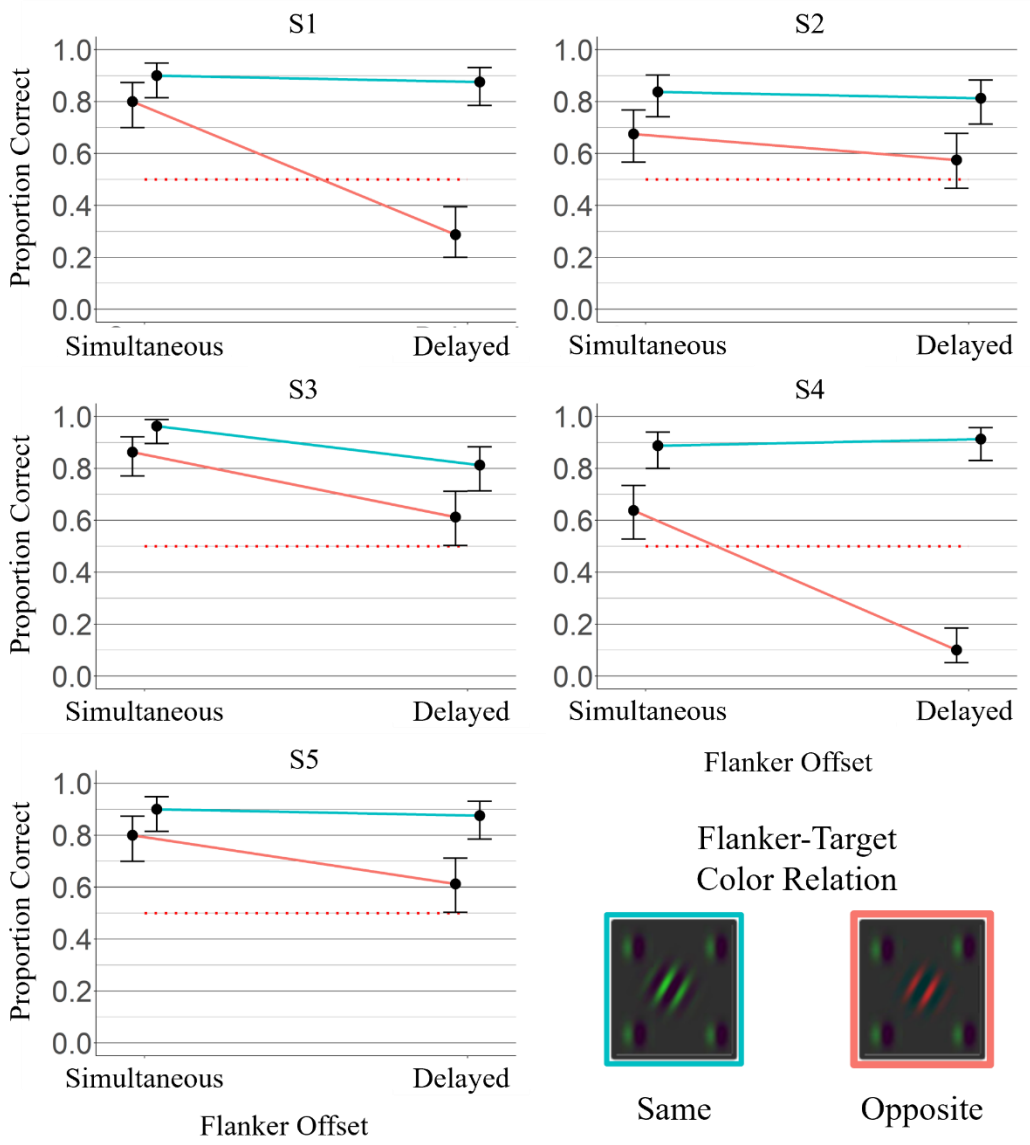

Figure 2-8. Color recall in Exp. 1B. Each point represents mean across 80 trials. Error bars represent 95% confidence intervals; red dotted line indicates chance.

Subject	Predictor	Log estimate (SE)	p-value
1	Flanker Offset (Simultaneous–Delayed)	2.294 (0.373)	< **0.001**
	Flanker-Target Color Relation (Same–Opposite)	2.853 (0.419)	< **0.001**
	Flanker Offset × Color Relation	-2.043 (0.626)	**0.001**
2	Flanker Offset (Simultaneous–Delayed)	0.429 (0.329)	0.192
	Flanker-Target Color Relation (Same–Opposite)	1.164 (0.365)	**0.001**
	Flanker Offset × Color Relation	-0.255 (0.531)	0.631
3	Flanker Offset (Simultaneous–Delayed)	1.378 (0.398)	< **0.001**
	Flanker-Target Color Relation (Same–Opposite)	1.009 (0.367)	**0.006**
	Flanker Offset × Color Relation	0.400 (0.766)	0.601
4	Flanker Offset (Simultaneous–Delayed)	2.76 (0.439)	< **0.001**
	Flanker-Target Color Relation (Same–Opposite)	4.54 (0.544)	< **0.001**
	Flanker Offset × Color Relation	-3.04 (0.689)	< **0.001**
5	Flanker Offset (Simultaneous–Delayed)	0.852 (0.357)	**0.017**
	Flanker-Target Color Relation (Same–Opposite)	1.093 (0.373)	**0.003**
	Flanker Offset × Color Relation	-0.457 (0.573)	0.425

Table 2-3. Logistic regression models for color recall in Exp. 1B. 4/5 subjects showed significant main effects of flanker offset, indicating OSM. 5/5 subjects showed significant main effects of flanker-target color relation. 2/5 subjects showed significant interaction effects.

For tilt recall, two of five subjects showed significant masking. No subject showed a significant main effect of flanker-target color relation, nor did any subject show a significant interaction effect of the two. See Figure 2-9 for subjects' tilt recall in Exp. 1B, and Table 2-4 for corresponding regression models.

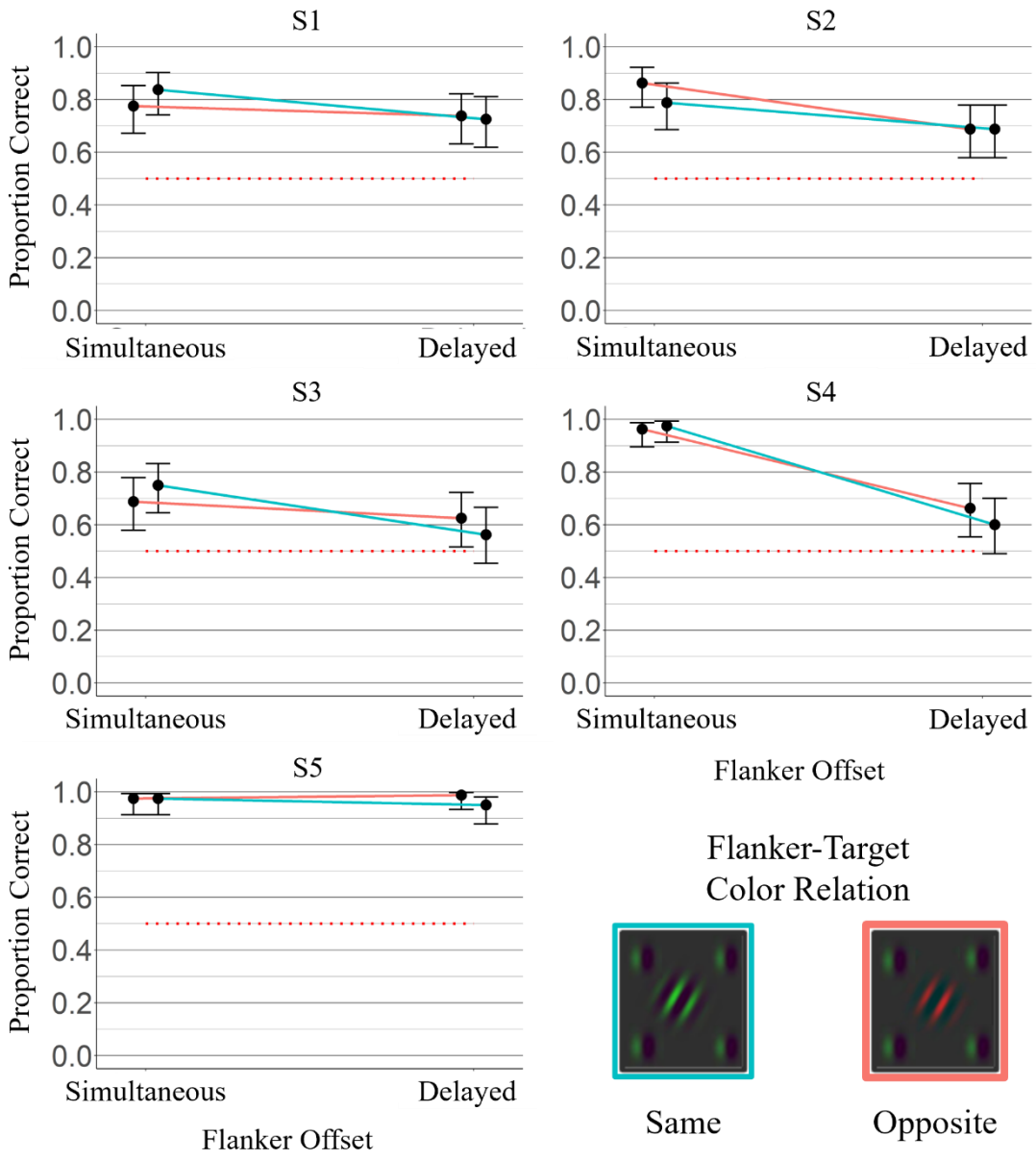

Figure 2-9. Tilt recall in Exp. 1B. Each point represents mean across 80 trials. Error bars represent 95% confidence intervals; red dotted line indicates chance. **Note**: Tilt recall for S5 was near ceiling for all conditions.

Subject	Predictor	Log estimate (SE)	p-value
1	Flanker Offset (Simultaneous–Delayed)	0.231 (0.369)	0.581
	Flanker-Target Color Relation (Same–Opposite)	-0.064 (0.357)	0.858
	Flanker Offset × Color Relation	0.466 (0.539)	0.387
2	Flanker Offset (Simultaneous–Delayed)	1.048 (0.404)	**0.001**
	Flanker-Target Color Relation (Same–Opposite)	0.000 (0.341)	1.000
	Flanker Offset × Color Relation	-0.526 (0.544)	0.334
3	Flanker Offset (Simultaneous–Delayed)	0.278 (0.831)	0.406
	Flanker-Target Color Relation (Same–Opposite)	-0.260 (0.323)	0.421
	Flanker Offset × Color Relation	0.570 (1.190)	0.234
4	Flanker Offset (Simultaneous–Delayed)	2.571 (0.634)	< **0.001**
	Flanker-Target Color Relation (Same–Opposite)	-0.269 (0.329)	0.413
	Flanker Offset × Color Relation	0.687 (0.983)	0.485
5	Flanker Offset (Simultaneous–Delayed)	-0.706 (1.24)	0.568
	Flanker-Target Color Relation (Same–Opposite)	-1.425 (1.13)	0.207
	Flanker Offset × Color Relation	1.425 (1.52)	0.348

Table 2-4. Logistic regression models for tilt recall in Exp. 1B. 2/5 subjects showed significant masking. No subjects showed significant main effects of flanker-target color relation or significant interaction effects. Note: Tilt recall for S5 was near ceiling for all conditions.

2.4.3 Exp. 1C Results: Colored versus grayscale flanker effects on OSM

Reported here are results for Exp. 1C, in which effects of flanker color condition (colored versus grayscale) were tested for OSM of color and tilt. Recall accuracy figures and binomial logistic regression models are given for 1) overall recall (correct color *and* tilt); 2) color recall (irrespective of tilt); and 3) tilt recall (irrespective of color). Each is reported on a per-subject basis; for each subject, all three measures are derived from the same four-alternative forced choice recall task.

For overall recall, all five subjects showed significant masking. Two subjects showed significant main effects of flanker color, such that recall was higher with grayscale than colored flankers. All five subjects showed interaction effects in the same direction, such that masking was greater with colored than grayscale flankers; however, logß values for these interactions were generally small and the interaction was significant for only one subject. See Figure 2-10 for overall recall in Exp. 1C, and Table 2-5 for corresponding regression models.

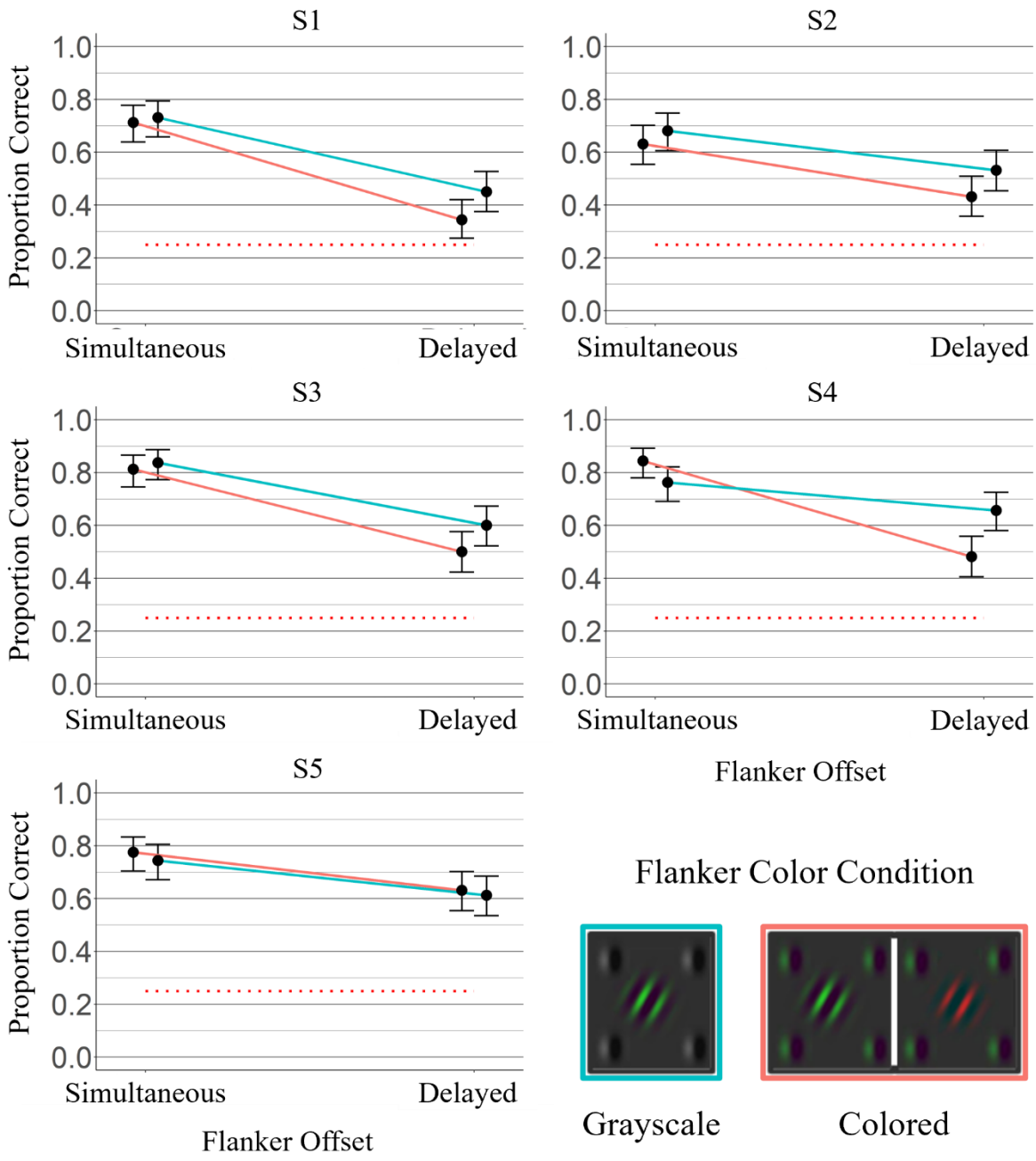

Figure 2-10. Overall recall in Exp. 1C. Each point represents mean across 160 trials. Error bars represent 95% confidence intervals; red dotted line indicates chance.

Subject	Predictor	Log estimate (SE)	p-value
1	Flanker Offset (Simultaneous–Delayed)	1.554 (0.241)	< **0.001**
	Flanker Color (Grayscale–Colored)	0.446 (0.230)	0.053
	Flanker Offset × Flanker Color	-0.353 (0.340)	0.299
2	Flanker Offset (Simultaneous–Delayed)	0.814 (0.229)	< **0.001**
	Flanker Color (Grayscale–Colored)	0.402 (0.225)	0.074
	Flanker Offset × Flanker Color	-0.180 (0.326)	0.581
3	Flanker Offset (Simultaneous–Delayed)	1.466 (0.148)	< **0.001**
	Flanker Color (Grayscale–Colored)	0.405 (0.130)	**0.002**
	Flanker Offset × Flanker Color	-0.232 (0.215)	0.279
4	Flanker Offset (Simultaneous–Delayed)	1.761 (0.269)	< **0.001**
	Flanker Color (Grayscale–Colored)	0.722 (0.230)	**0.002**
	Flanker Offset × Flanker Color	-1.242 (0.367)	< **0.001**
5	Flanker Offset (Simultaneous–Delayed)	0.699 (0.250)	**0.005**
	Flanker Color (Grayscale–Colored)	-0.0797 (0.231)	0.729
	Flanker Offset × Flanker Color	-0.0915 (0.349)	0.793

Table 2-5. Logistic regression models for overall recall in Exp. 1C. 5/5 subjects showed significant masking. 2/5 subjects showed significant main effects of flanker color, such that recall was higher with grayscale than colored flankers. 1/5 subjects showed a significant interaction effect, such that masking was stronger with colored than grayscale flankers.

For color recall, four subjects showed significant masking. Three subjects showed significant main effects of flanker color, such that recall was higher with grayscale than colored flankers. Only one subject showed a significant interaction effect, such that masking was

stronger with colored than grayscale flankers. See Figure 2-11 for color recall in Exp. 1C, and Table 2-6 for corresponding regression models.

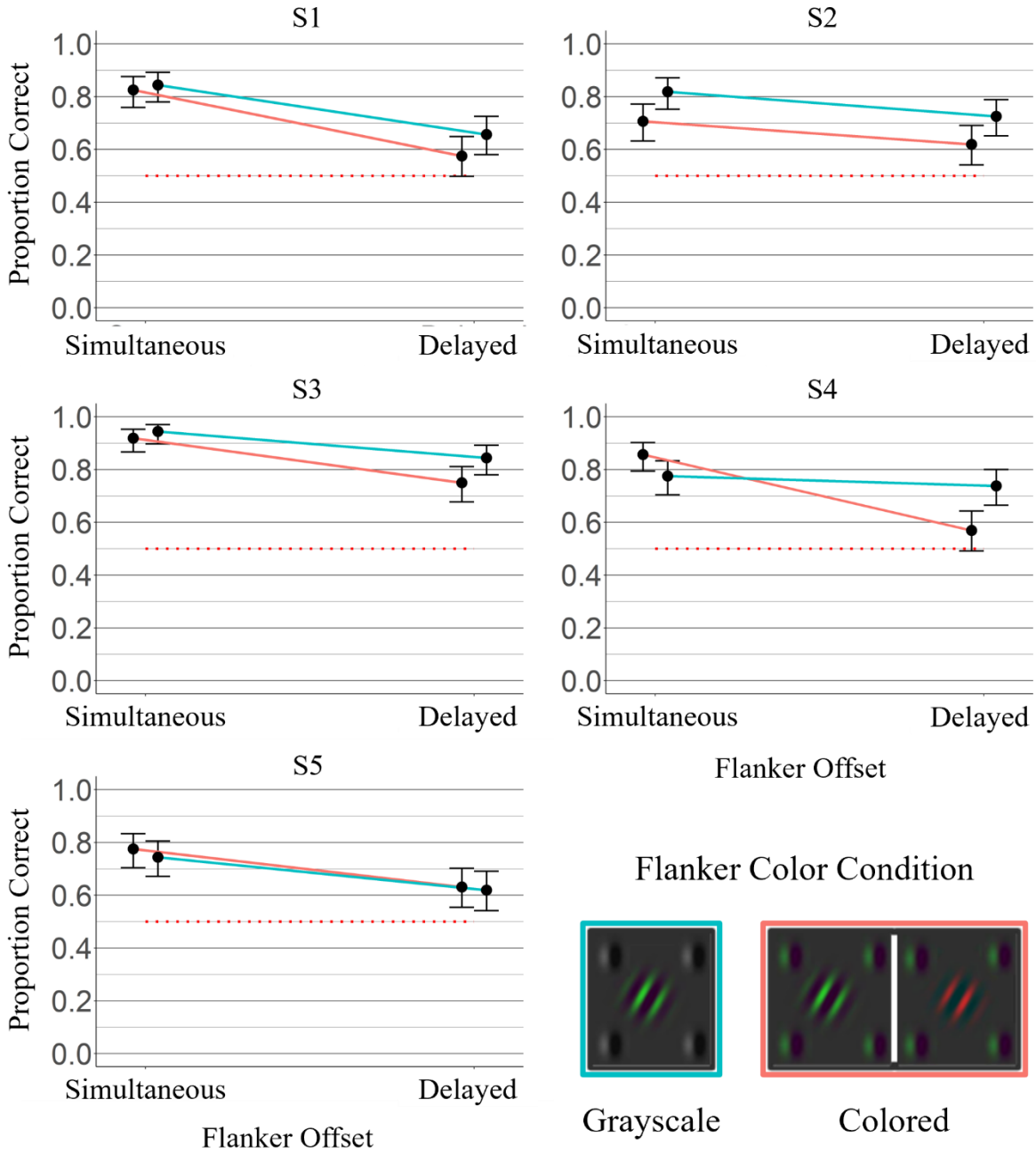

Figure 2-11. Color recall in Exp. 1C. Each point represents mean across 160 trials. Error bars represent 95% confidence intervals; red dotted line indicates chance.

Subject	Predictor	Log estimate (SE)	p-value
1	Flanker Offset (Simultaneous–Delayed)	1.248 (0.262)	< **0.001**
	Flanker Color (Grayscale–Colored)	0.344 (0.231)	0.136
	Flanker Offset × Flanker Color	-0.209 (0.379)	0.583
2	Flanker Offset (Simultaneous–Delayed)	0.393 (0.238)	0.099
	Flanker Color (Grayscale–Colored)	0.485 (0.241)	**0.044**
	Flanker Offset × Flanker Color	0.146 (0.361)	0.687
3	Flanker Offset (Simultaneous–Delayed)	1.327 (0.198)	< **0.001**
	Flanker Color (Grayscale–Colored)	0.588 (0.164)	< **0.001**
	Flanker Offset × Flanker Color	-0.193 (0.307)	0.529
4	Flanker Offset (Simultaneous–Delayed)	1.508 (0.276)	< **0.001**
	Flanker Color (Grayscale–Colored)	0.756 (0.240)	**0.002**
	Flanker Offset × Flanker Color	-1.304 (0.380)	< **0.001**
5	Flanker Offset (Simultaneous–Delayed)	0.700 (0.250)	**0.005**
	Flanker Color (Grayscale–Colored)	-0.053 (0.231)	0.817
	Flanker Offset × Flanker Color	-0.118 (0.349)	0.736

Table 2-6. Logistic regression models for color recall in Exp. 1C. 4/5 subjects showed significant masking. 3/5 subjects showed significant main effects of flanker color, such that recall was higher with grayscale than colored flankers. 1/5 subjects showed a significant interaction effect, such that color masking was stronger with colored than grayscale flankers.

For tilt recall, four subjects showed significant masking. No subject showed a significant main effects of flanker color, or significant interaction effect. One subject (S5) showed tilt recall at or near ceiling for all trial types. See Figure 2-12 for tilt recall in Exp. 1C, and Table 2-7 for corresponding regression models.

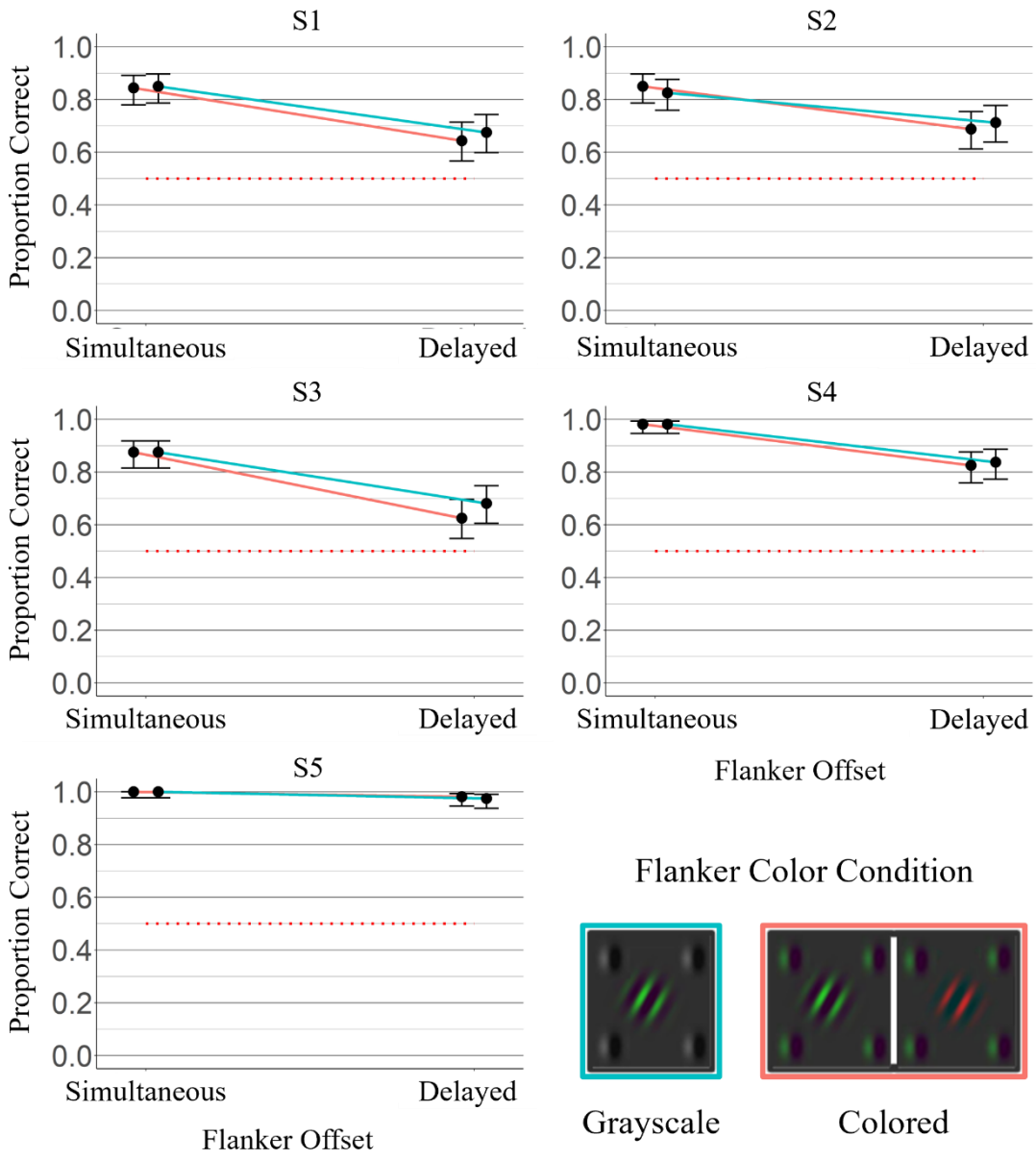

Figure 2-12. Tilt recall in Exp. 1C. Each point represents mean across 160 trials. Error bars represent 95% confidence intervals; red dotted line indicates chance. Note: Tilt recall for S5 was at or near ceiling under all conditions.

Subject	Predictor	Log estimate (SE)	p-value
1	Flanker Offset (Simultaneous–Delayed)	1.095 (0.273)	< **0.001**
	Flanker Color (Grayscale–Colored)	0.139 (0.236)	0.555
	Flanker Offset × Flanker Color	-0.091 (0.390)	0.816
2	Flanker Offset (Simultaneous–Delayed)	0.946 (0.279)	< **0.001**
	Flanker Color (Grayscale–Colored)	0.119 (0.244)	0.626
	Flanker Offset × Flanker Color	-0.303 (0.390)	0.437
3	Flanker Offset (Simultaneous–Delayed)	1.435 (0.1671)	< **0.001**
	Flanker Color (Grayscale–Colored)	0.249 (0.136)	0.067
	Flanker Offset × Flanker Color	-0.249 (0.2379)	0.296
4	Flanker Offset (Simultaneous–Delayed)	2.407 (0.619)	< **0.001**
	Flanker Color (Grayscale–Colored)	0.089 (0.299)	0.765
	Flanker Offset × Flanker Color	-0.089 (0.877)	0.919
5	Flanker Offset (Simultaneous–Delayed)	17.608 (2311)	0.994
	Flanker Color (Grayscale–Colored)	-0.294 (0.772)	0.703
	Flanker Offset × Flanker Color	0.294 (3268)	1.000

Table 2-7. Logistic regression models for tilt recall in Exp. 1C. 4/5 subjects showed significant masking effects. No subject showed significant main effects of flanker color or significant interaction effects. Note: Tilt recall for S5 was at or near ceiling under all conditions.

2.5 Conclusions

The three object-substitution masking experiments described here show 1) masking of tilt for grayscale Gabor stimuli, with little effect of flanker-target similarity; 2) overall masking of colored, tilted Gabor stimuli, which is primarily masking of color rather than of tilt; and 3)

overall masking of colored, tilted Gabor stimuli by either colored or grayscale flankers, with little evidence of an interaction effect between degree of masking and flanker color. These findings support some but not all aspects of current theories about the roles of object representations, object similarity, and feature integration in OSM.

Exp. 1A partially replicated the findings of Goodhew et al. (2015) with modified stimuli. The masking effects found in this experiment were mixed: three subjects showed a significant main effect of flanker offset, while the fourth subject (S2) did not show a significant main effect of flanker offset but did show a significant interaction effect of mask type × flanker offset, with masking stronger with Gabor flankers than Gaussian ones. These findings are consistent with the prior authors' assertion that OSM can act on objects defined by single features, rather than only on feature-integration mechanisms (Bouvier & Treisman, 2010). However, they do not corroborate Goodhew et al's (2015) other primary result, which showed significantly greater masking of Gabor targets' tilts by similar Gabor flankers than lower-spatial-frequency, un-oriented Gaussian-dot flankers. Why does the difference in spatial frequency (power and directionality) between stimuli and flankers not appear to be as salient to masking in the present study as in Goodhew et al. (2015)? Several differences in the stimulus and mask parameters between the two studies may be important. In Goodhew et al. (2015), stimuli and flankers were 4.0 cpd and had 100% Michelson luminance contrast, whereas in this experiment they were 3.0 cpd and had 75% Michelson luminance contrast; this was done to keep the spatial frequency and contrast parameters in this experiment consistent with those in Experiments 1B and 1C. The Weber luminance contrast for Gaussian flankers, meanwhile, was 75% in the current study and 100% in the Goodhew et al. (2015) study.

The prior study's analysis may also have permitted more sensitive testing for contrasts, as they used a repeated-measures ANOVA on subject-average masking across n=20 subjects. Unfortunately, such a between-subjects design was not feasible for the current experiments, which required five to seven experimental sessions per subject including color vision pre-testing and photometry.

Exp. 1B established object-substitution masking of colored Gabor stimuli; this masking appears to be primarily of color and not tilt. All subjects showed significant overall masking, and four of five showed significant color masking. However, only two of five showed significant tilt masking, and the magnitude of tilt masking for those who did show it was lower than for color masking. This effect is most pronounced for S5, who consistently showed ceiling performance across conditions for tilt recall, but who showed significant color masking. If masking is of integrated object representations, the degree of masking for each feature should be equal, and there should be no pattern to errors in masking trials; that is, "correct color/incorrect tilt," "incorrect color/correct tilt," and "incorrect color/incorrect tilt" should occur in roughly equal proportions. Instead, subjects showed a strong bias toward "incorrect color/correct tilt" when they made errors.

Exp. 1B reveals a second bias in subjects' responses: All subjects showed higher color recall when the target was the same color as the flankers as when it was opposite in color. This would seem to go directly against the flanker-similarity effect on masking. However, two findings suggest that this trend was due to response bias, not a differential effect on masking. First, this trend was also apparent for offset-simultaneous trials, for which no masking could occur. Second, two subjects showed very low apparent color recall in the offset-delayed condition when the flankers were opposite in color to the target—significantly below chance

(35% correct for S1; 10% correct for S4). Conversely, these two (along with S2 and S5) showed very high apparent color recall—above 90%—when the flankers were the same color as the target. These results suggest that subjects may have tended to report the color of the flankers when they were unsure about the color of the target. Subsequent experiments will either average across "flankers-same" and "flankers-opposite" color conditions (as in Exp. 1C) or introduce mixed-color flankers (as in Exps. 2-3) to compensate for any bias toward reporting the color of the flankers. It should be noted that there was no measurable effect of flanker-target color similarity on tilt recall—no subject showed a significant main effect of color similarity, nor did any subject show an interaction between color similarity and tilt masking.

Exp. 1C, like Exp. 1B, showed object-substitution masking of colored Gabor stimuli. All subjects showed significant masking effects on overall recall; four of five showed significant masking effects for color and four of five showed significant masking effects for tilt (with the fifth near ceiling across conditions). Only one subject (S4) showed a significant interaction effect between masking and flanker color condition; this interaction was significant for overall and color recall, but not for tilt recall.

Exp. 1C introduced grayscale flankers, and compared masking between trials with these grayscale flankers and trials with colored flankers. The "colored flanker" condition represented the average of "flankers same" and "flankers opposite" flanker-target color relations. In averaging across these conditions, the intent was to average out the bias, shown in Exp. 1B, toward reporting the color of the flankers: As long as subjects' bias was the same for "flankers same" and "flankers opposite" trials, any decrease in accuracy for "flankers opposite" should be counterbalanced in the results by a corresponding increase in accuracy for "flankers same" trials, and the resulting average should reflect the mean color-masking effect for colored flankers. After

this averaging, subjects still showed significant color masking ($p<0.05$ for 5/5 subjects); however, only one subject showed significantly greater color masking with colored flankers than grayscale flankers. This does not follow the prediction of the "shared-axis model" of similarity effects, which predicted that because both *+l* ("red-and-dark") and *–l* ("green-and-dark") flankers modulated the L/(L+M) axis, they would mask target color more strongly than the grayscale flankers, which did not modulate the L/(L+M) axis.

In Exp. 1C four of five subjects showed significant tilt masking, whereas in Exp. 1B only two of five subjects did. In both experiments, S5 gave tilt recall >95% across all conditions with single-frame (16.7 ms) target-and-distractor array display time; this precluded any possibility of significant tilt masking with the present analysis. However, other subjects differed between Exp. 1B and Exp. 1C in the target-and-flanker display times established from the practice trials. In Exp. 1B, S1-S3 all required target-and-flanker display times of three frames (50 ms) to achieve average overall recall >70% in offset-simultaneous trials. In Exp. 1C, these same three subjects all showed optimal performance (70%-90%) on offset-simultaneous trials with target-and-flanker display times of two frames (33.3 ms). While no definite conclusions can be drawn from this, it does raise the question: Does masking of luminance-defined tilt require shorter target-and-flanker display times than masking of color? Further study is needed to explore this question.

Overall, these experiments establish that our OSM paradigm can be used to mask target color—and, to a lesser extent, tilt—for tilted Gabors defined in the cone-opponent *l* and luminance *Y* chromaticity axes. They failed to replicate flanker-target similarity effects on masking for grayscale Gabor targets' tilt (with Gabor versus Gaussian-blur flankers, Exp. 1A) (Goodhew et al., 2015). They also did not show flanker-target similarity effects for color. In Exp. 1B, which used "same-color" versus "opposite-color" flankers, the similarity effect was opposite

that predicted by the feature-level (Gellatly et al., 2006) and object-level similarity hypotheses (Goodhew et al., 2015); however, this effect was not significant overall and is likely to reflect a response bias rather than a true differential masking effect.

In Exp. 1C, there was no significant flanker-target color similarity effect with "colored" versus "grayscale" flankers (Exp. 1C). This did not follow the prediction of the "feature axis masking" hypothesis. However, as noted previously, the targets, distractors, and flankers in Exp. 1B-1C were designed to selectively activate color-and-luminance selective, "double-opponent" edge-detecting V1 neurons (Johnson et al., 2008; Nunez et al., 2021). Could the dual selectivity of these neurons have contributed to cross-masking of targets' color by grayscale flankers in this paradigm? This leads to two follow-up questions. First, could flankers with color and luminance-defined tilt effectively mask each feature when flanker-target relations are parameterized to maximize similarity *and* when parameterized to maximize dissimilarity for each? This will be tested in Experiment 2.

Second, would cross-masking of color (and/or of luminance) occur when targets, distractors, and flankers are designed to maximally stimulate feature-processing neurons with single-opponent color (±*l* or ±*s*) or spatially low-pass luminance (±*Y*) receptive field properties? This will be tested in Experiment 3.

CHAPTER 3

EXPERIMENT 2: COLOR AND TILT EFFECTS ON OSM

3.1 Rationale

Experiment 2 tested for effects of flanker-target similarity on color and tilt masking using an expanded set of similarity parameterizations for both color and tilt. As in Experiment 1, it used targets, distractors, and flankers modulated along the lsY *l* and *Y* chromaticity axes. This experiment was divided into four sub-experiments, Exps. 2A-2D, each designed to test a specific, related hypothesis. Exps. 2A-2D were designed follow up on the results of Exps. 1A-1C, which showed masking of tilt (Exp. 1A) and dissociable "feature-level" masking of color and tilt (Exps. 1B and 1C), but did not show expected similarity effects on masking of either feature. Exp. 1A did not replicate the finding of reduced tilt OSM of grayscale Gabor targets with lower-spatial-frequency Gaussian flankers (Goodhew et al., 2015). Exp. 1B did not find the color-similarity effect on color masking shown by Gellatly et al. (2006) with a paradigm using tilted Gabor targets and neutral-tilt Gabor flankers defined in lsY *l* and *Y* chromaticity axes. Finally, Exp. 1C did not show any differential effects on flanker chromaticity axes on masking. That is, flankers that were modulated along both lsY chromaticity axes the target was modulated along—the L/(L+M) cone-opponent *l* axis and the luminance (grayscale) *Y* axis—did not show significantly greater masking than flankers that were modulated in the grayscale *Y* axis only.

Additionally, the results of Exp. 1B, which showed masking of color and tilt but no effect of flanker-target color similarity on masking, were potentially affected by response bias toward reporting the color of the flankers (Gellatly et al., 2006). Exps. 2A-2D introduced flanker Gabors of mixed color or tilt to reduce this response bias (definition of "mixed" colors and tilts is given

in Section 3.3). In each experiment subjects reported only one feature of the target, and either the task-relevant or the task-irrelevant feature was parameterized to maximize or minimize predicted masking under the alternative hypothesis, while the other feature was held constant across trials.

In Exps. 2A (report color) and 2B (report tilt), the condition of the task-relevant feature was parameterized to be "mixed" in one half of trials and "neutral" in the other half. Across all trials, the task-irrelevant feature of the flankers was identical to that of the target to control for that feature's effect. The null hypothesis for Exps. 2A-2B was that there would be no difference in masking between flankers "mixed" and "neutral" in the task-relevant feature. This would be consistent either with no role of flanker-target similarity in masking under this paradigm, or with the similarity effect of "neutral" flankers being equivalent to that of "mixed" flankers—for example, if the net similarity effect were based on a linear, unweighted space-averaging. The alternative hypothesis was that masking would be stronger with one of the two similarity conditions than the other. This would be consistent with either an object-similarity or a feature-similarity hypothesis in which "mixed" flankers are not equivalent to "neutral flankers" in their masking efficacy—for example, if the net similarity effect were not based on an unweighted space-averaging. If such an asymmetric effect on masking were found, its direction would be indicative of the type of nonlinearity or weighting function in the system, though it would not necessarily distinguish between object-level and feature-level similarity effects.

In Exps. 2C (report color) and 2D (report tilt), the condition of the task-irrelevant feature was parameterized to be "mixed" in one half of trials and "opposite" in the other half. Across all trials, the task-relevant feature of the flankers was neutral to control for that feature's effect. The null hypothesis for Exps. 2C-2D was that there would be no difference in masking between the flankers-mixed and flankers-opposite conditions. This would be consistent with a feature-

similarity model, wherein dissimilarity of the task-irrelevant feature does not affect masking (Gellatly et al., 2006), or with a thresholded object-similarity model, in which dissimilarity of a single feature is an equally effective object-segmentation cue as dissimilarity of two features. The alternative hypothesis was that masking would be stronger with flankers mixed than flankers opposite. This would be consistent with a non-thresholded object-similarity model, wherein difference of either the task-relevant or task-irrelevant feature would effectively cue object segmentation, irrespective of whether the other feature was similar or different. See Table 3-1 for the parameters for task-relevant and task-irrelevant features in Exps. 2A-2D.

3.2 Subjects

Six subjects (three men, mean age 26.5 years) completed this experiment. Author RL was one subject; the other five were naïve to the purpose and design of the study. Each subject gave informed consent, had normal or corrected-to-normal visual acuity, had normal color vision, and completed photometry to equate monitor phosphors' luminance.

3.3 Stimuli and Protocol

Each trial had five phases, as described in General Methods. Stimuli consisted of Gabor targets, distractors, and flankers with varying colors and tilts. At the end of each trial (phase five), a probe array was displayed until the subject indicated which probe matched the target via button press. In this experiment, the subject reported color or tilt singly; thus, the probe array consisted of two probes: one the correct color (or tilt), and the other the opposite color (or tilt). Both probes matched the target for the non-reported feature. For example, when subjects reported the color of the target, one probe was "red-and-dark" and the other "green-and-dark;" both had the same tilt as the target. Thus, the correct probe always fully matched the target.

Gabor targets, distractors, and flankers were always modulated in luminance (lsY *Y*). They could also be modulated in color along the cone-opponent L/(L+M) *l* axis. Targets and distractors were always colored, but flankers could be either colored or grayscale ("neutral color," modulated in *Y* only). Targets', distractors', and flankers' tilts were defined by the axis of modulation of luminance. When color was also modulated, this occurred along the same tilt axis as lightness modulation, and either in phase or in antiphase with the lightness modulation. Thus, target, distractor, and flanker Gabors could appear either "red-and-dark" (+*l* in phase with +*Y*) or "green-and-dark" (–*l* in phase with +*Y*). Targets and distractors were always tilted ±22.5° from vertical, but flankers could be either tilted ±22.5° from vertical, or tilted vertically ("neutral tilt," axis 90°).

This experiment had four different types of trial blocks, each analyzed separately. These are referred to as "Exp. 2A" through "Exp. 2D." In each block type, the four flanker Gabors were parameterized differently for color and tilt, and subjects would report either color or tilt for all trials in the block. In Exp. 2A (report color) and 2B (report tilt), the task-relevant (reported) feature of the flankers was parameterized to be either mixed or neutral, and the task-irrelevant feature of the flankers was the same as the target. In Exps. 2C (report color) and 2D (report tilt), the task-irrelevant (unreported) feature of the flankers was parameterized to be either mixed or opposite the target, and the task-relevant (reported) feature of the flankers was neutral.

In all four block types, the colors and tilts of the Gabor distractors were assigned randomly and independently. When flankers were "mixed" in a feature, the positions of the two (+) and the two (–) flanker Gabors were randomized independently for each trial. As in Exp. 1, flanker offset was either simultaneous with target offset, or delayed by 250 ms. See Table 3-1 for

specifications of the flanker conditions for each block type, and Figure 3-1 for examples of stimulus arrays with targets, distractors, and flankers.

	Exp. 2A	**Exp. 2B**	**Exp. 2C**	**Exp. 2D**
Reported feature	Color	Tilt	Color	Tilt
Flanker colors	Mixed *or* all neutral (grayscale)	All same as target	All neutral (grayscale)	Mixed *or* all opposite target
Flanker tilts	All same as target	Mixed *or* all neutral (90°)	Mixed *or* all opposite target	All neutral (90°)

Table 3-1. Parameters for Exps. 2A–2D. In each block type, subjects reported one feature. Target and distractor Gabors were always mixed in both features at the group level; flanker Gabors could be 1) neutral in a feature; 2) mixed in a feature; 3) all the same as the target in a feature; or 4) all opposite to the target in a feature.

Each subject completed 40 blocks of 16 trials each for each experiment. Each block was a randomized and fully counterbalanced 2×2×2×2 design: 2 levels of target color ("red-and-dark" and "green-and-dark") × 2 levels of target tilt ("left" and "right") × 2 levels of flanker-target similarity for either the task-relevant or task-irrelevant feature (see Table 3-1) × 2 levels of flanker offset ("simultaneous" and "delayed"). The levels of target color and target tilt were collapsed for analysis, giving 160 total trials per condition in each 2×2 binomial logistic regression analyses.

Prior to the experiment, each subject performed three to four practice blocks to familiarize them with the task and calibrate target-plus-flanker durations, as described in Section

2.3.5. Target-plus-flanker durations for each subject in Exps. 2A-2D can be found in Table B-1 in Appendix B Section B.1.

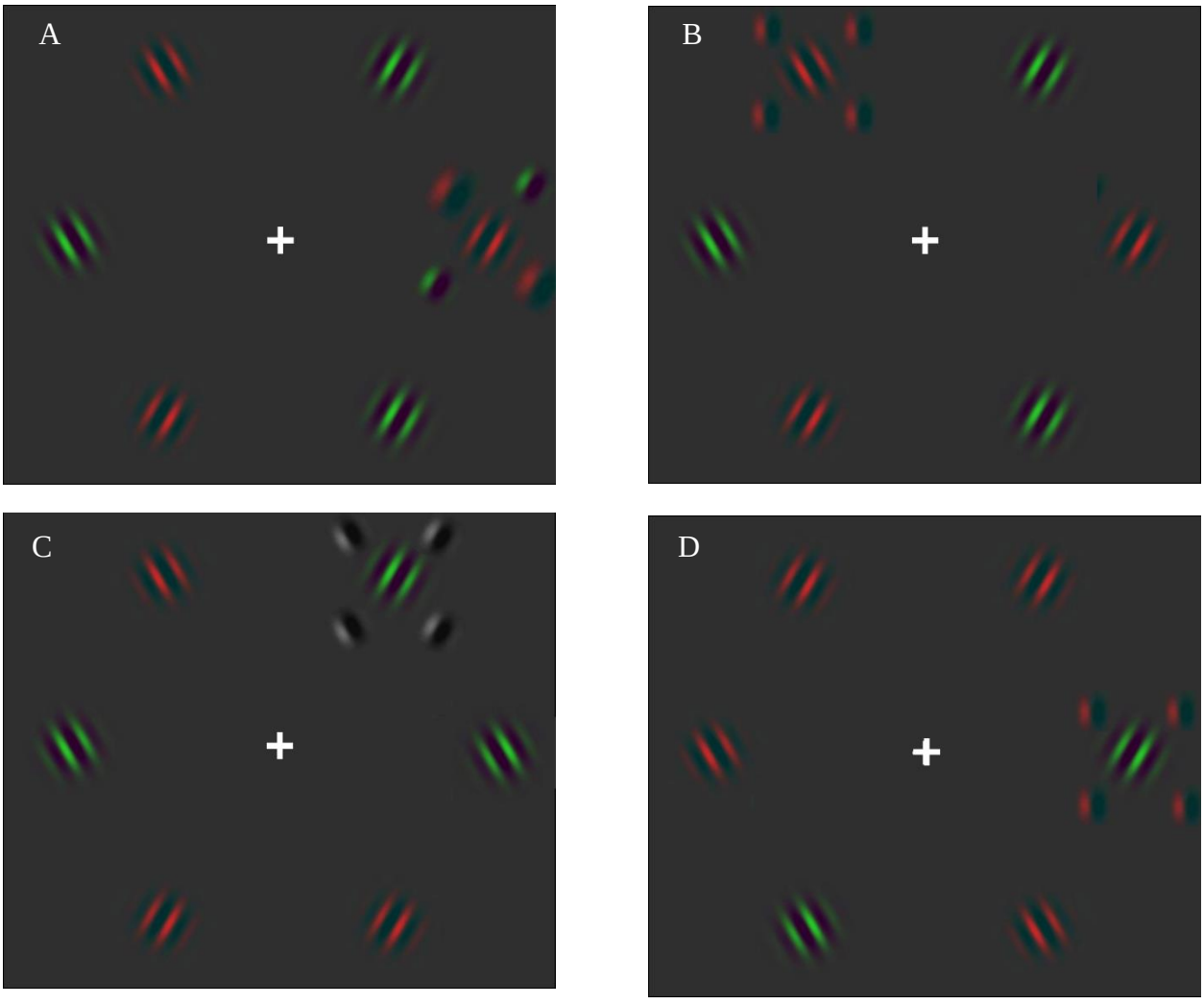

Figure 3-1. Example stimulus arrays in Exps. 2A-2D. a) Example of "flankers mixed colors" in Exp. 2A. b) Example of "flankers neutral tilt" in Exp. 2B. c) Example of "flankers mixed tilts" in Exp. 2C. d) Example of "flankers same color" in Exp. 2D. **Note**: These examples are for demonstration only, and do not precisely represent the actual stimuli used in experiments.

3.4 Results

For each subject in each experiment, proportion correct recall for the reported feature was analyzed with a 2×2 binomial logistic regression model, with main effects of flanker offset and flanker condition (for either color or tilt), and the interaction effect of the two.

In Exp. 2A, wherein subjects reported color and flanker color was parameterized, five of six subjects showed significant main effects of flanker offset ($p<0.05$), indicating masking. Directions of main effects of flanker color, and of masking-color interactions, were mixed across subjects. See Figure 3-2 for color recall in Exp. 2A, and Table 3-2 for corresponding regression models.

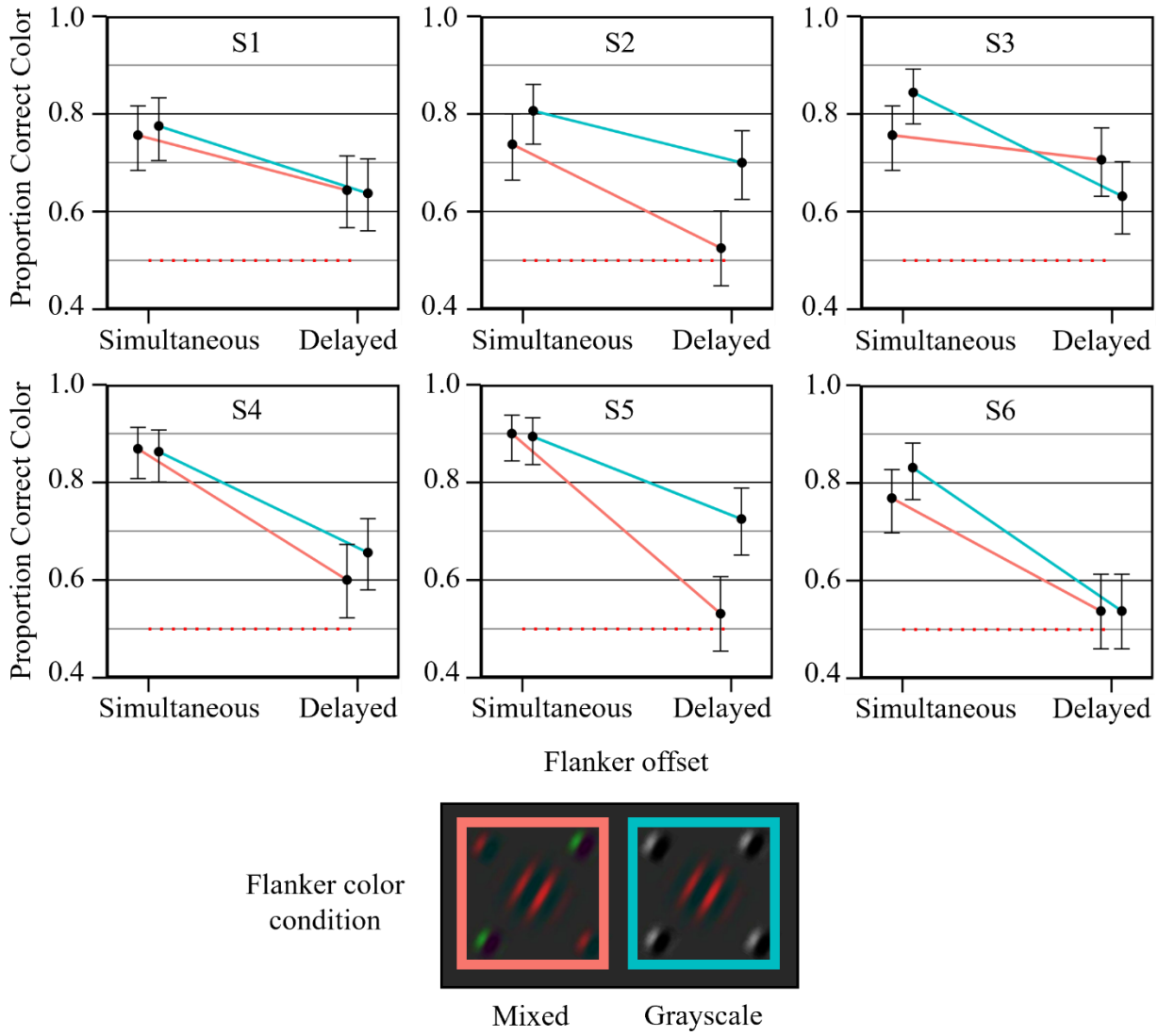

Figure 3-2. Color recall in Exp. 2A. Each point represents mean across 160 trials. Error bars represent 95% confidence intervals; red dotted line indicates chance. Line colors represent the color condition of the flankers: red lines are for the "flanker colors mixed" condition, and blue lines are for the "flankers grayscale" condition.

Subject	Predictor	Log estimate (SE)	p–value
1	Flanker Offset (Simultaneous – Delayed)	0.541 (0.247)	**0.029**
	Flanker Color (Grayscale – Mixed)	-0.027 (0.233)	0.907
	Flanker Offset × Flanker Color	0.132 (0.352)	0.708
2	Flanker Offset (Simultaneous – Delayed)	0.932 (0.240)	< **0.0001**
	Flanker Color (Grayscale – Mixed)	0.747 (0.234)	**0.001**
	Flanker Offset × Flanker Color	–0.354 (0.357)	0.320
3	Flanker Offset (Simultaneous – Delayed)	0.225 (0.253)	0.314
	Flanker Color (Grayscale – Mixed)	–0.340 (0.239)	0.155
	Flanker Offset × Flanker Color	0.894 (0.372)	**0.016**
4	Flanker Offset (Simultaneous – Delayed)	1.485 (0.284)	< **0.0001**
	Flanker Color (Grayscale – Mixed)	0.241 (0.232)	0.298
	Flanker Offset × Flanker Color	–0.295 (0.402)	0.463
5	Flanker Offset (Simultaneous – Delayed)	2.072 (0.308)	< **0.0001**
	Flanker Color (Grayscale – Mixed)	0.844 (0.238)	< **0.001**
	Flanker Offset × Flanker Color	–0.912 (0.438)	**0.037**
6	Flanker Offset (Simultaneous – Delayed)	1.051 (0.246)	< **0.0001**
	Flanker Color (Grayscale – Mixed)	< 0.001 (0.224)	> 0.999
	Flanker Offset × Flanker Color	0.393 (0.361)	0.275

Table 3-2. Models for Exp. 2A, effect of flanker color on color OSM. Masking was significant for 5/6 subjects. Flanker color was significant for 2/6 subjects, such that recall was higher with grayscale flankers than mixed-color flankers. The interaction between masking and flanker color was significant for 2/6 subjects, but with opposite signs.

In Exp. 2B, wherein subjects reported tilt and flanker tilt was parameterized, all six subjects showed significant masking. Four of six showed significant main effects of flanker tilt, with recall higher for neutral-tilt than mixed-tilt flankers. Interactions were all nonsignificant in the same direction, with masking stronger with mixed tilt than neutral tilt flankers. See Figure 3-3 for tilt recall in Exp. 2B, and Table 3-3 for corresponding regression models.

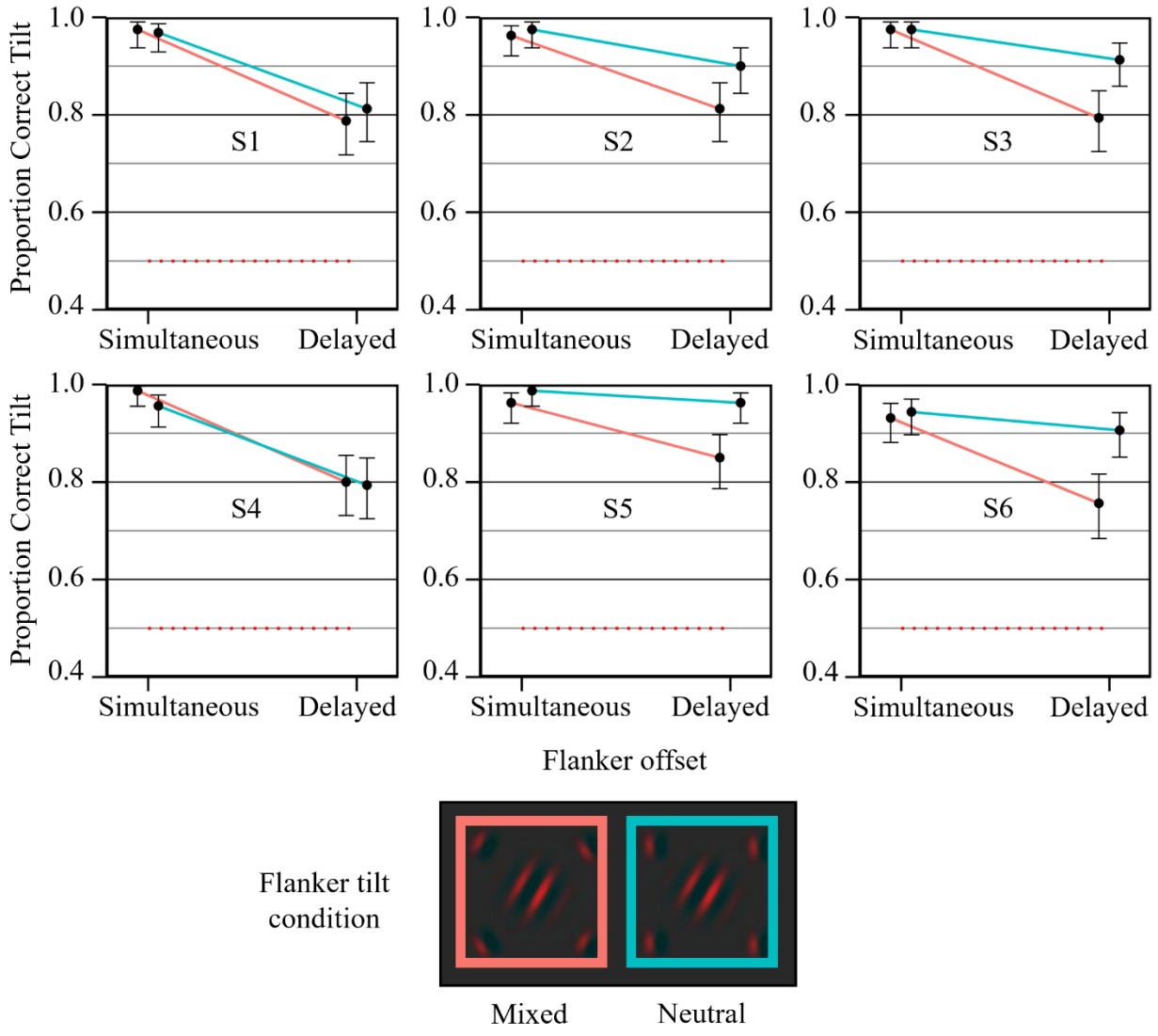

Figure 3-3. Tilt recall in Exp. 2B. Each point represents mean across 160 trials. Error bars represent 95% confidence intervals; red dotted line indicates chance. Line colors represent the tilt condition of the flankers: red lines are for the “flanker tilts mixed” condition, and blue lines are for the “flanker tilts neutral” condition.

Subject	Predictor	Log estimate (SE)	p–value
1	Flanker Offset (Simultaneous – Delayed)	2.354 (0.542)	< **0.0001**
	Flanker Tilt (Mixed – Neutral)	0.156 (0.280)	0.576
	Flanker Offset × Flanker Tilt	–0.386 (0.736)	0.600
2	Flanker Offset (Simultaneous – Delayed)	1.779 (0.463)	< **0.001**
	Flanker Tilt (Mixed – Neutral)	0.731 (0.332)	**0.028**
	Flanker Offset × Flanker Tilt	–0.313 (0.735)	0.671
3	Flanker Offset (Simultaneous – Delayed)	2.316 (0.543)	< **0.0001**
	Flanker Tilt (Mixed – Neutral)	0.997 (0.341)	**0.003**
	Flanker Offset × Flanker Tilt	–0.997 (0.793)	0.209
4	Flanker Offset (Simultaneous – Delayed)	2.983 (0.739)	< **0.0001**
	Flanker Tilt (Mixed – Neutral)	–0.039 (0.278)	0.889
	Flanker Offset × Flanker Tilt	–1.246 (0.856)	0.145
5	Flanker Offset (Simultaneous – Delayed)	1.511 (0.471)	**0.001**
	Flanker Tilt (Mixed – Neutral)	1.511 (0.471)	**0.001**
	Flanker Offset × Flanker Tilt	–0.386 (0.950)	0.684
6	Flanker Offset (Simultaneous – Delayed)	1.474 (0.363)	< **0.0001**
	Flanker Tilt (Mixed – Neutral)	1.137 (0.328)	< **0.001**
	Flanker Offset × Flanker Tilt	–0.923 (0.568)	0.104

Table 3-3. Models for Exp. 2B, effect of flanker tilt on tilt OSM. Masking was significant for 6/6 subjects. Flanker tilt was significant for 4/6 subjects, such that recall was higher with neutral-tilt flankers than mixed-tilt flankers. The interaction between masking and flanker tilt was not significant for any subject.

In Exp. 2C, wherein subjects reported color and flanker tilt was parameterized, 4/6 subjects showed significant masking, and one other was nearly significant (p=0.071). Directions of main effects of flanker tilt, and of the tilt-offset interactions, were mixed across subjects and not statistically significant. See Figure 3-4 for color recall in Exp. 2C, and Table 3-4 for corresponding regression models.

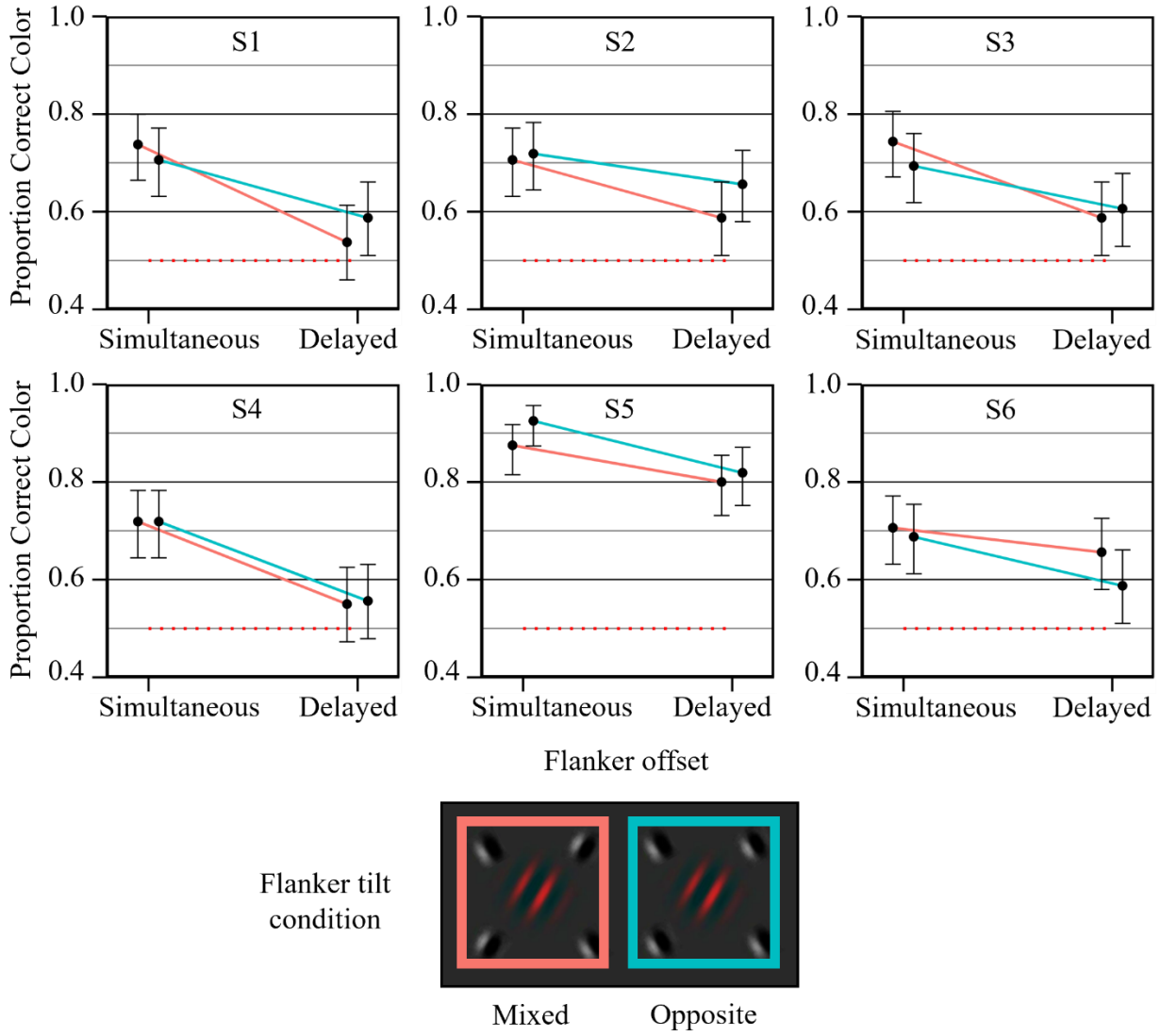

Figure 3-4. Color recall in Exp. 2C. Each point represents mean across 160 trials. Error bars represent 95% confidence intervals; red dotted line indicates chance. Line colors represent the tilt condition of the flankers: red lines are for the “flanker tilts mixed” condition, and blue lines are for the “flanker tilts opposite” condition.

Subject	Predictor	Log estimate (SE)	p–value
1	Flanker Offset (Simultaneous – Delayed)	0.883 (0.240)	< **0.001**
	Flanker Tilt (Opposite – Mixed)	0.203 (0.226)	0.368
	Flanker Offset × Flanker Tilt	–0.359 (0.337)	0.286
2	Flanker Offset (Simultaneous – Delayed)	0.524 (0.237)	**0.027**
	Flanker Tilt (Opposite – Mixed)	0.293 (0.231)	0.205
	Flanker Offset × Flanker Tilt	–0.232 (0.338)	0.493
3	Flanker Offset (Simultaneous – Delayed)	0.712 (0.242)	**0.003**
	Flanker Tilt (Opposite – Mixed)	0.078 (0.228)	0.732
	Flanker Offset × Flanker Tilt	–0.326 (0.338)	0.335
4	Flanker Offset (Simultaneous – Delayed)	0.738 (0.237)	**0.002**
	Flanker Tilt (Opposite – Mixed)	0.025 (0.225)	0.910
	Flanker Offset × Flanker Tilt	–0.025 (0.335)	0.940
5	Flanker Offset (Simultaneous – Delayed)	0.560 (0.310)	0.071
	Flanker Tilt (Opposite – Mixed)	0.122 (0.285)	0.670
	Flanker Offset × Flanker Tilt	0.445 (0.478)	0.352
6	Flanker Offset (Simultaneous – Delayed)	0.231 (0.241)	0.338
	Flanker Tilt (Opposite – Mixed)	–0.293 (0.231)	0.205
	Flanker Offset × Flanker Tilt	0.204 (0.336)	0.543

Table 3-4. Models for Exp. 2C, effect of flanker tilt on color OSM. Masking was significant for 4/6 subjects. Flanker tilt was not significant for any subjects, nor was there a significant or consistent interaction-effect direction between masking and flanker tilt.

In Exp. 2D, wherein subjects reported tilt and flanker color was parameterized, 4/6 subjects showed significant masking, and the other two were nearly significant ($p<0.1$). Directions of main effects of flanker color, and of the color-offset interactions, were mixed across subjects. See Figure 3-5 for tilt recall in Exp. 2D, and Table 3-5 for corresponding regression models.

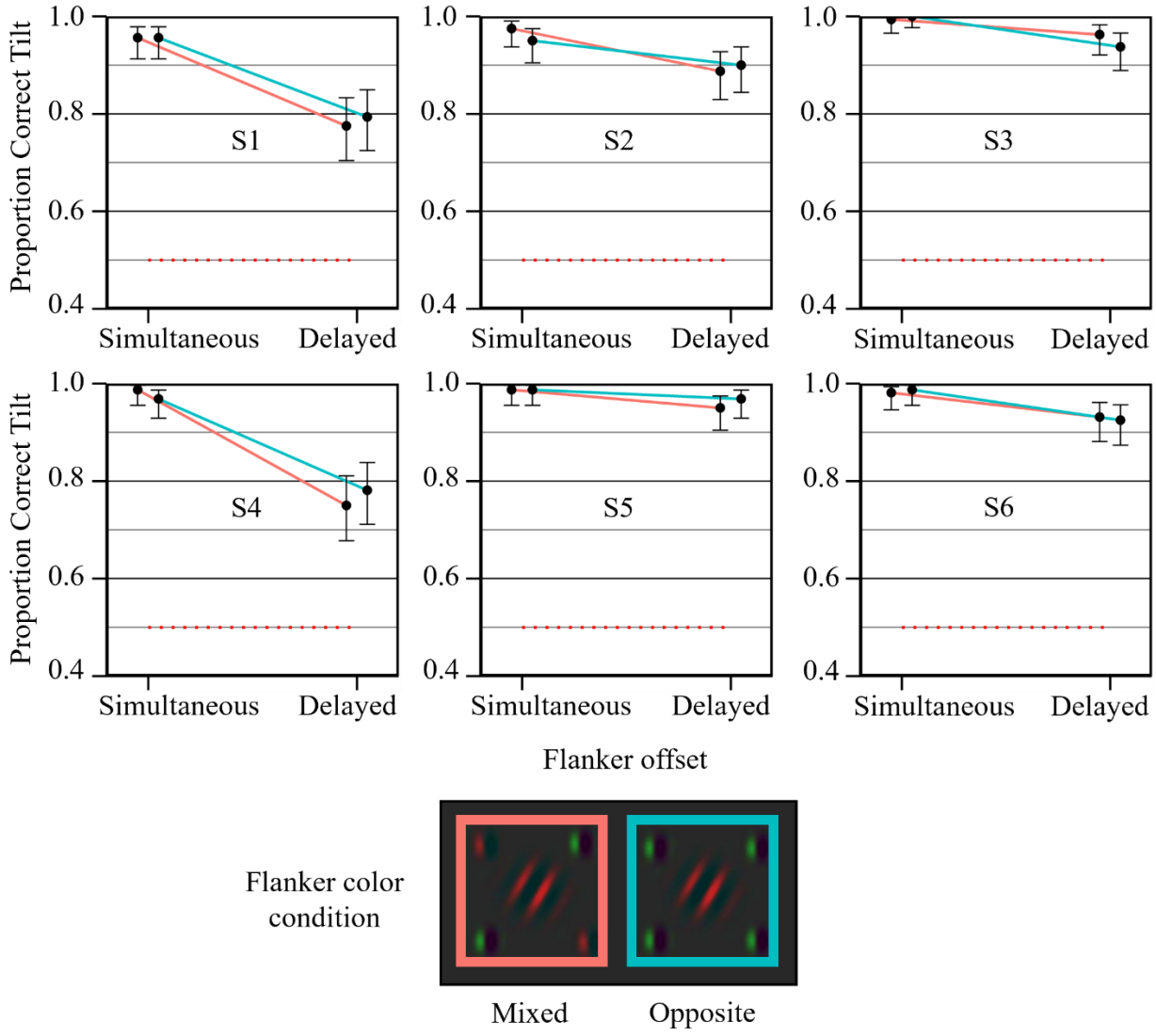

Figure 3-5. Tilt recall in Exp. 2D. Each point represents the mean across 160 trials. Error bars represent 95% confidence intervals; red dotted line indicates chance. Line colors represent the color condition of the flankers: red lines are for the "flanker colors mixed" condition, and blue lines are for the "flanker colors opposite" condition.

Subject	Predictor	Log estimate (SE)	p–value
1	Flanker Offset (Simultaneous – Delayed)	1.848 (0.460)	< **0.0001**
	Flanker Color (Opposite – Mixed)	0.111 (0.272)	0.684
	Flanker Offset × Flanker Color	–0.111 (0.611)	0.856
2	Flanker Offset (Simultaneous – Delayed)	1.598 (0.565)	**0.005**
	Flanker Color (Opposite – Mixed)	0.132 (0.363)	0.717
	Flanker Offset × Flanker Color	–0.851 (0.721)	0.238
3	Flanker Offset (Simultaneous – Delayed)	1.824 (1.086)	0.093
	Flanker Color (Opposite – Mixed)	–0.537 (0.529)	0.310
	Flanker Offset × Flanker Color	16.0 (1401.7)	> 0.99
4	Flanker Offset (Simultaneous – Delayed)	3.271 (0.735)	< **0.0001**
	Flanker Color (Opposite – Mixed)	0.174 (0.264)	0.510
	Flanker Offset × Flanker Color	–1.110 (0.885)	0.210
5	Flanker Offset (Simultaneous – Delayed)	1.425 (0.799)	0.074
	Flanker Color (Opposite – Mixed)	0.490 (0.581)	0.400
	Flanker Offset × Flanker Color	–0.490 (1.162)	0.674
6	Flanker Offset (Simultaneous – Delayed)	1.352 (0.661)	**0.041**
	Flanker Color (Opposite – Mixed)	–0.094 (0.433)	0.829
	Flanker Offset × Flanker Color	0.506 (1.017)	0.619

Table 3-5. Models for Exp. 2D, effect of flanker color on tilt OSM. Masking was significant for 4/6 subjects ($p<0.05$), and nearly significant for the remaining 2 subjects ($p<0.1$). Flanker color was not significant for any subject, nor was there any significant or consistent interaction effect between masking and flanker tilt.

3.5 Conclusions

In Exps. 2A-2D, object-substitution masking of color or tilt as a single feature was shown across a variety of contexts. This further contradicts the hypothesis that OSM acts solely at the level of object-feature integration (Bouvier & Treisman, 2010). These four experiments parameterized flanker-target similarity for either the task-relevant feature (Exps. 2A-2B) or the task-irrelevant feature (Exps. 2C-2D). These parameterizations included conditions in which flankers were mixed in one of the two target features; that is, two flankers had (+) modulation along a feature axis and the other two flankers had (-) modulation of equal magnitude along that same feature axis. Across Exps. 2A-2D, these "flankers-mixed" conditions were shown to effectively induce masking of both color and tilt. The usefulness of this is twofold: First, when flankers are mixed with respect to the task-relevant feature, they cannot bias responses in the same way that non-mixed flankers do. Second, if the neural function that outputs the "flanker-target similarity effect" is treated as an unweighted spatial average, then the net flanker-target similarity effect for flankers mixed in a feature is equivalent to that of flankers neutral in that feature. Thus, this model of the flanker-target similarity effect as the output of an unweighted spatial averaging function predicts that any effect of flanker-target similarity on masking ought to be identical for flankers mixed or neutral in a feature. The contrapositive of this assertion is that if mixed flankers and neutral flankers show different effects on masking, one can rule out this unweighted spatial averaging model of similarity effects.

The results of Exps. 2A-2D as they relate to the models of flanker-target similarity effects outlined in the Rationale section are as follows:

In Exp. 2A, 2/6 subjects showed significant interaction effects between flanker color condition and color masking. However, the directions of these effects were mixed, both among

the two significant interactions and among the remaining four subjects. In Exp. 2B, no subjects showed significant interaction effects between flanker tilt condition and tilt masking. However, all six interactions were in the same direction, such that masking was greater for flankers with mixed tilts than those with neutral tilt. These results show clear evidence of color and tilt masking, and the pattern of masking-flanker tilt effects in Exp. 2B is more consistent with the alternative hypothesis, that masking has either an object-level or feature-level similarity effect that is not based on a linear, unweighted space-averaging function.

In Exp. 2C, directions of interaction effects between flanker tilt condition and color masking were mixed across subjects, with none significant. Finally, in Exp. 2D, directions of interaction effects between flanker color condition and tilt masking were mixed across subjects, with none significant. These results show further evidence of color and tilt masking. They show no evidence, even in patterns of nonsignificant results, of any interaction effects between masking and flanker-target similarity condition for the task-irrelevant feature. No evidence, therefore, was found in support of a non-thresholded object-similarity model of flanker-target similarity effects.

It should be noted that, across experiments, tilt recall was generally higher than color recall, despite the calibration procedure employed at the start of each experiment. In particular, tilt recall for flanker offset-simultaneous conditions was ≥90% for all subjects in Exp. 2B, and ≥95% for all subjects in Exp. 2D. This near-ceiling performance almost certainly decreased sensitivity of the binomial logistic regression model, and could have obscured variance across conditions in tilt OSM. For consistency with Exp. 1, the stimuli in Exp. 2A-2D had high (75%) Michelson luminance contrast, and target, distractor, and flanker tilts were ±22.5° from vertical. Using stimuli with lower luminance contrast and/or smaller tilt gradations may allow for better

calibration of tilt-recall performance and more sensitive modeling. Interestingly, the tilt differences among targets, distractors, and flankers in this protocol were much smaller than in other experiments that showed substantially stronger masking of tilt than of color (Gellatly et al., 2006; Koivisto & Silvanto, 2011). This discrepancy is explored in the General Discussion.

Future OSM paradigms testing masking of color and tilt should precisely equate the salience these features to increase sensitivity to variance in tilt recall. They should also test flanker-target similarity parameterizations not included in these experiments, such as flankers all-same versus all-opposite in the task-irrelevant feature. The finding that flankers mixed in a feature can effectively induce masking opens up opportunities for testing various hypotheses about possible sources of unequal signal-weighting or nonlinearity in flanker-target similarity effects, including half-wave rectification, full-wave rectification, and thresholding. The final experiment of this dissertation tests for such effects on masking of targets defined along single cone-opponent or luminance axes.

CHAPTER 4

EXPERIMENT 3: OSM OF SINGLE-FEATURE COLOR AND LUMINANCE REPRESENTATIONS

4.1 Rationale

The three sub-experiments comprising Experiment 3 were performed to investigate masking, and similarity effects thereon, of single-feature color and luminance stimuli. They used stimuli defined along single cone-opponent or luminance axes, designed to selectively stimulate luminance-processing or single-opponent color- processing neurons (Johnson et al., 2008). The four flankers were always mixed in modulation of one chromaticity axis; that is, two (+) and two (–), to reduce potential response bias. These experiments had four primary predictions:

1) Cone-opponent *l* and *s* axis-isolating targets, and luminance *Y* axis-isolating targets, would all be masked in this paradigm.
2) There would be flanker-target similarity effects on masking. That is, for at least some flanker-target axis pairings, flankers defined on the same chromaticity axis as their target would induce OSM more effectively than flankers defined on a different axis.
3) Targets of different colors would be masked differently.
4) Masking efficacy would vary by both flanker and target chromaticity axis, irrespective of any flanker-target similarity effects.

While similarity-effect models motivated predictions 1) and 2), the properties of color and luminance signaling neurons—particularly the dynamics of S cone signaling neurons—motivated predictions 3) and 4) (Blake et al., 2008; Lee et al., 2009; Pietersen et al., 2014).

4.2 Subjects

Experiment 3 was divided into three sub-experiments, Exps. 3A-3C; in each, 10 subjects completed two experimental sessions. Author RL completed all three sub-experiments; no other subject completed multiple sets of conditions, and all other subjects were naïve to the design and purpose of the experiment. The demographics of subjects for each set of conditions are as follows. Exp. 3A: Mean age 26 years; four men. Exp. 3B: Mean age 25 years; three men. Exp. 3C: Mean age 26 years; two men. Five additional subjects did not complete Exps. 3A-3C due to attrition, or abnormal anomaloscope or photometry measurements. All subjects completed color vision screening and photometry, and gave informed consent, as outlined in Chapter 2.2, Exp. 1 Subjects.

4.3 Stimuli and Protocol

Each trial had the five phases described in Chapter 2.3, Exp. 1 Stimuli and Protocol: General. Targets and distractors were arranged in the same imaginary regular hexagon, with the target and distractors similarly randomized. The background was an equal-energy gray, with lsY coordinates of [l=0.665, s=1.0, Y=16.0 cd/m^2]. Targets, distractors, flankers, and probes were all Gaussian-like blurred circular dots defined by (+) or (–) modulation of a single chromaticity axis (l, s, or Y) away from the background chromaticity. This gave six possible stimulus colors: "red" (+l), "green" (–l), "purple" (+s), "lime" (–s), "light" (+Y), and "dark" (–Y). Target and distractor dots had maximal spatial frequency power at 0.6 cpd, and flanker dots had maximum spatial frequency power at 0.7 cpd. See Appendix C, Section C.1 for more details of the Exp. 3 stimuli, including the method of generation and chromaticity modulations.

The three sets of sub-experiments, Exps. 3A-3C, varied the chromaticity axes used to define the target, distractors, and flankers. Each sub-experiment used two chromaticity axes to

define flankers, targets, and distractors; the three sub-experiments thus represented all possible pairwise combinations of *l*, *s*, and *Y* defined stimuli. Within each sub-experiment there were two sessions; for each session, flankers were always one chromaticity axis while targets and distractors could be either of two chromaticity axes. Each session was analyzed and reported separately. See Table 4-1 for flanker, target, and distractor parameters for Exps. 3A-3C, and Figure 4-1 for illustration of example target, flanker, and distractor arrays.

Sub-experiment (Chromaticity axes compared)	Flanker colors (Chromaticity axis)	Target and distractor colors (Chromaticity axes)
3A	2 red, 2 green (±*l*)	red (+*l*) *or* green (–*l*) *or* purple (+*s*) *or* lime (–*s*)
l vs *s*	2 purple, 2 lime (±*s*)	
3B	2 red, 2 green (±*l*)	red (+*l*) *or* green (–*l*) *or* light (+*Y*) *or* dark (–*Y*)
l vs *Y*	2 light, 2 dark (±*Y*)	
3C	2 purple, 2 lime (±*s*)	purple (+*s*) *or* lime (–*s*) *or* light (+*Y*) *or* dark (–*Y*)
s vs *Y*	2 light, 2 dark (±*Y*)	

Table 4-1. Parameters for Exps. 3A–3C. In each block type, flankers were always defined along one chromaticity axis; the target and distractors were a random mix of the flankers' axis and one other axis. Each experiment was subdivided into two sessions of testing (one for each of the two flanker chromaticity axes). These sessions were analyzed separately.

Before starting each day's testing, a subject completed 4-6 practice blocks. The first three had decreasing target-and-distractor display durations (of 500, 250, and 100 ms). The fourth practice onward was at full speed, with a target-and-distractor display duration of 33.3 ms (two frames). These full-speed practices were used to set the modulation magnitude of the target, distractors, and flankers. They were run, with both axes' modulation magnitude increased or decreased as appropriate, until the subject's performance in flanker-offset-simultaneous trials was 75-90% for both same-axis and different-axis flanker-target chromaticity relations. Once this

baseline was reached, the subject proceeded to the main experiment. Note that this calibration procedure differed from that of Exps. 1 and 2, which calibrated performance on flanker-offset-simultaneous trials to the number of frames shown. This change was made to keep target-and-flanker display times consistent across subjects, as the time courses of feedforward and feedback processes were of specific interest in this experiment. See Appendix C Section C.1 for details of the calibration procedure employed in Exps. 3A-3C, and Table C-1 for the *l*, *s*, and *Y* modulation values used.

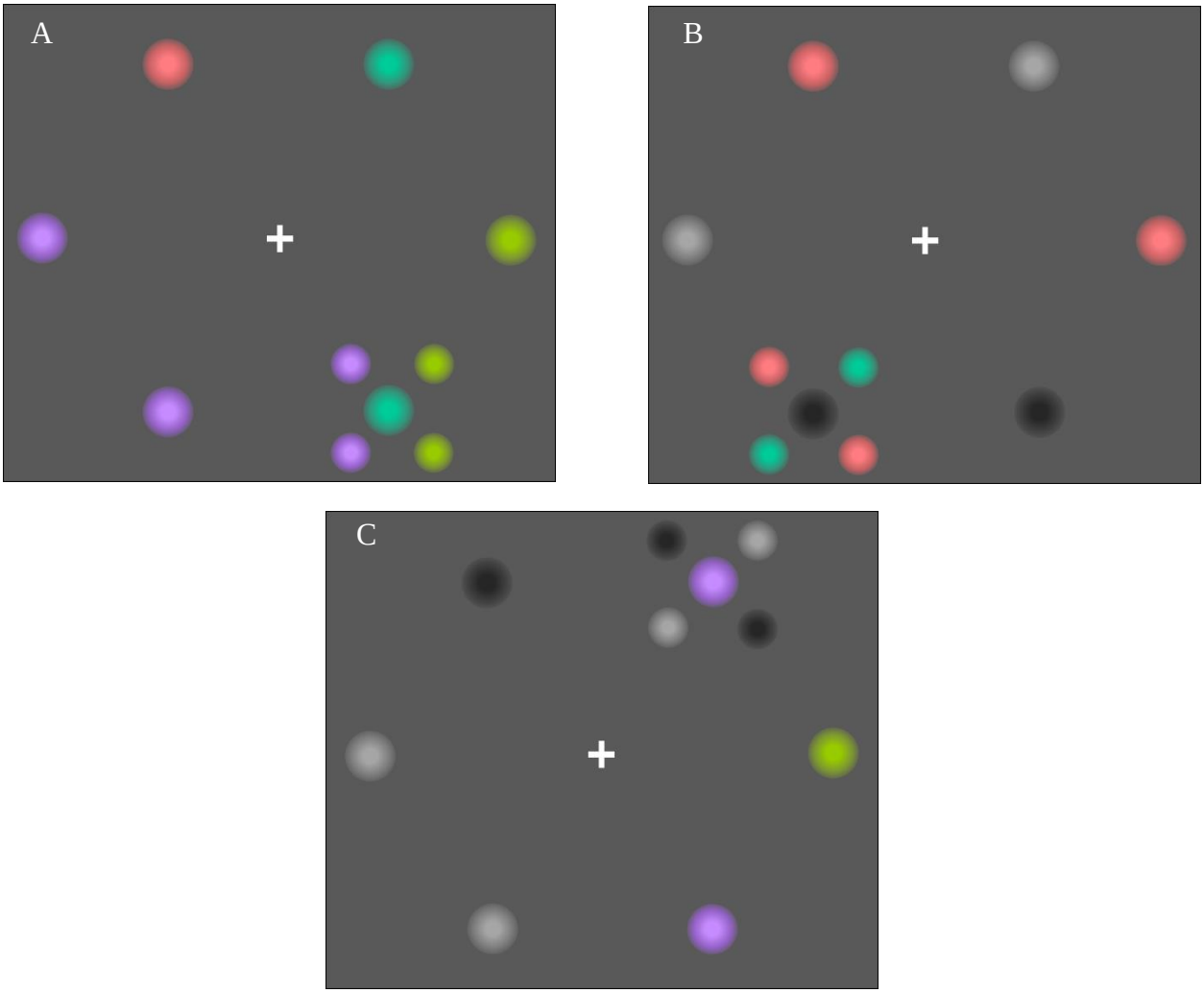

Figure 4-1. Example stimulus arrays in Exps. 3A-3C. a) Example stimulus array for "flankers ±*s*, target –*l*" in Exp. 3A. b) Example stimulus array for "flankers ±*l*, target –*Y*" in Exp. 3B. **c)** Example stimulus array for "flankers ±*Y*, target +*s*" in Exp. 3C. **Note**: These examples are for demonstration only, and do not precisely represent the actual stimuli used in experiments.

In the main experiment, the duration of target-and-flanker display in each trial was 33.3 ms (2 frames). After the stimulus display and a short blank period, the subject pressed a button on a gamepad to indicate which of two probe dots matched the color of the target dot. The two probe dots were always defined on the same chromaticity axis as the target; for example, if the target was "red" (+*l*), the two probes would be "red" (+*l*) and "green" (–*l*).

Each session of the main experiment was divided into 100 blocks of 8 trials each. Each block of trials was a fully randomized and counterbalanced 2×2×2 design, with factors of flanker offset ("simultaneous" versus "delayed"), flanker-target chromaticity axis relation ("same" versus "different"), and target axis modulation direction ("+" versus "–").

4.4 Results

For each of Exp. 3A, Exp. 3B, and Exp. 3C, there were two sessions, one each for the two possible chromaticity axes of the flankers. These sessions were each analyzed separately, giving six analyses, all run at the group level (n=10 subjects for each analysis). These analyses were 2×2 repeated-measures ANOVAs. Predictor factors were flanker offset ("simultaneous" versus "delayed") and flanker-target color-axis relation, henceforth referred to as "axis similarity" ("same" versus "different"); these were treated as within-subjects factors, with subject ID the error factor. Target modulation direction ("+" versus "–") was collapsed in the main analyses; analyses of masking for individual target colors may be found in Section 4.4.4. The outcome variable for the primary analyses was mean proportion correct recall, at each the four possible levels of flanker offset × flanker-target chromaticity axis relation, within each subject. These within-subject mean proportions were arcsine-transformed to approximate normality for analysis.

4.4.1 Exp. 3A: Masking with *l* and *s* targets, distractors, and flankers

In Exp. 3A, targets, flankers, and distractors were modulated along the "red vs green" *l* and "purple vs lime" *s* axes. Separate RMANOVA analyses were performed for the two sessions (flankers ±*l* and flankers ±*s*).

For the "flankers ±*l*" session, results were as follows: 1) Significant main effect of flanker offset, henceforth "masking" [$F(1,9)=145.6$, $p<0.001$]; 2) Significant main effect of flanker-target chromaticity axis similarity, henceforth "similarity effect" [$F(1,9)=8.942$, $p<0.05$]; and 3) Significant interaction of masking and axis similarity, henceforth "interaction" [$F(1,9)=19.05$, $p<0.01$], such that masking was stronger for similar *l* than dissimilar *s* targets.

For the "flankers ±*s*" session, results were as follows: 1) Significant masking [$F(1,9)=98.85$, $p<0.001$]; 2) Significant similarity effect [$F(1,9)=12.14$, $p<0.01$]; and 3) Significant interaction [$F(1,9)=5.579$, $p<0.05$], such that masking was *weaker* for similar *s* than dissimilar *l* targets. See Figure 4-2 for results of Exp. 3A.

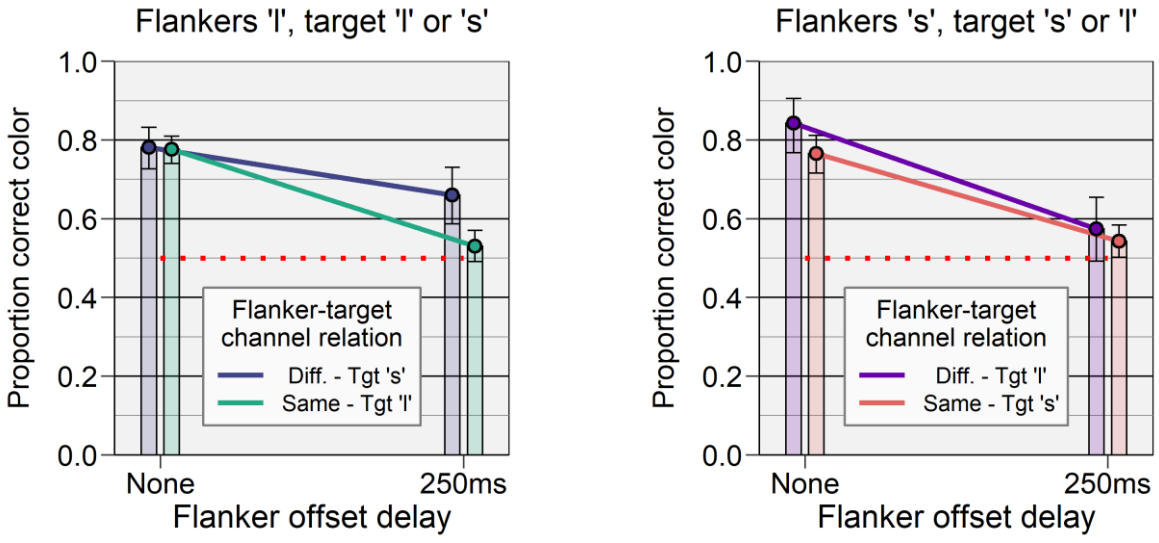

Figure 4-2. Recall for color in Exp. 3A. Each point represents mean across 10 subjects. Error bars represent 95% confidence intervals; red dotted line indicates chance. a) Recall for *l* and *s* targets with ±*l* flankers. Masking was significantly greater for *l* (similar) than *s* (dissimilar) targets [$F(1,9)=19.05$; $p<0.01$]. b) Recall for *l* and *s* targets with ±*s* flankers. Masking was significantly lower for *s* (similar) than *l* (dissimilar) targets [$F(1,9)=5.579$, $p<0.05$].

4.4.2 Exp. 3B: Masking with *l* and *Y* targets, distractors, and flankers

In Exp. 3B, targets, flankers, and distractors were modulated along the "red vs green" *l* and "dark vs light" *Y* axes. Separate RMANOVA analyses were performed for the two sessions (flankers ±*l* and flankers ±*Y*).

For the "flankers ±*l*" session, results were as follows: 1) Significant masking [$F(1,9)=44.94$, $p<0.001$]; 2) Non-significant similarity effect [$F(1,9)=0.218$, $p=0.652$]; and 3) Significant interaction [$F(1,9)=10.6$, $p<0.01$], such that masking was stronger for similar *l* than dissimilar *Y* targets.

For the "flankers ±*Y*" session, results were as follows: 1) Significant masking [$F(1,9)=10.31$, $p<0.05$]; 2) Significant similarity effect [$F(1,9)=30.47$, $p<0.001$]; and 3) Near-significant interaction [$F(1,9)=4.833$, $p=0.055$], such that masking was stronger for similar *Y* than dissimilar *l* targets. See Figure 4-3 for results of Exp. 3B.

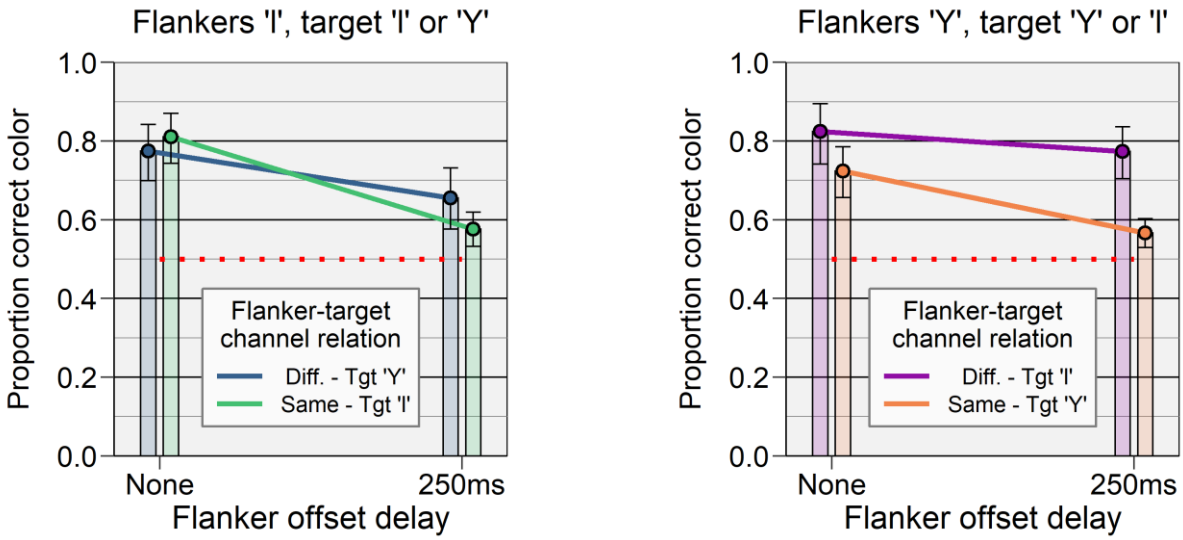

Figure 4-3. Recall for color in Exp. 3B. Each point represents mean across 10 subjects. Error bars represent 95% confidence intervals; red dotted line indicates chance. a) Recall for *l* and *Y* targets with ±*l* flankers. Masking was significantly greater for *l* (similar) than *Y* (dissimilar) targets [$F(1,9)=10.6$, $p<0.01$]. b) Recall for *l* and *s* targets with ±*s* flankers. Masking was near-significantly greater for *Y* (similar) than *l* (dissimilar) targets [$F(1,9)=4.833$, $p=0.055$].

4.4.3 Exp. 3C: Masking with *s* and *Y* targets, distractors, and flankers

In Exp. 3C, targets, flankers, and distractors were modulated along the "purple vs lime" *s* and "light vs dark" *Y* axes. Separate RMANOVA analyses were performed for the two sessions (flankers ±*s* and flankers ±*Y*).

For the "flankers ±*s*" session, results were as follows: 1) Significant masking [F(1,9)=126.5, p<0.0001]; 2) Non-significant similarity effect [F(1,9)=1.932, p=0.198]; and 3) Non-significant interaction [F(1,9)=1.079, p=0.326].

For the "flankers ±*Y*" session, results were as follows: 1) Significant masking [F(1,9)=52.44, p<0.0001]; 2) Significant similarity effect [F(1,9)=68.06, p<0.001]; and 3) Non-significant interaction [F(1,9)=1.382, p=0.27]. See Figure 4-4 for results of Exp. 3C.

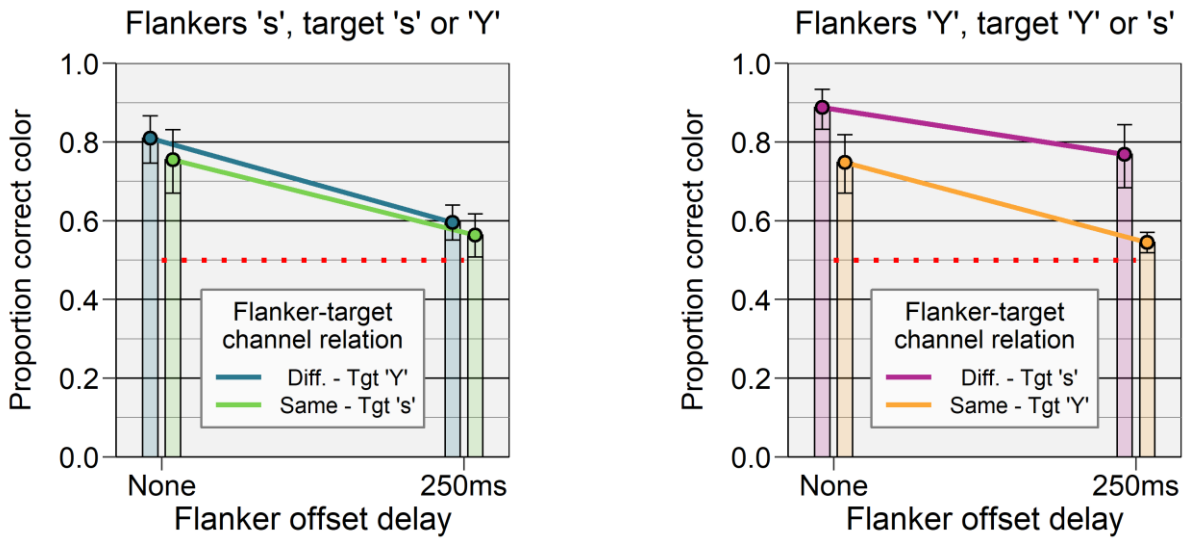

Figure 4-4. Recall for color in Exp. 3C. Each point represents mean across 10 subjects. Error bars represent 95% confidence intervals; red dotted line indicates chance. **A.** Recall for *s* and *Y* targets with ±*s* flankers. The interaction effect was not significant [F(1,9)=1.079, p=0.326]. **B.** Recall for *l* and *s* targets with ±*s* flankers. The interaction effect was not significant [F(1,9)=1.382, p=0.27].

4.4.4 Masking of individual target colors

The analyses reported above each averaged across modulation directions for each target axis. For example, results for recall of *s* targets with ±*l* flankers reflect the average recall for +*s* "purple" and –*s* "lime" targets. However, also of interest is a breakdown of masking by individual target colors. For each experiment, masking of each target color by each flanker axis was analyzed using four planned comparisons to the grand mean of masking for that flanker axis. Masking magnitude was defined as performance on "flanker offset simultaneous" minus performance on "flanker offset delayed" trials.

Variance of masking differed widely across target colors in each experiment, violating assumptions for parametric contrasts. Thus, non-parametric repeated-measures contrasts were calculated using the function `mctp.rm()` in the `R` package `nparcomp` (Konietschke et al., 2015, 2019; R Core Team, 2022). This function computes simultaneously any number *q* of "*t*-type" test statistics $\tilde{\mathbf{T}}$ based on any contrasts, including non-orthogonal ones such as contrasts of each condition to the grand mean (Konietschke et al., 2012; Noguchi et al., 2020). Significance for each contrast is assessed by the location of the test statistic $\tilde{\mathbf{T}}$ in a multivariate *t*-distribution, here with numerator degrees of freedom df_{num}=3 and denominator degrees of freedom df_{den}=9. This test requires only that data points be ordered (ordinal, discrete, or continuous), and that subject-level effects be random; no other assumptions are made about the variables' distributions' variances or shapes (Konietschke et al, 2010; 2012; 2015). This procedure adjusts the critical α for significance depending on the number of contrasts, protecting against multiple comparisons by controlling the family-wise error rate in the strong sense. This adjustment is said to be conservative for high correlations and small sample sizes, though less conservative than

Bonferroni adjustment (Konietschke et al., 2012; Noguchi et al., 2020). Power is generally comparable to ANOVA (Konietschke et al., 2013).

In Exp. 3A, when flankers were ±*l*, only +*s* "purple" targets ($\widetilde{\mathbf{T}}$=–6.09; p<0.001) were masked differently than the grand mean (0.183). When flankers were ±*s*, both –*s* "lime" targets ($\widetilde{\mathbf{T}}$=2.86; p=0.042) and +*s* "purple" targets ($\widetilde{\mathbf{T}}$=–3.76; p=0.011) were masked differently than the grand mean (0.245). See Table 4-2 for mean masking magnitudes for each target color-flanker axis condition in Exp. 3A, and p-values for the corresponding contrasts.

Exp. 3A		Target color					
		–*l* "green"	+*l* "red"	–*s* "lime"	+*s* "purple"	–*Y* "dark"	+*Y* "light"
Flanker axis; Grand mean masking	±*l* 0.183	0.325 (0.283)	0.166 (0.999)	0.208 (0.089)	**0.034 (<0.001)**	--	--
	±*s* 0.245	0.369 (0.313)	0.167 (0.461)	**0.378 (0.043)**	**0.067 (0.011)**	--	--
	±*Y*	--	--	--	--	--	--

Table 4-2. Masking by target color and flanker axis in Exp. 3A. In each cell, the top number gives the mean masking magnitude for that color target with that flanker axis; the bottom value gives the p-value of the associated contrast with the grand mean. **Black boldface**: Masking significantly greater than the grand mean. **Red boldface**: Masking significantly less than the grand mean (α=0.05, family-wise error controlled for each flanker axis).

In Exp. 3B, when flankers were ±*l*, only +*Y* "light" targets ($\widetilde{\mathbf{T}}$=–3.64; p=0.017) were masked differently than the grand mean (0.177). When flankers were ±*Y*, only –*Y* "dark" targets ($\widetilde{\mathbf{T}}$=4.05; p<0.01) were masked differently than the grand mean (0.104). See Table 4-3 for mean

masking magnitudes for each target color in Exp. 3B, and p-values for the corresponding contrasts.

Exp. 3B		Target color					
		–l "green"	*+l* "red"	*–s* "lime"	*+s* "purple"	*–Y* "dark"	*+Y* "light"
Flanker axis; Grand mean masking	±*l* 0.177	0.254 (0.519)	0.215 (0.636)	--	--	0.216 (0.912)	**0.022 (0.017)**
	±*s*	--	--	--	--	--	--
	±*Y* 0.104	0.050 (0.322)	0.052 (0.218)	--	--	**0.271 (0.009)**	0.044 (0.870)

Table 4-3. Masking by target color and flanker axis in Exp. 3B. In each cell, the top number gives the mean masking magnitude for that color target with that flanker axis; the bottom value gives the p-value of the associated contrast with the grand mean. **Black boldface**: Masking significantly greater than the grand mean. **Red boldface**: Masking significantly less than the grand mean (α=0.05, family-wise error controlled for each flanker axis).

In Exp. 3C, when flankers were ±*s*, both *–Y* "dark" targets ($\tilde{\mathbf{T}}$=9.51; p<0.001) and *+Y* "light" targets ($\tilde{\mathbf{T}}$=–14.0; p<0.001) were masked differently from the grand mean (0.203). When flankers were ±*Y*, both *+s* "purple" targets ($\tilde{\mathbf{T}}$=–4.68; p=0.004) and *–Y* "dark" targets ($\tilde{\mathbf{T}}$=9.41; p<0.001) were masked differently than the grand mean (0.162). See Table 4-4 for mean masking magnitudes for each target color in Exp. 3C, and p-values for the corresponding contrasts to the grand mean masking. See Appendix D for graphs of masking amounts for each color by each flanker axis in Exps. 3A-3C (Figure D-4 to D-6), along with the ANOVA table-style weights used for the planned contrasts.

Exp. 3C		Target color					
		–l “green”	*+l* “red”	*–s* “lime”	*+s* “purple”	*–Y* “dark”	*+Y* “light”
Flanker axis; Grand mean masking	*±l*	--	--	--	--	--	--
	±s 0.203	--	--	0.328 (0.375)	0.056 (0.123)	**0.441 (<0.001)**	**–0.012 (<0.001)**
	±Y 0.162	--	--	0.206 (0.470)	**0.033 (0.004)**	**0.341 (<0.001)**	0.066 (0.056)

Table 4-4. Masking by target color and flanker axis in Exp. 3C. In each cell, the top number gives the mean masking magnitude for that color target with that flanker axis; the bottom value gives the p-value of the associated contrast with the grand mean. **Black boldface**: Masking significantly greater than the grand mean. **Red boldface**: Masking significantly less than the grand mean (α=0.05, family-wise error controlled for each flanker axis).

4.4.5 Masking magnitude by target and flanker axis, and interactions

For each sub-experiment, a secondary analysis was performed on “masking magnitude” data across the two sessions, as reported in prior studies (Goodhew et al., 2015; Huang et al., 2018; Moore & Lleras, 2005). The goals of these secondary analyses were to test for effects of flanker axis, target axis, and their interaction on the magnitude of masking.

Each analysis was a 2×2 two-way repeated-measures ANOVA with factors of flanker axis, target axis, and their interaction, with a step-down procedure: If the interaction was significant, simple main effects were calculated for flanker axis at each level of target axis and vice-versa. These contrasts were calculated using the `R emmeans` library functions `emmeans()` and `contrast()`, with Holm correction for multiplicity (Lenth et al., 2022).

In Exp. 3A (targets and flankers *l* or *s*), two-way RMANOVA showed significant main effects of both flanker axis and target axis, with a non-significant interaction effect [$F(1,9)=3.62$, $p=0.09$, $\eta^2=0.29$]. The effect of flanker axis was such that masking was less with ±*l* than ±*s* flankers, with a mean difference of –0.062 [$F(1,9)=6.63$, $p=0.03$, $\eta^2=0.42$]. The effect of target axis was such that masking was greater with *l* targets than *s* targets, with a mean difference of 0.085 [$F(1,9)=20.3$, $p=0.001$, $\eta^2=0.69$]. These results show that *s*-defined flankers masked more effectively, and that *s*-defined targets were less susceptible to masking, but that there was no significant overall flanker axis × target axis interaction on masking magnitude. This is consistent with the opposite directions of similarity effects (flanker-target similarity × flanker-offset interactions) in "flankers ±*l*" and "flankers ±*s*" sessions (see Figure 4-2). See Table 4-5 for mean masking magnitudes for each flanker and target axis in Exp. 3A, along with ANOVA and contrast significance values.

Exp. 3A			Target axis		
			l	*s*	Δ (*l* – *s*)
		MEAN	0.183	0.245	Target axis main effect: **–0.062 ***
Flanker axis	±*l*	0.257	0.245	0.121	Target axis simple effect (flankers ±*l*) --
	±*s*	0.172	0.268	0.223	Target axis simple effect (flankers ±*s*) --
	Δ (*l* – *s*)	Flanker axis main effect: **0.085 ****	Flanker axis simple effect (targets *l*) --	Flanker axis simple effect (targets *s*) --	Interaction: n.s.

Table 4-5. ANOVA table of masking by target and flanker axis in Exp. 3A. Cells weighted equally. n.s. Not significant; *p<0.05; **p<0.01; ***p<0.001 (Holm adjusted for multiplicity).

In Exp. 3B (targets and flankers *l* or *Y*), two-way RMANOVA showed a significant main effect of flanker axis on masking magnitude [$F(1,9)=7.28$, $p=0.025$, $\eta^2=0.45$]. The effect of target axis was not significant [$F(1,9)=0.113$, $p=0.75$, $\eta^2=0.01$]. The interaction effect was significant [$F(1,9)=17.3$, $p=0.002$, $\eta^2=0.66$]. Thus, planned non-orthogonal contrasts were performed to test for simple main effects of flanker axis at each level of target axis, and vice-versa. The simple effect of flanker axis was significant with *l* targets (Δ masking with flankers

l–*Y*=0.184; p=0.009), but not with *Y* targets (Δ masking with flankers *l*–*Y*=0.031; p=0.248). The simple effects of target axis were significant with both ±*l* flankers (Δ masking with targets *l*–*Y*=0.116; p=0.009) and ±*Y* flankers (Δ masking with targets *l*–*Y*=0.107; p=0.0015). These results show that ±*l* flankers were more effective in masking *l* targets than *Y* targets, but ±*Y* flankers did not significantly differ in masking *l* versus *Y* targets. However, both *l* and *Y* targets were more effectively masked by same-axis than different-axis flankers. This is consistent with the significant flanker-target similarity effect shown with ±*l* flankers, but not with ±*Y* flankers, in Exp. 3B, and with ±*l* flankers being overall more effective in masking than ±*Y* flankers (see Figure 4-3). See Table 4-6 for mean masking magnitudes for each target and flanker axis in Exp. 3B, along with ANOVA and contrast significance values.

Exp. 3B			Target axis		
			l	*Y*	Δ (*l* – *Y*)
		MEAN	0.143	0.138	Target axis main effect: 0.005 n.s.
Flanker axis	±*l*	0.178	0.235	0.119	Target axis simple effect (flankers ±*l*): **0.116 ****
	±*Y*	0.104	0.051	0.158	Target axis simple effect (flankers ±*Y*): **–0.107 ***
	Δ (*l* – *Y*)	Flanker axis main effect: **0.073** *	Flanker axis simple effect (targets *l*): **0.184 ****	Flanker axis simple effect (targets *Y*): –0.039 n.s.	Interaction: ******

Table 4-6. ANOVA table of masking by target and flanker axis in Exp. 3B. Cells weighted equally. n.s:. Not significant; *p<0.05; **p<0.01; ***p<0.001 (Holm adjusted for multiplicity).

In Exp. 3C (targets and flankers *s* or *Y*), two-way RMANOVA showed a significant main effect of target axis on masking magnitude, such that masking was greater with *Y* targets than *s* targets, with a mean difference of 0.053 [$F(1,9)=5.55$, $p=0.043$, $\eta^2=0.38$]. [$F(1,9)=20.3$, $p=0.001$, $\eta^2=0.69$]. The effect of flanker axis was not significant [$F(1,9)=2.11$, $p=0.181$, $\eta^2=0.19$], nor was the interaction effect [$F(1,9)=1.09$, $p=0.323$, $\eta^2=0.11$]. These results showed that *s* targets were masked less effectively than *Y* targets, but with no effect of flanker type. This is consistent with

the results seen in Figure 4-4. See Table 4-7 for mean masking magnitudes for each flanker and target axis in Exp. 3C, along with ANOVA and contrast significance values. See Figure D-4 to D-6 (Appendix D) for graphs of masking amounts across flanker and target axes in Exps. 3A-3C.

Exp. 3C			Target axis		
			s	*Y*	Δ (*s* – *Y*)
		MEAN	0.156	0.209	Target axis main effect: **–0.053 ***
Flanker axis	±*s*	0.203	0.192	0.215	Target axis simple effect (flankers ±*s*): --
	±*Y*	0.162	0.120	0.204	Target axis simple effect (flankers ±*Y*): --
	Δ (*s* – *Y*)	Flanker axis main effect: 0.042 n.s.	Flanker axis simple effect (targets *s*): --	Flanker axis simple effect (targets *Y*): --	Interaction: n.s.

Table 4-7. ANOVA table of masking by target and flanker axis in Exp. 3C. Cells weighted equally. n.s:. Not significant; *p<0.05; **p<0.01; ***p<0.001 (Holm adjusted for multiplicity).

4.5 Conclusions

These experiments showed that OSM can occur with targets, distractors, and flankers defined solely by single-axis modulation in the *lsY* cone excitation space. They reveal a pattern of flanker-target similarity tests inconsistent with predictions of the "object-similarity" and

"feature-similarity" models of similarity effects on OSM, and instead suggest masking mediated by the properties of low-level feature-processing neurons.

In all three experiments, OSM was significant for these single-feature targets with a flanker-and-target display duration of 33.3 ms. The targets, flankers, and distractors in this experiment were all designed to match feature-selectivity profiles of V1 luminance selective or "single-opponent" hue selective cells (Johnson et al., 2004), and to minimally excite other populations of feature-selective neurons such as color-, luminance-, or color/luminance-selective "double-opponent" edge-detecting neurons (Johnson et al., 2008). While other studies have investigated the effect of flanker-target luminance relations (Luiga & Bachmann, 2008) or color relations (Gellatly et al., 2006; Huang et al., 2018) on OSM, none has shown masking of either of these as single features of visual objects, nor have any parameterized both flanker and target features to selectively activate low-level feature-processing neurons.

4.5.1 Target-axis, flanker-axis, and similarity effects varied across sub-experiments

In this paradigm, flanker-target similarity is maximized when the target is defined on the same axis as the flankers, as it then shares color with two of the flankers. Conversely, when the target is defined on a different axis from the flankers, it shares color with none. Thus, for these experiments, both "object-similarity" and "feature-similarity" hypotheses predict that masking of "same-axis" targets should always be stronger than masking of "different-axis" targets.

In Exp. 3A, both ±*l* and ±*s* flankers were significantly more effective in masking *l*-defined than *s*-defined targets. In the secondary analysis, both flanker axis and target axis showed significant overall main effects on masking magnitude, but no significant overall interaction. That is, *s*-defined flankers were more effective in masking, while *s*-defined targets were less susceptible to masking, when compared to *l*-defined flankers and targets; however, the

interaction between flanker and target axes showed no significant effect on masking magnitude. Taken together, these results do not universally support a straightforward effect of flanker-target similarity on masking in Exp. 3A.

In Exp. 3B, ±*l* flankers were significantly more effective in masking *l*-defined than *Y*-defined targets, while ±*Y* flankers were not quite significantly more effective in masking *Y*-defined than *l*-defined targets. In the secondary analysis, there was a significant overall interaction effect of flanker axis × target axis on masking magnitude, indicating an overall flanker-target similarity effect on masking. Contrasts testing simple effects showed that both *l* and *Y* targets were masked more effectively by same-axis than different-axis flankers, confirming the similarity effect in this case.

In Exp. 3C, neither ±*s* nor ±*Y* flankers showed significant differences in masking efficacy for same-axis versus different-axis targets. In the secondary analysis, only target axis showed a significant effect on masking, with *Y* targets masked more effectively than *s* targets. The interaction between target type and flanker type was not significant. This is consistent with the results shown in Figure 4-4, which indicated stronger masking for *Y* than *s* targets in both experimental sessions.

Why, in Exp. 3A, might *s*-defined flankers mask more effectively—and *s*-defined targets be less effectively masked—than *l*-defined flankers and targets, regardless of flanker-target similarity? Why, of the three pairs of feature axes tested against each other in these experiments, do only *l* versus *Y* targets and flankers (Exp. 3B) show a significant overall similarity effect on masking? Why do *s* versus *Y* defined flankers and targets in Exp. 3C show neither similarity nor chromaticity-axis effects on masking, instead giving roughly equal masking across conditions? These questions are explored in Chapter 5: General Discussion.

4.5.2 Masking depended on target color in all sub-experiments

Individual target colors showed consistent patterns of masking across the three sub-experiments. "Purple" +*s* and "light" +*Y* targets were masked less than average by all flanker axes across experiments, whereas "lime" –*s* and "dark" –*Y* targets were masked more than average by all flanker axes across all experiments. Masking magnitudes for "green" –*l* and "red" +*l* targets did not significantly differ from average masking in any experiment.

Why, within both the *s* and *Y* target axes, was one color masked more effectively than its opposite? This is particularly curious for masking of same-axis flankers—since flanker colors were mixed ±, the two possible target colors should have been equally similar—or dissimilar—to same-axis flankers. This question is explored in Chapter 5: General Discussion.

CHAPTER 5

GENERAL DISCUSSION

5.1 Summary of results

The three sets of experiments communicated here tested feature-level contributions to object-substitution masking (OSM), using stimuli parameterized in luminance, tilt, and cone-opponent color. They showed three primary results:

1) Masking of luminance-defined tilt was replicated (Exp. 1A; Figure 2-6), and dissociable, feature-level masking of color and tilt were established (Exps. 1B-1C; Figures 2-8 to 2-13).
2) Experiments that modulated flanker-target similarity of color and tilt did not show significant flanker-target similarity effects on masking of either feature (Exps. 1–2):
    a. There were no significant differences in tilt masking between Gaussian versus neutral-tilt Gabor flankers (Exp. 1A; Figure 2-6).
    b. There were no significant differences in color or tilt masking with flankers same versus opposite color and neutral tilt (Exp. 1B; Figures 2-8 to 2-10).
    c. There were no significant differences in color or tilt masking with flankers colored versus grayscale and neutral tilt (Exp. 1C; Figures 2-11 to 2-13).
    d. There were no significant differences in color or tilt masking with flankers mixed versus all-neutral for the task-relevant feature, and all-same for the task-irrelevant feature (Exps. 2A-2B; Figures 3-2 and 3-3).

e. There were no significant differences in color or tilt masking with flankers mixed versus all-opposite for the task-irrelevant feature, and all-neutral for the task-relevant feature (Exps. 2C-2D; Figures 3-4 and 3-5).

3) There were significant flanker-target similarity effects, significant target and flanker chromaticity-axis effects, and significant target-color effects on masking of color and luminance in single-feature paradigms (Exp. 3; Figures 4-2 to 4-4).

5.2 There is a feature-level component in OSM

Object-level masking theories posit that OSM is not affected by neural processing at the feature level, but rather that a fully integrated neural "object" representation is built for the target-and-flankers, only to be completely replaced by a new neural object representation for the flankers only (Enns & Di Lollo, 1997; Goodhew et al., 2013; Moore & Lleras, 2005). Such object-level masking theories predict implicitly that different features of objects should always be equally masked. Mixed masking theories, on the other hand, predict that OSM can disrupt feature-level processing in addition to object-level processing (Gellatly et al., 2006; Huang et al., 2018), and thus that masking of different features can be "asymmetric." In the current Exps. 1B-1C, subjects reported both color and tilt in a four-alternative forced-response recall task, and showed consistently stronger masking of color than of tilt. This asymmetric masking of these two features is incompatible with a purely object-level masking theory, and supports a role for feature-level masking.

Exps. 3A-3C showed evidence of masking of targets defined by a single chromaticity axis in the *lsY* space. In each of these three sub-experiments, a target could represent either (+) or (–) modulation of one of two possible cone-opponent or luminance axes, making these stimuli even "simpler," from a representational standpoint, than the grayscale tilted Gabor targets used

in Exp. 1A and in Goodhew et al. (2015). Masking of these targets—and the feature-axis level effects discussed later—also supports a role for feature-level masking in OSM.

5.3 Flanker-target similarity plays a complex role in masking in these paradigms

The results of Exps. 1 and 2 are inconsistent in part with previous studies of similarity effects on OSM. Unlike in Goodhew et al. (2015), Exp. 1A did not show a significant effect of similar Gabor versus dissimilar Gaussian flankers in masking of grayscale the Gabor's tilt. Exps. 1B-1C did not show significant effects of flanker-target color similarity in masking of a Gabor's color, and Exps. 2A-2D showed no significant effects of flanker-target similarity in either the task-relevant or task-irrelevant feature for masking of color or tilt. Exps. 3A-3C only showed a significant overall flanker-target similarity effect in Exp. 3B (*l* and *Y* targets and flankers); while individual flanker axes showed flanker-target similarity effects in Exp. 3A (*l* and *s* targets and flankers), these effects were opposite in direction, such that ±*s* flankers were *less* effective in masking "similar" *s* targets. Exp. 3C (*s* and *Y* targets and flankers) showed no flanker-target similarity effects. These results are contrary to prior experiments that have shown similarity effects for either the task-relevant (Gellatly et al., 2006; Huang et al., 2018) or task-irrelevant feature (Lleras & Moore, 2003; Moore & Lleras, 2005) in OSM paradigms featuring targets and flankers defined in multiple features.

Methodological differences between the current and previous experiments may have contributed to the discrepancies between results from Exps. 1 and 2 and those from prior studies. First, Exps. 1 and 2 used within-subjects designs, whereas previous experiments used between-subjects designs with 20 or more subjects per experiment. The duration of each experiment here drove the use of within-subjects designs in Exps. 1 and 2: Each subject needed four or more sessions of flicker photometry to generate accurate equiluminant cone-excitation stimuli, and this

meant that each subject required seven or more sessions to complete the full Exp. 1, and eight or more sessions to complete the full Exp. 2.

Second, Exps. 1B-1C and 2A-2D parameterized color and tilt differently from prior studies. The present experiments used oblique-tilted Gabor stimuli parameterized to the receptive-field properties of edge detecting "non-opponent" (luminance-only preferring) and "double-opponent" (color- and sometimes also luminance-preferring) V1 cells. In contrast, prior studies of color and tilt OSM used hard-edged vertical or horizontal bars, luminance-equated to each other but not defined with respect to any particular low-level color axes (Gellatly et al., 2006; Huang et al., 2018). Distinctions between the current and former experiments' stimuli, and how these distinctions may have contributed to discrepancies in results, are detailed below.

5.4 Reconciling Exps. 1 and 2 with similarity effects in prior studies

Color, luminance, and tilt of stimuli in these experiments were parameterized with respect to the receptive-field properties of feature-processing neurons well-characterized by both physiological and psychophysical studies (Chatterjee & Callaway, 2003; Cottaris & De Valois, 1998; Derrington et al., 1984; Johnson et al., 2001, 2008; Mollon & Krauskopf, 1973; Tailby et al., 2008). Stimuli in Exps. 1 and 2 were parameterized with respect to the receptive-field properties of "non-opponent" and "double-opponent" edge-detecting neurons, commonly found in V1 (Johnson et al., 2004, 2008). Stimuli in Exp. 3 were parameterized with respect to the receptive-field properties of luminance-selective and "single-opponent" color-selective, non-edge-detecting neurons, found in both LGN and V1 (Casagrande et al., 2007; Chatterjee & Callaway, 2003; Derrington et al., 1984; Ding & Casagrande, 1997; Johnson et al., 2004, 2008).

In parameterizing stimulus features to these feature-processing neurons' receptive-field properties, the goal was to control for their respective contributions to perception. Matching

stimulus parameters to receptive field properties narrowed the potential range of types of neurons required for representation of a stimulus, and made it easier to predict changes in neural activity from changes in a stimulus. While contributions from appropriate populations of V1 feature-processing neurons were almost certainly not sufficient for target perception in this paradigm, they were likely necessary; thus, failures of feature processing by these neurons could be inferred here from masking. That is, when a target was masked, it could be inferred that such feature-processing neurons did not contribute sufficiently to an accurate representation of the target—at least at the level of conscious recall. This raises several questions. What information about the targets in these experiments might feature-processing neurons have transmitted? How might transmission of that information have been disrupted in object-substitution masking? These questions will be explored in order.

First, in Exps. 1 and 2, stimuli were parameterized with respect to the receptive-field properties of "non-opponent" and "double-opponent" edge-detecting neurons, commonly found in V1 (Johnson et al., 2004, 2008). "Non-opponent" neurons are most selective for luminance-defined, achromatic stimuli, and tend to have band-pass tuning for spatial frequency and tilt (tilt tuning bandwidth roughly 10°–60°). "Double-opponent" neurons have slightly wider-band tuning for spatial frequency and tilt; they are characterized by having cone-opponent responses. Some are most sensitive to isoluminant chromatic edges with little selectivity for grayscale luminance edges, while most respond strongly to either color- or luminance-defined edges (Johnson et al., 2004, 2008).

The spatial-frequency and tilt selectivity properties of these edge-detecting neurons match up well to the "spatial frequency and orientation channels" that underlie the human oriented contrast sensitivity function, originally measured psychophysically via selective

adaptation (Blakemore & Campbell, 1969; Campbell & Kulikowski, 1966). Could spatial-frequency and tilt selectivity of edge-detecting neurons be reflected in feature-similarity effects in OSM? In an experiment using oriented grayscale Gabor targets like those in Exp. 1A, Goodhew et al. (2015) showed that flanker-target relations for both tilt and spatial frequency co-varied with efficacy of masking. Increasing the difference in angle between target and flanker Gabors monotonically decreased masking out to 45°; beyond that, masking was nonsignificant. Changing the flankers from tilted Gabors (at a spatial frequency like the target's) to Gaussian blur dots also made masking nonsignificant in their paradigm (Goodhew et al., 2015).

This effect of flanker-target tilt difference on masking aligns well with psychophysically and physiologically measured orientation tuning of neural edge detectors (Blakemore & Campbell, 1969; Campbell & Kulikowski, 1966; Greenlee & Magnussen, 1988; Johnson et al., 2008; Mazer et al., 2001; Phillips & Wilson, 1984). That these edge detectors' orientation tuning becomes narrower at higher spatial frequencies (Phillips & Wilson, 1984) and higher luminance contrasts (Johnson et al., 2008) may help explain the discrepancy in results between Goodhew et al. (2015) and the present Exp. 1A, which did not show a significant difference in masking between Gabor and Gaussian flankers. Notably, the Gabor targets in Exp. 1A had lower spatial frequency and Michelson contrast (3.0 cycles/degree; 75% contrast) than those in Goodhew et al (2015) (4.0 cycles/degree; 100% contrast). It is possible that because the Exp. 1A Gabors had lower spatial frequency and lower contrast, they may have stimulated a broader range of edge-detecting neurons, and thus been less distinguishable from the lower-spatial-frequency Gaussian-dot flankers. Further experiments are needed to relate flanker-target similarity in tilt masking to the receptive-field properties of the spatial-frequency and orientation selective neurons that subserve edge detection.

Exps. 1B and 1C did not show any significant effect of flanker-target color similarity on masking of either color or tilt. These experiments used Gabor targets modulated in luminance (75% Michelson contrast) and cone-opponent color (with *l* modulation of ±0.05 from the neutral background value of *l*=0.665). This differs from color definition in prior experiments that have investigated the effect of color as either a task-relevant or task-irrelevant feature. Previous experiments for which color was a task-relevant feature showed that flanker-target color dissimilarity affected masking of color, but not of tilt (Gellatly et al., 2006; Huang et al., 2018). Both prior experiments used photometrically luminance-matched color stimuli that were otherwise not specified with respect to specific known color-processing neurons; in one, targets and flankers could be either "red" or "orange," and in the other targets could be "red" or "yellow." These stimuli were also hard-edged shapes with stroke widths of 0.2° to 0.5° and lengths of 0.3° to 1.1°. As such, it is likely that these stimuli activated strongly both single-opponent and double-opponent color-selective neurons, with various chromaticity (and for double-opponent neurons, spatial-frequency) tunings. Because these stimuli likely activated a wide variety of neurons selective for color, tilt, or their conjunction, it would be difficult to attribute masking effects in these paradigms to disruption of processing at any one level. Likewise, it would be difficult to define or separate neural "color" and "tilt" signals, or their contributions to flanker-target similarity, beyond the level of identity.

Because the stimuli in the current experiments are more narrowly parameterized with respect to receptive-field properties, it is possible to speculate about relations between feature-processing neurons' properties, reentrant processing, and OSM in this paradigm. Exps. 1B-1C and Exps. 2A-2D showed masking of both color and tilt, with color masking comparatively stronger, and with no significant effects of flanker-target color similarity on masking of either

feature in either the two-feature report (Exps. 1B-1C) or the single-feature report paradigm (Exps. 2A-2D). This fails to support the object-similarity model, in which dissimilarity of any feature would be predicted to reduce masking (Goodhew et al., 2015; Moore & Lleras, 2005). It also fails to support the feature-similarity model, in which dissimilarity for a given feature would be predicted to reduce masking of that feature only (Gellatly et al., 2006; Huang et al., 2018).

5.5 Ventral and dorsal stream processing and the "dynamic blackboard" model

The stimuli used in Exps. 1B-1C and Exps. 2A-2D were designed to most selectively activate edge-detecting "double-opponent" neurons sensitive to both color and luminance contrast, along with similar edge-detecting "non-opponent" neurons selective for luminance contrast only. Might feedforward form signals from these populations be redundant? And might reentrant signals for form be faster than those for color? This latter point is consistent with the dynamics of the temporally faster magnocellular-dominated dorsal pathway (Foxe & Simpson, 2002; Merigan & Maunsell, 1993), which has been shown to play a role in form processing (Bar, 2003; Tapia & Breitmeyer, 2011). Dorsal areas such as MT have been shown to send modulatory feedback signals to V1 within 10 ms from initial V1 activation (Hupé et al., 2001). This forms the basis of the "dynamic blackboard" theory of processing in V1 and V2, in which fast feedback signals from the magnocellular pathway are proposed to influence the tuning of V1 and V2 neurons (Bullier, 2001).

Predictions of the "dynamic blackboard" theory have been corroborated in studies of OSM, which have shown increased masking when magnocellular inputs to the dorsal stream are "saturated" with pulsed-pedestal luminance signals (Goodhew et al., 2014). Recently, a more specific neural mechanism for this has been proposed: Dorsal-stream activity is thought to rapidly encode coarse representations of objects based on topological properties, and transmit

these representations as “templates” to ventral-stream areas for confirmation (Wang et al., 2020). In OSM paradigms, flanker-target topological dissimilarity has been shown to reduce masking of target color, tilt, and topology features; this has in turn been interpreted as evidence that these “template” representations from the dorsal stream assist in neural object representation and individuation (Huang et al., 2018).

Integrating these findings and theories, a clearer picture of a reentrant processing model begins to emerge. During normal vision, when an object appears the magnocellular-driven dorsal stream rapidly generates a coarse “template” representation, which is transmitted to ventral-stream areas such as V1 (Bullier, 2001; Goodhew et al., 2014; Huang et al., 2018). This template signal modifies the activity of these lower-level neurons, facilitating signals consistent with the template and perhaps suppressing signals inconsistent with it. As this template is generated, slower parvocellular- and koniocellular-driven signals for color and finer form are processed in V1 and transmitted up the ventral processing hierarchy, likely with some crossover into the dorsal stream (Perry & Fallah, 2014). Successive ventral and dorsal regions send their own recurrent signals to V1, with each arriving in sequence and reflecting some more integrated level of feature or object processing. Like the initial template signal from the dorsal stream, these recurrent signals each modify feedforward signaling in their postsynaptic, lower-level neurons. Throughout this process, recurrent signals can “match” with feedforward signals; these “matches” serve to confirm feature- or object-level neural representations, making them available for conscious perception (Di Lollo, 2010; Di Lollo et al., 2000).

5.6 Questions on the feature specificity of reentrant processing

This account of reentrant processing, dorsal-ventral integration, and OSM is elegant, and it provides a framework for asking new questions about more specific neural processes involved

in OSM, and in iterative reentrant processing more generally: What are the reentrant signals like? What types of neurons at each level do they project to and from? Are these signals separated by specific features at all? If so, how?

Prior studies have shown evidence that, for targets with multiple types of features, flanker-target similarity effects for one type of feature do not "cross over" to affect masking of another type of feature, with the exception of topological features (Gellatly et al., 2006; Huang et al., 2018). This would be consistent with at least some reentrant signals being separated by feature. Further evidence of feature separation in reentrant signals comes from studies that show strong correlations between the receptive-field properties of pre-synaptic (higher-level) neurons and those of the post-synaptic (lower-level) neurons to which they send recurrent projections (Marques et al., 2018; Shmuel et al., 2005).

5.7 Proposed modifications to reentrant-processing theory, and further questions

Returning to Exps. 1 and 2, how might their findings—that color was masked more strongly than tilt, and that flanker-target similarity for neither feature showed significant effects on masking of either—now be addressed? In a flanker-offset-delayed trial, it is likely that the first target-representing recurrent signal to reach V1 would be the dorsal "template" signal. This template signal would be more likely to be involved in confirmation of the luminance-defined tilt representation—perhaps at the level of the non-opponent luminance-only neurons, perhaps at the level of the double-opponent color-and-luminance selective neurons, or perhaps both. This signal, arriving first, would be more likely to be "confirmed" by the residual tilt signal from the initial feedforward sweep. A recurrent target color-representing signal from higher levels of ventral processing, on the other hand, would likely arrive later, after the feedforward sweep representing the new flankers-only image had "caught up." Thus, this later recurrent color signal

would be unable to confirm the target color, and instead the confirmed neural color representation would be for the flankers only.

Since color-and-luminance double-opponent neurons have selectivity for both chromatic contrast and grayscale contrast, it is possible that they receive feedback from some higher-level neurons that are selective for color and some that are not. If this is the case, then any flankers with appropriate luminance contrast could mask their color. This could explain the lack of flanker-target color similarity effects on color masking in Exps. 1B-1C and 2A. Similarly, it is possible that the tilt discrepancy between targets and "neutral-tilt" flankers in Exp. 2B (22.5°) was insufficient to selectively activate different tilt-processing neurons. This could have led to the creation of very similar "templates" for target-and-flankers and target-only even in these "flankers-neutral" conditions, and thus no expected reduction of masking due to the flanker-target tilt similarity. Experiments that parameterize target color and tilt differently—for example, with isoluminant color stimuli designed to selectively activate color-only selective double-opponent neurons—could be used to test further hypotheses about reentrant processing and OSM for color and tilt features.

In Exps. 3A-3C, stimuli were parameterized according to the receptive-field properties of spatially low-pass neurons selective for single features: Either luminance *Y* or cone-opponent, isoluminant color *l* or *s*. Neurons with such receptive field properties are common in V1 and LGN (Derrington & Lennie, 1984; Johnson et al., 2008). With mixed-modulation flankers (like those used in Exps. 2A-2D), these spatially low-pass, single-feature targets were effectively masked. Flanker-target similarity appeared to affect masking only in Exp. 3B, in which targets and flankers were modulated either in *l* or *Y* axes. In Exp. 3A, *s*-defined flankers were more effective at masking, and *s*-defined targets were masked less effectively—even when flankers

were defined on the ±*l* axis, and were therefore more unlike their *s* target. In fact, "purple" +*s* targets were masked significantly less than average by both types of flanker in Exps. 3A and 3C. Similarly, "light" +*Y* targets were masked less than average for two flanker conditions in Exps. 3B and 3C, while "dark" –*Y* targets were masked more than average for the other two flanker conditions.

Returning to the role of signal speed in reentrant processing, the inefficacy of masking of *s* targets, and particularly "purple" +*s* ones, fits well. S-cone signals are transmitted significantly slower than opponent L- and M-cone signals (Cottaris & De Valois, 1998; Johnson et al., 2010; Pietersen et al., 2014; Tailby et al., 2008), and this is reflected in psychophysical phenomena (Lee et al., 2009; McKeefry et al., 2003; Mollon & Krauskopf, 1973; Stromeyer et al., 1991), including the apparent "lag" of the blue half of a moving blue-red bipartite bar (Blake et al., 2008). In this paradigm, the slower transmission of S-cone signals leads their initial feedforward signal to be relatively delayed, perhaps until after the critical period for masking. There is a similar asymmetry in transmission speeds for –*Y* luminance decrements versus +*Y* increments: Luminance increment signals through the "ON" pathway are transmitted slower than luminance decrement signals through the "OFF" pathway (Komban et al., 2011; Rekauzke et al., 2016). Thus, like "purple" +*s* signals, "light" +*Y* signals would be expected to be delayed, and perhaps to arrive after the critical period for masking via OSM. Further experiments are needed to test these hypotheses relating signal speed, feedforward-feedback interactions, and OSM.

5.8 Conclusions

The experiments communicated here showed evidence of feature-level masking for color and tilt in an OSM paradigm, using stimuli parameterized to match receptive-field properties of feature-processing neurons in V1 and LGN. The first two sets of experiments did not show

significant evidence of object-level or feature-level similarity effects on masking of either color or tilt. The third set of experiments showed evidence of target and flanker chromaticity-axis effects on masking of cone-opponent *l* and *s* color representations, and flanker-target similarity effects on masking of cone-opponent *l* color and luminance *Y* representations. These findings are related to the stimulus parameters used, and modifications to the current theory of OSM and of iterative reentrant processing, along with experiments to test new predictions, are suggested. Taken together, the findings of this dissertation suggest an expanded role of feature-level effects in OSM, and a path toward better understanding of the role of feedback in perceptual processing.

BIBLIOGRAPHY

Alpern, M. (1953). Metacontrast. *Journal of the Optical Society of America*, *43*(8), 648–657.

Amano, K., Wandell, B. A., & Dumoulin, S. O. (2009). Visual field maps, population receptive field sizes, and visual field coverage in the human MT complex. *Journal of Neurophysiology*, *102*, 2704–2718. https://doi.org/10.1152/jn.00102.2009

Andersen, R. A., Snowden, R. J., Treue, S., & Graziano, M. (1990). Hierarchical processing of motion in the visual cortex of monkey. *Cold Spring Harbor Symposium on Computational Biology*, *55*, 741–748.

Angelucci, A., Levitt, J. B., Walton, E. J. S., Hupé, J.-M., Bullier, J., & Lund, J. S. (2002). Circuits for Local and Global Signal Integration in Primary Visual Cortex. *Journal of Neuroscience*, *22*(19), 8633–8646. https://doi.org/10.1523/JNEUROSCI.22-19-08633.2002

Anstis, S. M., & Cavanagh, P. (1983). A minimum motion technique for judging equiluminance. In J. D. Mollon & L. T. Sharpe (Eds.), *Colour Vision: Psychophysics and Physiology* (pp. 66–77). Academic Press.

Bachmann, T., & Allik, J. (1976). Integration and interruption in the masking of form by form. *Perception*, *5*(1), 79–97.

Bar, M. (2003). A cortical mechanism for triggering top-down facilitation in visual object recognition. *J Cogn Neurosci*, *15*(4), 600–609. https://doi.org/10.1162/089892903321662976

Becker, H. G. T., Haarmeier, T., Tatagiba, M., & Gharabaghi, A. (2013). Electrical stimulation of the human homolog of the medial superior temporal area induces visual motion blindness. *Journal of Neurophysiology*, *33*(46), 18288–18297. https://doi.org/10.1523/JNEUROSCI.0556-13.2013

Bischof, W. F., & Di Lollo, V. (1995). Motion and metacontrast with simultaneous onset of stimuli. *Journal of the Optical Society of America A*, *12*(8), 1623–1636. https://doi.org/10.1364/josaa.12.001623

Blake, Z., Land, T., & Mollon, J. (2008). Relative latencies of cone signals measured by a moving vernier task. *Journal of Vision*, *8*(16), 16. https://doi.org/10.1167/8.16.16

Blakemore, C., & Campbell, F. W. (1969). On the existence of neurones in the human visual system selectively sensitive to the orientation and size of retinal images. *Journal of Physiology*, *203*(1), 237–260.

Boehler, C. N., Schoenfeld, M. A., Heinze, H. J., & Hopf, J. M. (2008). Rapid recurrent processing gates awareness in primary visual cortex. *Proceedings of the National Academy of Sciences of the United States of America*, *105*(25), 8742–8747. https://doi.org/10.1073/pnas.0801999105

Bouvier, S., & Treisman, A. (2010). Visual feature binding requires reentry. *Psychological Science*, *21*(2), 200–204. https://doi.org/10.1177/0956797609357858

Boycott, B. B., & Dowling, J. E. (1969). Organization of the primate retina: Light microscopy. *Philosophical Transactions of the Royal Society of London, Series B: Biological Sciences*, *255*(799), 109–184.

Boynton, R. M. (1986). A system of photometry and colorimetry based on cone excitations. *Color Research and Application*, *11*(4), 244–252.

Brainard, D. H. (1997). The Psychophysics Toolbox. *Spatial Vision*, *10*(4), 433–436. https://doi.org/10.1163/156856897X00357

Brainard, D., & Pelli, D. (2022). *Psychtoolbox-3*. http://psychtoolbox.org/

Breitmeyer, B. G., & Ganz, L. (1976). Implications of sustained and transient channels for theories of visual pattern masking, saccadic suppression, and information processing. *Psychological Review*, *83*(1), 83–118. https://doi.org/10.4324/9781351156288-14

Britten, K. H., & Van Wezel, R. J. A. (1998). Electrical microstimulation of cortical area MST biases heading perception in monkeys. *Nature Neuroscience*, *1*(1), 59–63. https://doi.org/10.1038/259

Bullier, J. (2001). Integrated model of visual processing. *Brain Research Reviews*, *36*(2–3), 96–107. https://doi.org/10.1016/S0165-0173(01)00085-6

Campbell, F. W., & Kulikowski, J. J. (1966). Orientational selectivity of the human visual system. *The Journal of Physiology*, *187*(2), 437–445. https://doi.org/10.1113/jphysiol.1966.sp008101

Cao, D., Lee, B. B., & Sun, H. (2010). Combination of rod and cone inputs in parasol ganglion cells of the magnocellular pathway. *Journal of Vision*, *10*(11), 4–4. https://doi.org/10.1167/10.11.4

Casagrande, V. A., Yazar, F., Jones, K. D., & Ding, Y. (2007). The morphology of the koniocellular axon pathway in the macaque monkey. *Cerebral Cortex*, *17*, 2334–2345. https://doi.org/10.1093/cercor/bhl142

Chatterjee, S., & Callaway, E. M. (2003). Parallel colour-opponent pathways to primary visual cortex. *Nature*, *426*(6967), 668–671. https://doi.org/10.1038/nature02167

Cohen, A., & Rafal, R. D. (1991). Attention and feature integration: Illusory conjunctions in a patient with a parietal lobe lesion. *Psychological Science*, *2*(2), 106–110.

Cottaris, N. P., & De Valois, R. L. (1998). Temporal dynamics of chromatic tuning in macaque primary visual cortex. *Nature*, *395*(6705), 896–900. https://doi.org/10.1038/27666

Dacey, D. M., & Lee, B. B. (1994). The "blue-on" opponent pathway in primate retina originates from a distinct bistratified ganglion cell type. *Nature*, *367*(February).

Derrington, A. M., Krauskopft, J., & Lennie, P. (1984). Chromatic mechanisms in lateral geniculate nucleus of macaque. *Journal of Physiology*, *357*, 241–265.

Derrington, A. M., & Lennie, P. (1984). Spatial and temporal contrast sensitivities of neurones in lateral geniculate nucleus of macaque. *The Journal of Physiology*, *357*(1), 219–240. https://doi.org/10.1113/jphysiol.1984.sp015498

Desimone, R., Albright, T., Gross, C., & Bruce, C. (1984). Stimulus-selective properties of inferior temporal neurons in the macaque. *Journal of Neuroscience*, *4*(8), 2051–2062. https://doi.org/10.1523/JNEUROSCI.04-08-02051.1984

Desimone, R., & Schein, S. J. (1987). Visual properties of neurons in area V4 of the macaque: Sensitivity to stimulus form. *Journal of Neurophysiology*, *57*(3), 835–868. https://doi.org/10.1152/jn.1987.57.3.835

Di Lollo, V. (1980). Temporal integration in visual memory. *Journal of Experimental Psychology: General*, *109*(1), 75–97.

Di Lollo, V. (2010). Iterative reentrant processing: A conceptual framework for perception and cognition (The binding problem? No worries, mate). In V. Coltheart (Ed.), *Tutorials in Visual Cognition* (pp. 9–42). Psychology Press.

Di Lollo, V. (2018). Attention is a sterile concept; iterative reentry is a fertile substitute. *Consciousness and Cognition*, *64*(February), 45–49. https://doi.org/10.1016/j.concog.2018.02.005

Di Lollo, V., Bischof, W. F., & Dixon, P. (1993). Stimulus-onset asynchrony is not necessary for motion perception or metacontrast masking. *Psychological Science*, *4*(4), 260–263.

Di Lollo, V., Enns, J. T., & Rensink, R. A. (2000). Competition for consciousness among visual events: The psychophysics of reentrant visual processes. *Journal of Experimental Psychology: General*, *129*(4), 481–507.

Ding, Y., & Casagrande, V. A. (1997). The distribution and morphology of LGN K pathway axons within the layers and CO blobs of owl monkey VI. *Visual Neuroscience*, *14*, 691–704. https://doi.org/10.1017/S0952523800012657

Enns, J. T., & Di Lollo, V. (1997). Object substitution: A new form of masking in unattended visual locations. *Psychological Science*, *8*(2), 135–139. https://doi.org/10.1111/j.1467-9639.1993.tb00256.x

Fahrenfort, J. J., Scholte, H. S., & Lamme, V. A. F. (2008). The spatiotemporal profile of cortical processing leading up to visual perception. *Journal of Vision*, *8*(1), 12–12. https://doi.org/10.1167/8.1.12

Field, D. T., Biagi, N., & Inman, L. A. (2020). The role of the ventral intraparietal area (VIP/pVIP) in the perception of object-motion and self-motion. *NeuroImage*, *213*, 116679. https://doi.org/10.1016/j.neuroimage.2020.116679

Foxe, J. J., & Simpson, G. V. (2002). Flow of activation from V1 to frontal cortex in humans: A framework for defining "early" visual processing. *Experimental Brain Research*, *142*(1), 139–150. https://doi.org/10.1007/s00221-001-0906-7

Freeman, J., Ziemba, C. M., Heeger, D. J., Simoncelli, E. P., & Movshon, J. A. (2013). A functional and perceptual signature of the second visual area in primates. *Nature Neuroscience*, *16*(7), 974–981. https://doi.org/10.1038/nn.3402

Friedman-Hill, S. R., Robertson, L. C., & Treisman, A. (1995). Parietal contributions to visual feature binding: Evidence from a patient with bilateral lesions. *Science*, *269*(5225), 853–855.

Gegenfurtner, K. R., Kiper, D. C., & Fenstemaker, S. B. (1996). Processing of color, form, and motion in macaque area V2. *Visual Neuroscience*, *13*(1), 161–172. https://doi.org/10.1017/S0952523800007203

Gellatly, A., Pilling, M., Cole, G., & Skarratt, P. (2006). What is being masked in object substitution masking? *Journal of Experimental Psychology: Human Perception and Performance*, *32*(6), 1422–1435. https://doi.org/10.1037/0096-1523.32.6.1422

Goodhew, S. C. (2017). What have we learned from two decades of object-substitution masking? Time to update: Object individuation prevails over substitution. *Journal of Experimental Psychology: Human Perception and Performance*, *43*(6), 1249–1262.

Goodhew, S. C., Boal, H. L., Edwards, M., & Author, C. (2014). A magnocellular contribution to conscious perception via temporal object segmentation. *Journal of Experimental Psychology: Human Perception and Performance*, *40*(3), 948–959.

Goodhew, S. C., Dux, P. E., Lipp, O. V, & Visser, T. A. W. (2012). Understanding recovery from object substitution masking. *Cognition*, *122*(3), 405–415. https://doi.org/10.1016/j.cognition.2011.11.010

Goodhew, S. C., Edwards, M., Boal, H. L., & Bell, J. (2015). Two objects or one? Similarity rather than complexity determines objecthood when resolving dynamic input. *Journal of Experimental Psychology: Human Perception and Performance*, *41*(1), 102–110. https://doi.org/10.1037/xhp0000022

Goodhew, S. C., Pratt, J., Dux, P. E., & Ferber, S. (2013). Substituting objects from consciousness: A review of object substitution masking. *Psychonomic Bulletin and Review*, *20*(5), 859–877. https://doi.org/10.3758/s13423-013-0400-9

Greenlee, M. W., & Magnussen, S. (1988). Interactions among spatial frequency and orientation channels adapted concurrently. *Vision Research*, *28*(12), 1303–1310. https://doi.org/10.1016/0042-6989(88)90061-2

Grill-Spector, K., Kourtzi, Z., & Kanwisher, N. (2001). The lateral occipital complex and its role in object recognition. *Vision Research*, *41*(10–11), 1409–1422. https://doi.org/10.1016/S0042-6989(01)00073-6

Gross, C. G., Rocha-Miranda, C. E., & Bender, D. B. (1972). Visual properties of neurons in inferotemporal cortex of the macaque. *Journal of Neurophysiology*, *35*(1), 96–111. https://doi.org/10.1152/JN.1972.35.1.96

Guest, D., Gellatly, A., & Pilling, M. (2011). The effect of spatial competition between object-level representations of target and mask on object substitution masking. *Attention, Perception, and Psychophysics*, *73*(8), 2528–2541. https://doi.org/10.3758/s13414-011-0196-5

Hanazawa, A., & Komatsu, H. (2001). Influence of the direction of elemental luminance gradients on the responses of V4 cells to textured surfaces. *Journal of Neuroscience*, *21*(12), 4490–4497. https://doi.org/10.1523/JNEUROSCI.21-12-04490.2001

Harada, T., Goda, N., Ogawa, T., Ito, M., Toyoda, H., Sadato, N., & Komatsu, H. (2009). Distribution of colour-selective activity in the monkey inferior temporal cortex revealed by functional magnetic resonance imaging. *European Journal of Neuroscience*, *30*(10), 1960–1970. https://doi.org/10.1111/j.1460-9568.2009.06995.x

Harris, J. A., Donohue, S. E., Schoenfeld, M. A., Hopf, J.-M., Heinze, H.-J., & Woldorff, M. G. (2016). Reward-associated features capture attention in the absence of awareness: Evidence from object-substitution masking. *NeuroImage*, *137*, 116–123. https://doi.org/10.1016/j.neuroimage.2016.05.010

Harth, E., Unnikrishnan, K. P., & Pandya, A. S. (1987). The inversion of sensory processing by feedback pathways: A model of visual cognitive functions. *Science*, *237*(4811), 184–187. https://doi.org/10.1126/science.3603015

Hei, X., Stoelzel, C. R., Zhuang, J., Bereshpolova, Y., Huff, J. M., Alonso, J.-M., & Swadlow, H. A. (2014). Directional selective neurons in the awake LGN: Response properties and modulation by brain state. *J Neurophysiol*, *112*, 362–373. https://doi.org/10.1152/jn.00121.2014.-Directionally

Hirose, N., & Osaka, N. (2010). Asymmetry in Object Substitution Masking Occurs Relative to the Direction of Spatial Attention Shift. *Journal of Experimental Psychology: Human Perception and Performance*, *36*(1), 25–37. https://doi.org/10.1037/a0017165

Huang, Y., He, L., Wang, W., Meng, Q., Zhou, T., & Chen, L. (2018). What determines the object-level visual masking: The bottom-up role of topological change. *Journal of Vision*, *18*(1), 1–14. https://doi.org/10.1167/18.1.3

Hubel, D. H., & Wiesel, T. N. (1959). Receptive fields of single neurones in the cat's striate cortex. *The Journal of Physiology*, *148*(3), 574–591. https://doi.org/10.1113/jphysiol.1959.sp006308

Hubel, D. H., & Wiesel, T. N. (1962). Receptive fields, binocular interaction and functional architecture in the cat's visual cortex. In *Journal of Physiology* (Vol. 160).

Hubel, D. H., & Wiesel, T. N. (1968). Receptive fields and functional architecture of monkey striate cortex. In *Journal of PHysiology* (Vol. 195).

Hupé, J. M., James, A. C., Girard, P., Lomber, S. G., Payne, B. R., & Bullier, J. (2001). Feedback connections act on the early part of the responses in monkey visual cortex. *Journal of Neurophysiology*, *85*(1), 134–145. https://doi.org/10.1152/jn.2001.85.1.134

Hupe, J. M., James, A. C., Payne, B. R., Lomber, S. G., Girard, P., & Bullier, J. (1998). Cortical feedback improves discrimination between figure and background in V1, V2 and V3 neurons. *Nature*, *394*, 784–787.

Ichida, J. M., Schwabe, L., Bressloff, P. C., & Angelucci, A. (2007). Response Facilitation From the "Suppressive" Receptive Field Surround of Macaque V1 Neurons. *Journal of Neurophysiology*, *98*(4), 2168–2181. https://doi.org/10.1152/jn.00298.2007

Johnson, E. N., Hawken, M. J., & Shapley, R. (2001). The spatial transformation of color in the primary visual cortex of the macaque monkey. *Nature Neuroscience*, *4*(4). https://doi.org/10.1038/86061

Johnson, E. N., Hawken, M. J., & Shapley, R. (2004). Cone inputs in macaque primary visual cortex. *Journal of Neurophysiology*, *91*(6). https://doi.org/10.1152/jn.01043.2003

Johnson, E. N., Hawken, M. J., & Shapley, R. (2008). The orientation selectivity of color-responsive neurons in macaque V1. *The Journal of Neuroscience*, *28*(32), 8096–8106. https://doi.org/10.1523/JNEUROSCI.1404-08.2008

Johnson, E. N., Hooser, S. D. V., & Fitzpatrick, D. (2010). The Representation of S-Cone Signals in Primary Visual Cortex. *Journal of Neuroscience*, *30*(31), 10337–10350. https://doi.org/10.1523/JNEUROSCI.1428-10.2010

Kahan, T. A., & Enns, J. T. (2010). Object trimming: When masking dots alter rather than replace target representations. *Journal of Experimental Psychology: Human Perception and Performance*, *36*(1), 88–102. https://doi.org/10.1037/a0016466

Kahan, T. A., & Lichtman, A. S. (2006). Looking at object-substitution masking in depth and motion: Toward a two-object theory of object substitution. *Perception and Psychophysics*, *68*(3), 437–446. https://doi.org/10.3758/BF03193688

Kahneman, D. (1967). An onset-onset law for one case of apparent motion and metacontrast. *Perception and Psychophysics*, *2*(12), 577–584.

Kahneman, D. (1968). Method, findings, and theory in studies of visual masking. *Psychological Bulletin*, *70*(6 PART 1), 404–425. https://doi.org/10.1037/h0026731

Kahneman, D., Treisman, A., & Gibbs, B. J. (1992). The reviewing of object files: Object-specific integration of information. *Cognitive Psychology*, *24*(2), 175–219.

Koivisto, M., & Silvanto, J. (2011). Visual feature binding: The critical time windows of V1/V2 and parietal activity. *Neuroimage, 59*(2): 1608-1614. https://doi.org/10.1016/j.neuroimage.2011.08.089

Kolb, H., & Dekorver, L. (1991). Midget ganglion cells of the parafovea of the human retina: A study by electron microscopy and serial section reconstructions. *Journal of Comparative Neurology*, *303*(4), 617–636. https://doi.org/10.1002/CNE.903030408

Komban, S. J., Alonso, J.-M., & Zaidi, Q. (2011). Darks are processed faster than lights. *Journal of Neuroscience*, *31*(23), 8654–8658. https://doi.org/10.1523/JNEUROSCI.0504-11.2011

Konietschke, F., Bathke, A.C., Hothorn, L.A., Brunner, E. (2010). Testing and estimation of purely nonparametric effects in repeated measures designs. *Computational Statistics and Data Analysis, 54*(8): 1895-1905.

Konietschke, F., Hothorn, L.A., Brunner, E. (2012). Rank-based multiple test procedures and simultaneous confidence intervals. *Electronic Journal of Statistics, 6*: 738-759.

Konietschke, F., Noguchi, K., & Rubarth, K. (2019). *nparcomp: Multiple Comparisons and Simultaneous Confidence Intervals* (3.0) [Computer software]. https://CRAN.R-project.org/package=nparcomp

Konietschke, F., Placzek, M., Schaarschmidt, F., & Hothorn, L. A. (2015). nparcomp: An R software package for nonparametric multiple comparisons and simultaneous confidence intervals. *Journal of Statistical Software*, *64*, 1–17. https://doi.org/10.18637/jss.v064.i09

Kulli, J. C. (1967). *Metacontrast and evoked potentials: A possible neural substrate*. Harvard University.

Lachica, E. A., & Casagrande, V. A. (1992). Direct W-like geniculate projections to the cytochrome oxidase (CO) blobs in primate visual cortex: Axon morphology. *The Journal of Comparative Neurology*, *319*, 141–158.

Lamme, V. A. F. (2000). Neural Mechanisms of Visual Awareness: A Linking Proposition. In *Brain and Mind* (Vol. 1, pp. 385–406).

Lamme, V. A. F., Zipser, K., & Spekreijse, H. (1998). Figure-ground activity in primary visual cortex is suppressed by anesthesia. *Proceedings of the National Academy of Sciences*, *95*, 3263–3268.

Lee, R. J., Mollon, J. D., Zaidi, Q., & Smithson, H. E. (2009). Latency characteristics of the short-wavelength-sensitive cones and their associated pathways. *Journal of Vision*, *9*(12), 5. https://doi.org/10.1167/9.12.5

Lennie, P., Krauskopf, J., & Sclar, G. (1990). Chromatic mechanisms in striate cortex of macaque. *The Journal of Neuroscience*, *10*(2), 649–669.

Lenth, R. V., Buerkner, P., Herve, M., Love, J., Miguez, F., Riebl, H., & Singmann, H. (2022). *emmeans: Estimated Marginal Means, aka Least-Squares Means* (1.7.5) [Computer software]. https://CRAN.R-project.org/package=emmeans

Lleras, A., & Enns, J. T. (2004). Negative compatibility or object updating? A cautionary tale of mask-dependent priming. *Journal of Experimental Psychology: General*, *133*(4), 475–493. https://doi.org/10.1037/0096-3445.133.4.475

Lleras, A., & Moore, C. M. (2003). When the target becomes the mask: Using apparent motion to isolate the object-level component of object substitution masking. *Journal of Experimental Psychology: Human Perception and Performance*, *29*(1), 106–120. https://doi.org/10.1037/0096-1523.29.1.106

Lueck, C. J., Zeki, S. M., Friston, K. J., Deiber, M.-P., Cope, P., Cunningham, V. J., Lammertsma, A. A., Kennard, C., & Frackowiak, R. S. J. (1989). The colour centre in the cerebral cortex of man. *Nature*, *340*, 386–389.

Luiga, I., & Bachmann, T. (2008). Luminance processing in object substitution masking. *Vision Research*, *48*(7), 937–945. https://doi.org/10.1016/j.visres.2008.01.001

Marques, T., Nguyen, J., Fioreze, G., & Petreanu, L. (2018). The functional organization of cortical feedback inputs to primary visual cortex. *Nature Neuroscience*, *21*(5), 757–764. https://doi.org/10.1038/S41593-018-0135-Z

Martin, P. R., Blessing, E. M., Buzás, P., Szmajda, B. A., & Forte, J. D. (2011). Transmission of colour and acuity signals by parvocellular cells in marmoset monkeys. *The Journal of Physiology*, *589*(11), 2795–2812. https://doi.org/10.1113/JPHYSIOL.2010.194076

Martin, P. R., White, A. J. R., Goodchild, A. K., Wilder, H. D., & Sefton, A. E. (1997). Evidence that blue-on cells are part of the third geniculocortical pathway in primates. *European Journal of Neuroscience*, *9*, 1536–1541. https://doi.org/10.1111/j.1460-9568.1997.tb01509.x

MathWorks. (2022). *MATLAB R2018a*. https://www.mathworks.com/products/matlab.html

Mazer, J. A., Vinje, W. E., McDermott, J., Schiller, P. H., & Gallant, J. L. (2001). *Spatial frequency and orientation tuning dynamics in area V1* (Vol. 99, Issue 3, pp. 1645–1650). www.pnas.orgcgidoi10.1073pnas.022638499

McKeefry, D. J., Parry, N. R. A., & Murray, I. J. (2003). Simple Reaction Times in Color Space: The Influence of Chromaticity, Contrast, and Cone Opponency. *Investigative*

Ophthalmology & Visual Science, *44*(5), 2267–2276. https://doi.org/10.1167/iovs.02-0772

Mckeefry, D. J., & Zeki, S. M. (1997). The position and topography of the human colour centre as revealed by functional magnetic resonance imaging. In *Brain* (Vol. 120).

Merigan, W. H., & Maunsell, J. H. (1993). How parallel are the primate visual pathways? *Annual Review of Neuroscience*, *16*, 369–402. https://doi.org/10.1146/annurev.ne.16.030193.002101

Merigan, W. H., Nealey, T. A., & Maunsell, J. H. R. (1993). Visual effects of lesions of cortical area V2 in macaques. *Journal of Neuroscience*, *13*(7), 3180–3191. https://doi.org/10.1523/JNEUROSCI.13-07-03180.1993

Mishkin, M., Ungerleider, L. G., & Macko, K. A. (1983). Object vision and spatial vision: Two cortical pathways. *Trends in Neuroscience*, *6*, 414–417.

Mollon, J. D., & Krauskopf, J. (1973). Reaction time as a measure of the temporal response properties of individual colour mechanisms. *Vision Research*, *13*(1), 27–40. https://doi.org/10.1016/0042-6989(73)90162-4

Moore, C. M., & Lleras, A. (2005). On the role of object representations in substitution masking. *Journal of Experimental Psychology: Human Perception and Performance*, *31*(6), 1171–1180. https://doi.org/10.1037/0096-1523.31.6.1171

Neill, W. T., Hutchison, K. A., & Graves, D. F. (2002). Masking by object substitution: Dissociation of masking and cuing effects. *Journal of Experiment Psychology: Human Perception and Performance*, *28*(3), 682–694. https://doi.org/10.1037/0096-1523.28.3.682

Noguchi, K., Abel, R.S., Marmolejo-Ramos, F., Konietschke, F. (2020). Nonparametric multiple comparisons. Behavioral Research Methods, 52(2): 489-502.

Nunez, V., Gordon, J., & Shapley, R. M. (2021). A multiplicity of color-responsive cortical mechanisms revealed by the dynamics of cVEPs. *Vision Research*, *188*, 234–245. https://doi.org/10.1016/j.visres.2021.07.017

Pasupathy, A., & Connor, C. E. (1999). Responses to contour features in macaque area V4. *Journal of Neurophysiology*, *82*(5), 2490–2502. https://doi.org/10.1152/JN.1999.82.5.2490

Patterson, S. S., Neitz, M., & Neitz, J. (2019). Reconciling color vision models with midget ganglion cell receptive fields. *Frontiers in Neuroscience*, *13*(865), 1–12. https://doi.org/10.3389/fnins.2019.00865

Perry, C. J., & Fallah, M. (2014). Feature integration and object representations along the dorsal stream visual hierarchy. *Frontiers in Computational Neuroscience*, *0*(AUG), 84. https://doi.org/10.3389/FNCOM.2014.00084

Phillips, G. C., & Wilson, H. R. (1984). Orientation bandwidths of spatial mechanisms measured by masking. *JOSA A*, *1*(2), 226–232. https://doi.org/10.1364/JOSAA.1.000226

Pietersen, A. N. J., Cheong, S. K., Solomon, S. G., Tailby, C., & Martin, P. R. (2014). Temporal response properties of koniocellular (blue-on and blue-off) cells in marmoset lateral geniculate nucleus. *Journal of Neurophysiology*, *112*(6), 1421–1438. https://doi.org/10.1152/jn.00077.2014

R Core Team. (2022). *R: A language and environment for statistical computing.* R Foundation for Statistical Computing. https://www.R-project.org/

Rekauzke, S., Nortmann, N., Staadt, R., Hock, H. S., Schöner, G., & Jancke, D. (2016). Temporal Asymmetry in Dark–Bright Processing Initiates Propagating Activity across Primary Visual Cortex. *Journal of Neuroscience*, *36*(6), 1902–1913. https://doi.org/10.1523/JNEUROSCI.3235-15.2016

Ringach, D. L., Hawken, M. J., & Shapley, R. (1997). Dynamics of orientation tuning in macaque primary visual cortex. *Nature*, *387*(6630), 281–284.

Robertson, L., Treisman, A., Friedman-Hill, S., & Grabowecky, M. (1997). The interaction of spatial and object pathways: Evidence from Balint's syndrome. *Journal of Cognitive Neuroscience*, *9*(3), 295–317. https://doi.org/10.1162/jocn.1997.9.3.295

Rockland, K. S., & Pandya, D. N. (1979). Laminar origins and terminations of cortical connections of the occipital lobe in the rhesus monkey. *Brain Research*, *179*, 3–20.

Rust, N. C., & DiCarlo, J. J. (2010). Selectivity and tolerance ("invariance") both increase as visual information propagates from cortical area V4 to IT. *The Journal of Neuroscience*, *30*(39), 12978–12995. https://doi.org/10.1523/JNEUROSCI.0179-10.2010

Sanes, J. R., & Masland, R. H. (2015). The types of retinal ganglion cells: Current status and implications for neuronal classification. *Annual Review of Neuroscience*, *38*, 221–246. https://doi.org/10.1146/annurev-neuro-071714-034120

Schroeder, C. E., Mehta, A. E., & Givre, S. J. (1998). A spatiotemporal profile of visual system activation revealed by current source density analysis in the awake macaque. *Cerebral Cortex*, *8*(7), 575–592. https://doi.org/10.1093/CERCOR/8.7.575

Schwabe, L., Obermayer, K., Angelucci, A., & Bressloff, P. C. (2006). The Role of Feedback in Shaping the Extra-Classical Receptive Field of Cortical Neurons: A Recurrent Network Model. *Journal of Neuroscience*, *26*(36), 9117–9129. https://doi.org/10.1523/JNEUROSCI.1253-06.2006

Shafritz, K. M., Gore, J. C., & Marois, R. (2002). The role of the parietal cortex in visual feature binding. *Proceedings of the National Academy of Sciences of the United States of America*, *99*(16), 10917–10922. https://doi.org/10.1073/pnas.152694799

Sheinberg, D. L., & Logothetis, N. K. (1997). The role of temporal cortical areas in perceptual organization. *Proceedings of the National Academy of Sciences*, *94*, 3408–3413.

Shipp, S., & Zeki, S. M. (1989a). The Organization of Connections between Areas V5 and V1 in Macaque Monkey Visual Cortex. *European Journal of Neuroscience*, *1*(4), 309–332. https://doi.org/10.1111/j.1460-9568.1989.tb00798.x

Shipp, S., & Zeki, S. M. (1989b). The Organization of Connections between Areas V5 and V2 in Macaque Monkey Visual Cortex. *European Journal of Neuroscience*, *1*(4), 333–354. https://doi.org/10.1111/j.1460-9568.1989.tb00799.x

Shmuel, A., Korman, M., Sterkin, A., Harel, M., Ullman, S., Malach, R., & Grinvald, A. (2005). Retinotopic axis specificity and selective clustering of feedback projections from V2 to V1 in the owl monkey. *Journal of Neuroscience*, *25*(8), 2117–2131. https://doi.org/10.1523/JNEUROSCI.4137-04.2005

Siegel, R. M. (1998). Representation of visual space in area 7a neurons using the center of mass equation. In *Journal of Computational Neuroscience* (Vol. 5).

Sillito, A. M., Jones, H. E., Gerstein, G. L., & West, D. C. (1994). Feature-linked synchronization of thalamic relay cell firing induced by feedback from the visual cortex. *Nature*, *369*(6480), 479–482. https://doi.org/10.1038/369479a0

Silson, E. H., McKeefry, D. J., Rodgers, J., Gouws, A. D., Hymers, M., & Morland, A. B. (2013). Specialized and independent processing of orientation and shape in visual field maps LO1 and LO2. *Nature Neuroscience 2013 16:3*, *16*(3), 267–269. https://doi.org/10.1038/NN.3327

Sincich, L. C., & Horton, J. C. (2005). The circuitry of V1 and V2: Integration of color, form, and motion. *Annual Review of Neuroscience*, *28*, 303–326. https://doi.org/10.1146/ANNUREV.NEURO.28.061604.135731

Singer, W. (1977). Control of thalamic transmission by corticofugal and ascending reticular pathways in the visual system. *Psychological Reviews*, *57*(3), 386–420.

Singmann, H., Bolker, B., Westfall, J., Aust, F., Ben-Shachar, M. S., Højsgaard, S., Fox, J., Lawrence, M. A., Mertens, U., Love, J., Lenth, R., & Christensen, R. H. B. (2022). *afex: Analysis of Factorial Experiments* (1.1-1) [Computer software]. https://CRAN.R-project.org/package=afex

Sperling, G. (1964). What visual masking can tell us about temporal factors in perception. *Proceedings of the Seventeenth International Congress of Psychology*, 199–200.

Stromeyer, C. F., Eskew, R. T., Kronauer, R. E., & Spillmann, L. (1991). Temporal phase response of the short-wave cone signal for color and luminance. *Vision Research*, *31*(5), 787–803. https://doi.org/10.1016/0042-6989(91)90147-W

Tailby, C., Solomon, S. G., & Lennie, P. (2008). Functional asymmetries in visual pathways carrying S-cone signals in macaque. *J Neurosci*, *9*(15), 4078–4087. https://doi.org/10.1523/jneurosci.5338-07.2008

Tapia, E., & Breitmeyer, B. G. (2011). Visual Consciousness Revisited: Magnocellular and Parvocellular Contributions to Conscious and Nonconscious Vision. *Psychological Science*, *22*(7), 934–942. https://doi.org/10.1177/0956797611413471

Tata, M. S. (2002). Attend to it now or lose it forever: Selective attention, metacontrast masking, and object substitution. *Perception and Psychophysics*, *64*(7), 1028–1038. https://doi.org/10.3758/BF03194754

Tigges, J., Tigges, M., & Perachio, A. A. (1977). Complementary laminar terminations of afferents to area 17 originating in area 18 and in the lateral geniculate nucleus in squirrel monkey. *Journal of Computational Neuroscience*, *176*(1), 87–100.

Treisman, A. (1988). Features and Objects: The Fourteenth Bartlett Memorial Lecture. *The Quarterly Journal of Experimental Psychology Section A*, *40*(2), 201–237. https://doi.org/10.1080/02724988843000104

Treisman, A. M., & Gelade, G. (1980). A feature-integration theory of attention. *Cognitive Psychology*, *12*(1), 97–136. https://doi.org/10.1016/0010-0285(80)90005-5

Tsao, D. Y., Freiwald, W. A., Tootell, R. B.H., & Livingstone, M. S. (2006). A cortical region consisting entirely of face-selective cells. *Science*, *311*(5671), 670–674. https://doi.org/10.1126/science.1122096

Wagner, G., & Boynton, R. M. (1972). Comparison of four methods of heterochromatic photometry. *Journal of the Optical Society of America*, *62*(12), 1508–1515. https://doi.org/10.1364/JOSA.62.001508

Wang, W., Andolina, I. M., Lu, Y., Jones, H. E., & Sillito, A. M. (2018). Focal gain control of thalamic visual receptive fields by layer 6 corticothalamic feedback. *Cerebral Cortex*, *28*(1), 267–280. https://doi.org/10.1093/cercor/bhw376

Wang, W., Zhou, T., Zhuo, Y., Chen, L., & Huang, Y. (2020). *Subcortical magnocellular visual system facilities object recognition by processing topological property* (p. 2020.01.04.894725). bioRxiv. https://doi.org/10.1101/2020.01.04.894725

Warner, C. E., Goldshmit, Y., & Bourne, J. A. (2010). Retinal afferents synapse with relay cells targeting the middle temporal area in the pulvinar and lateral geniculate nuclei. *Frontiers in Neuroanatomy*, *4*(8), 1–16. https://doi.org/10.3389/NEURO.05.008.2010

Weller, R. E., & Kaas, J. H. (1983). Retinotopic patterns of connections of area 17 with visual areas V2 and MT in macaque monkeys. *Journal of Comparative Neurology*, *220*(3), 253–279.

Woodman, G. F., & Luck, S. J. (2003). Dissociations among attention, perception, and awareness during object-substitution masking. *Psychological Science*, *14*(6), 605–611. https://doi.org/10.1046/j.0956-7976.2003.psci_1472.x

Zeki, S. M. (1978). Functional specialisation in the visual cortex of the rhesus monkey. *Nature*, *274*(5670), 423–428. https://doi.org/10.1038/274423a0

Zeki, S. M., & Shipp, S. (1989). Modular Connections between Areas V2 and V4 of Macaque Monkey Visual Cortex. *European Journal of Neuroscience*, *1*(5), 494–506. https://doi.org/10.1111/j.1460-9568.1989.tb00356.x

Ziemba, C. M., Freeman, J., Movshon, J. A., & Simoncelli, E. P. (2016). Selectivity and tolerance for visual texture in macaque V2. *Proceedings of the National Academy of Sciences*, *113*(22), E3140–E3149. https://doi.org/10.1073/pnas.1510847113

Ziemba, C. M., Freeman, J., Simoncelli, E. P., & Movshon, J. A. (2018). Contextual modulation of sensitivity to naturalistic image structure in macaque V2. *Journal of Neurophysiology*, *120*(2), 409–420. https://doi.org/10.1152/JN.00900.2017

Zipser, K., Lamme, V. A. F., & Schiller, P. H. (1996). Contextual modulation in primary visual cortex. *Journal of Neuroscience*, *16*(22), 7376–7389. https://doi.org/10.1523/JNEUROSCI.16-22-07376.1996

APPENDIX A

SUPPLEMENTAL METHODS FOR EXPS. 1A-1C

A.1 Target-plus-flanker display times for subjects in Exps. 1A-1C

Exp. 1		Subject ID				
		S1	S2	S3	S4	S5
# Frames (ms)	A	1 (16.7)	1 (16.7)	1 (16.7)	1 (16.7)	--
	B	3 (50.0)	3 (50.0)	3 (50.0)	2 (33.3)	1 (16.7)
	1C	2 (33.3)	2 (33.3)	2 (33.3)	2 (33.3)	1 (16.7)

Table A-1. Target-plus-flankers display times for subjects in Exps. 1A-1C. All subjects who completed Exp. 1A showed optimal performance (75–90% correct on "offset-simultaneous" trials) with single-frame display times. S5 performed >90% in "offset-simultaneous" trials even with single-frame display times in Exp. 1A, and thus was disqualified from Exp. 1A.

A.2 Analyses and models used in Exps. 1A-1C

For each sub-experiment within Exps. 1A-1C, analyses were within-subject binomial logistic regression analyses, run using the `R` function `glm`. In each analysis, data were grouped by two manipulated factors. The first was flanker offset (`Simultaneous` versus `Delayed`), and the second was either: 1) Flanker type in Exp. 1A (`Gabor` versus `Gaussian`); 2) Flanker-target color relation in Exp. 1B (`Different` versus `Same` color); or 3) Flanker color condition in Exp. 1C (`Grayscale` versus `Colored`). Each binomial logistic regression analysis used

these two factors as predictors for performance in each trial (Correct `TRUE` or `FALSE`), using a logit link function. Tests for main effects and interactions used equal weight for cells.

In Exp. 1A, each cell of the 2×2 design represented 80 trials (giving 320 trials total). In Exp. 1B, each cell of the 2×2 design represented 120 trials (giving 480 trials total). In Exp. 1C, each cell of the 2×2 design represented 160 trials (giving 640 trials total).

APPENDIX B

SUPPLEMENTAL METHODS FOR EXPS. 2A-2D

B.1 Target-plus-flanker display times for subjects in Exps. 1A-1C

Exp. 2		Subject ID					
		S1	S2	S3	S4	S5	S6
# Frames (ms)	A	3 (50.0)	2 (33.3)	3 (50.0)	2 (33.3)	2 (33.3)	2 (33.3)
	B	3 (50.0)	1 (16.7)	1 (16.7)	1 (16.7)	2 (33.3)	1 (16.7)
	C	1 (16.7)	1 (16.7)	1 (16.7)	1 (16.7)	2 (33.3)	2 (33.3)
	D	1 (16.7)	1 (16.7)	1 (16.7)	1 (16.7)	2 (33.3)	1 (16.7)

Table B-1. Target-plus-flankers display times for subjects in Exps. 2A-2D.

APPENDIX C

SUPPLEMENTAL METHODS FOR EXPS. 3A-3C

C.1 Stimulus generation details and modulation amounts

Targets, distractors, and flankers in Exp. 3A-3C were Gabor-like blur dots. Each dot was modulated either positively or negatively on one axis of the *lsY* cone-excitation space. Each modulation was defined with respect to the neutral gray *lsY* values of *l*=0.665, *s*=1.0, *Y*=16 cd/m². Values for the modulated axis (*l*, *s*, or *Y*) were generated by applying a Gaussian blur kernel (with σ=22.5% of dot width) to a hard-edged dot, normalizing the resultant values to the maximum and minimum for the modulated axis, and merging the resultant normalized matrix with a same-sized matrix of background values for the other two axes. The resultant matrix of *lsY* coordinates was then transformed into CIE XYZ, corrected for that subject's photometric matches, and transformed into monitor RGB values for output.

To ensure that subjects' performance was not at ceiling (>90%) or floor (<75%) for "offset-simultaneous" trials, each subject completed one to four full-speed practice blocks before each session of Exps. 3A-3D. In each full-speed practice block, the modulation depth of the two *lsY* axes modulated in that experiment were set to a given value, and performance on "offset-simultaneous" trials was measured. If performance was >90%, the modulation depth was increased by one step in the next practice block; if performance was <75%, the modulation depth was decreased by one step in the next practice block. Each of the three axes had seven steps of modulation depth; see Table C-1 for modulation depths for *l*, *s*, and *Y* axes in Exps. 3A-3C. Note that steps for the *l* and *s* color axes are in arbitrary units, whereas steps for *Y* are in Weber contrast, and hence represent decimal proportions of the 16 cd/m² background luminance.

Exp. 3 Stimuli		Step #; Modulation depth						
		1	2	3	4	5	6	7
Axis modulated (background value)	*l* (0.665)	0.0250	0.0275	0.0300	0.0325	0.0350	0.0375	0.0400
	s (1.0)	0.5500	0.5833	0.6167	0.6500	0.6833	0.7167	0.7500
	Y (16.0)	0.0500	0.0667	0.0833	0.1000	0.1167	0.1333	0.1500

Table C-1. Stimulus *l*, *s*, and *Y* modulation depths in Exps. 3A-3C. For each session of each sub-experiment, subjects performed one to four full-speed practice blocks of trials to calibrate performance on "offset-simultaneous" trials to 75-90%. Each subject did the first full-speed practice block at step 4, and the modulation depth was stepped up or down in subsequent practice blocks until the subject's average performance on "offset-simultaneous" trials was 75-90%.

APPENDIX D

SUPPLEMENTAL MATERIALS FOR EXPS. 3A-3C

D.1 Masking by target color and flanker axis for Exps. 3A-3C

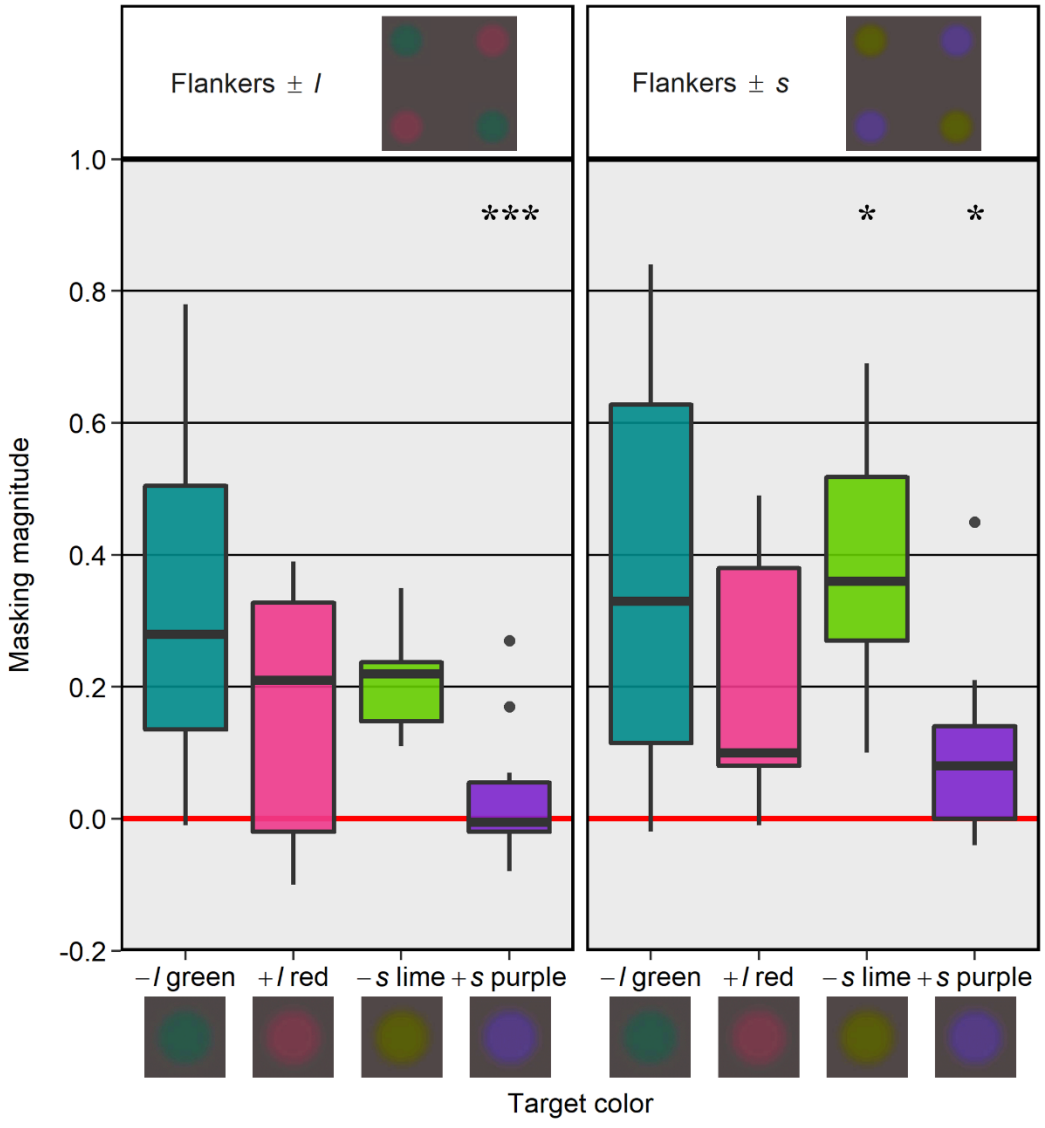

Figure D-1. Masking by target color and flanker axis in Exp. 3A. Dots represent outlier values for masking magnitudes. Contrasts are for each target color (within each of the two flanker axes) to the grand mean for that flanker axis. *p<0.05; **p<0.01; ***p<0.001. (Holm corrected for four comparisons).

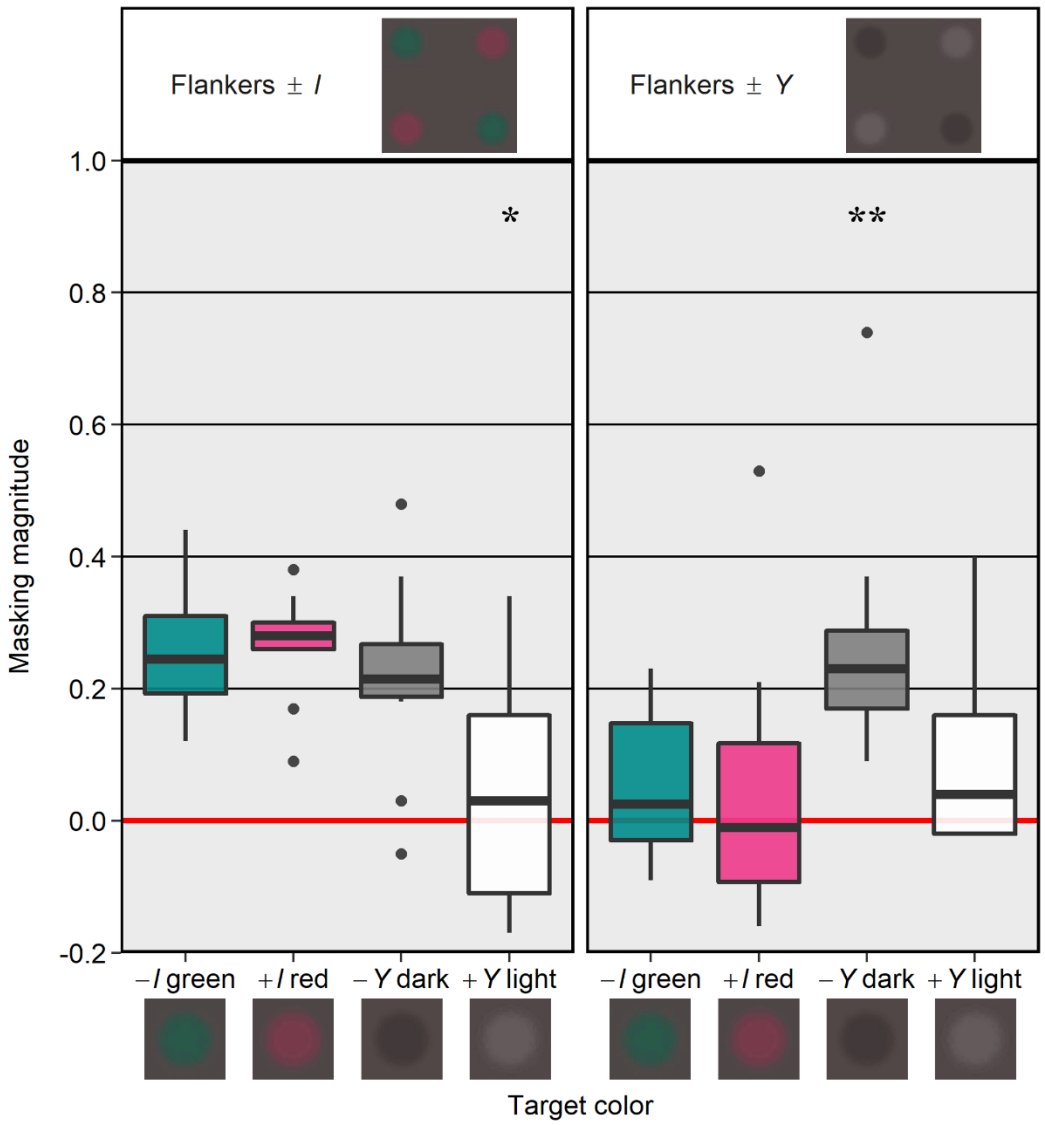

Figure D-2. Masking by target color and flanker axis in Exp. 3B. Dots represent outlier values for masking magnitudes. Contrasts are for each target color (within each of the two flanker axes) to the grand mean for that flanker axis. *p<0.05; **p<0.01; ***p<0.001 (Holm corrected for four comparisons).

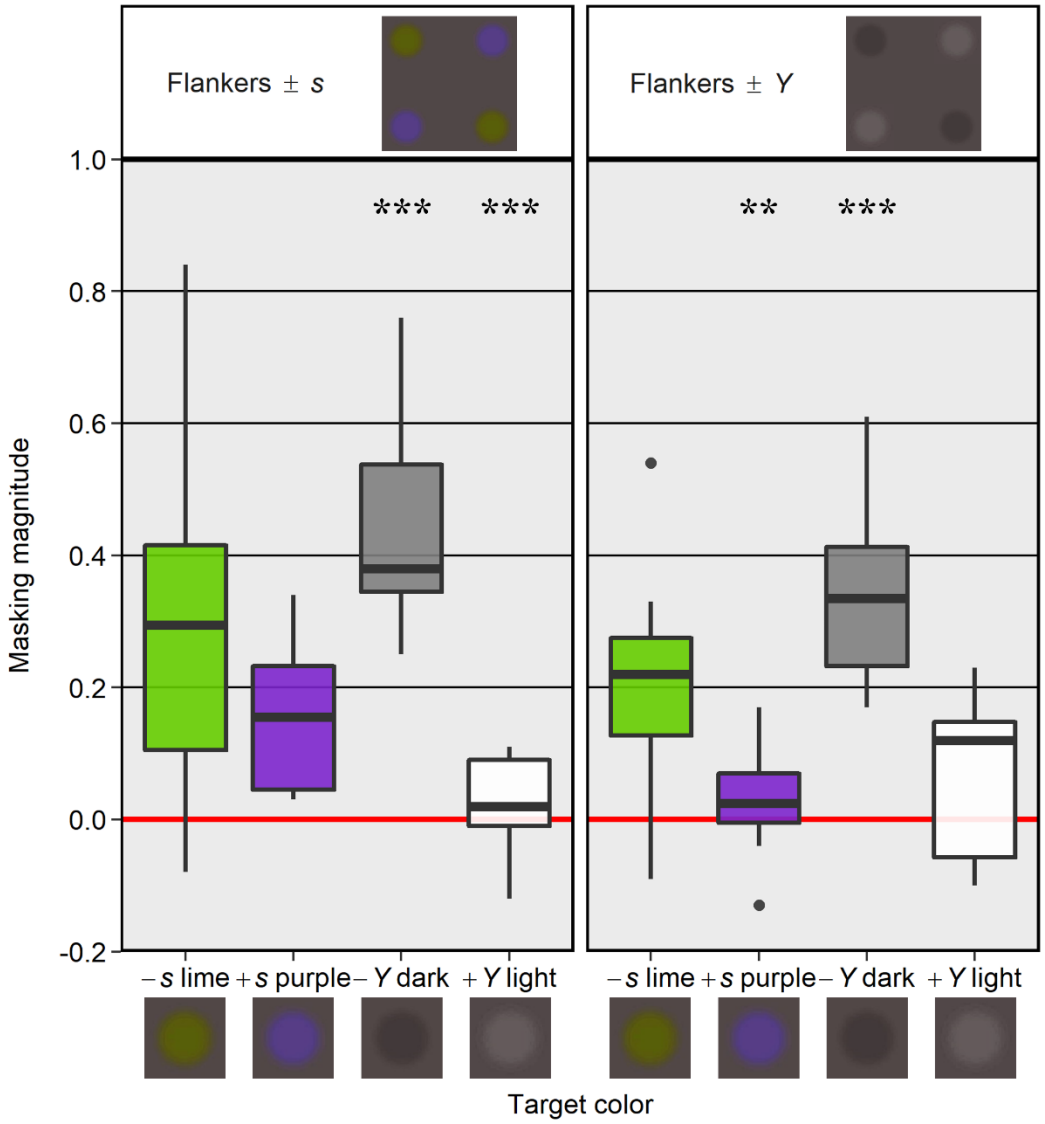

Figure D-3. Masking by target color and flanker axis in Exp. 3C. Dots represent outlier values for masking magnitudes. Contrasts are for each target color (within each of the two flanker axes) to the grand mean for that flanker axis. *p<0.05; **p<0.01; ***p<0.001. (Holm corrected for four comparisons).

D.2 Masking by flanker and target axes for Exps. 3A-3C

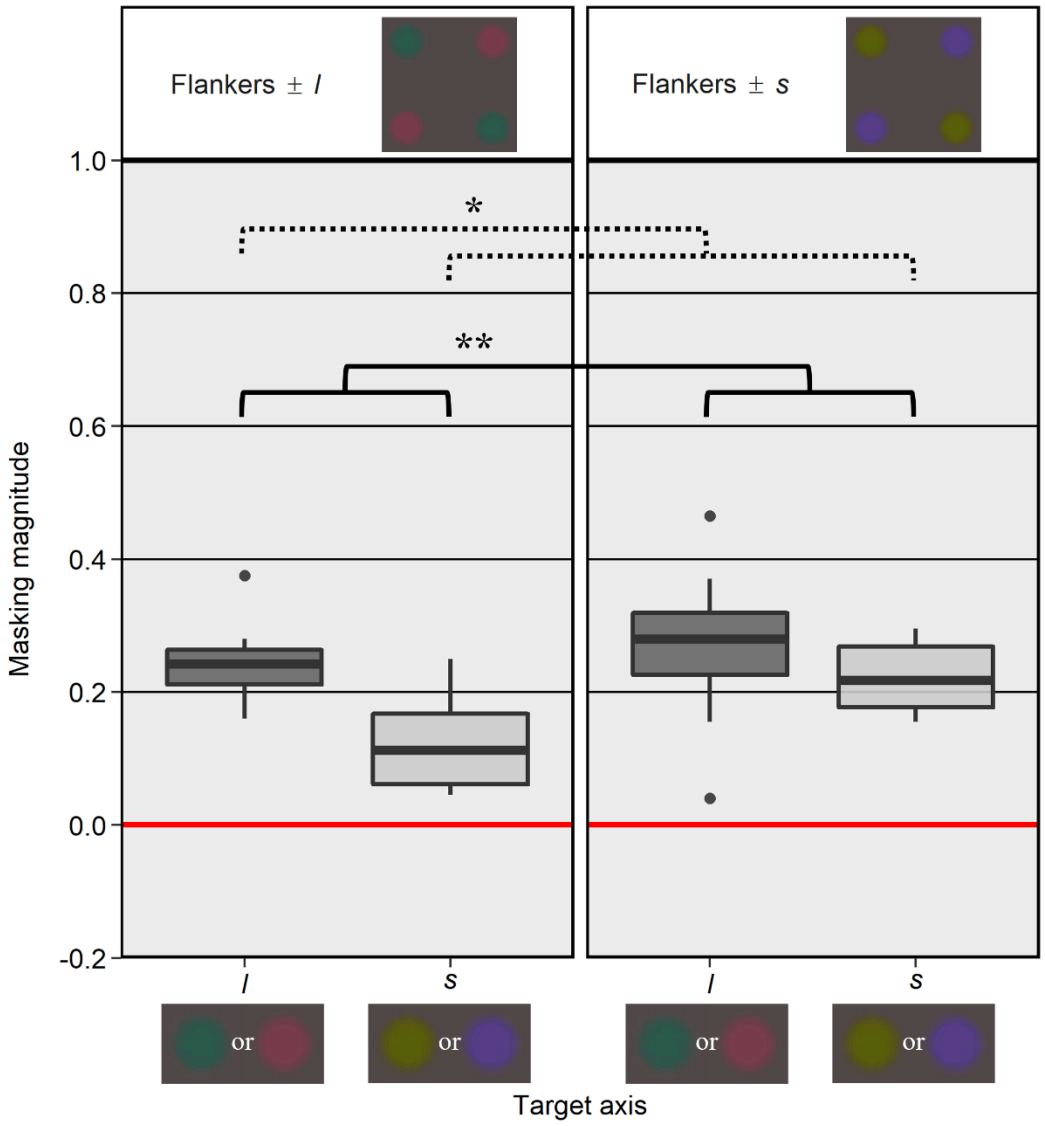

Figure D-4. Masking by flanker and target axes in Exp. 3A. Dots represent outlier values for masking magnitudes. Significant contrasts are indicated by groups of brackets as follows: Bracket group with solid lines: Main effect of flanker axis. Bracket group with dotted lines: Main effect of target axis. *p<0.05; **p<0.01. The flanker axis × target axis interaction was not significant (p=0.08).

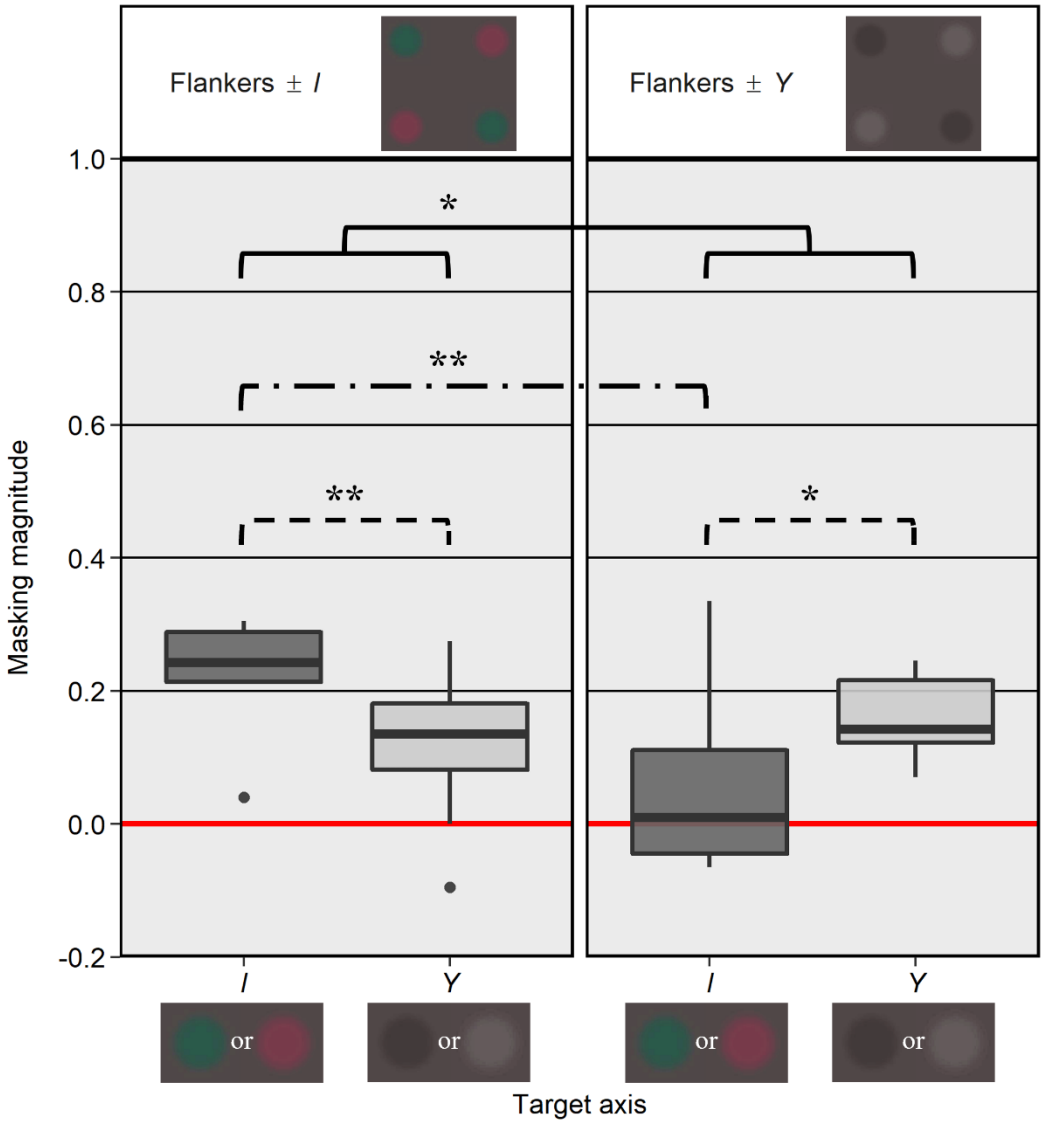

Figure D-5. Masking by flanker and target axes in Exp. 3B. Dots represent outlier values for masking magnitudes. Significant contrasts are indicated by brackets or groups of brackets as follows: Bracket group with solid lines: Main effect of flanker axis. Bracket with dash-dotted lines: Simple effect of flanker axis. Bracket with dashed lines: Simple effect of target axis. *p<0.05; **p<0.01. The flanker axis × target axis interaction was significant (p<0.01).

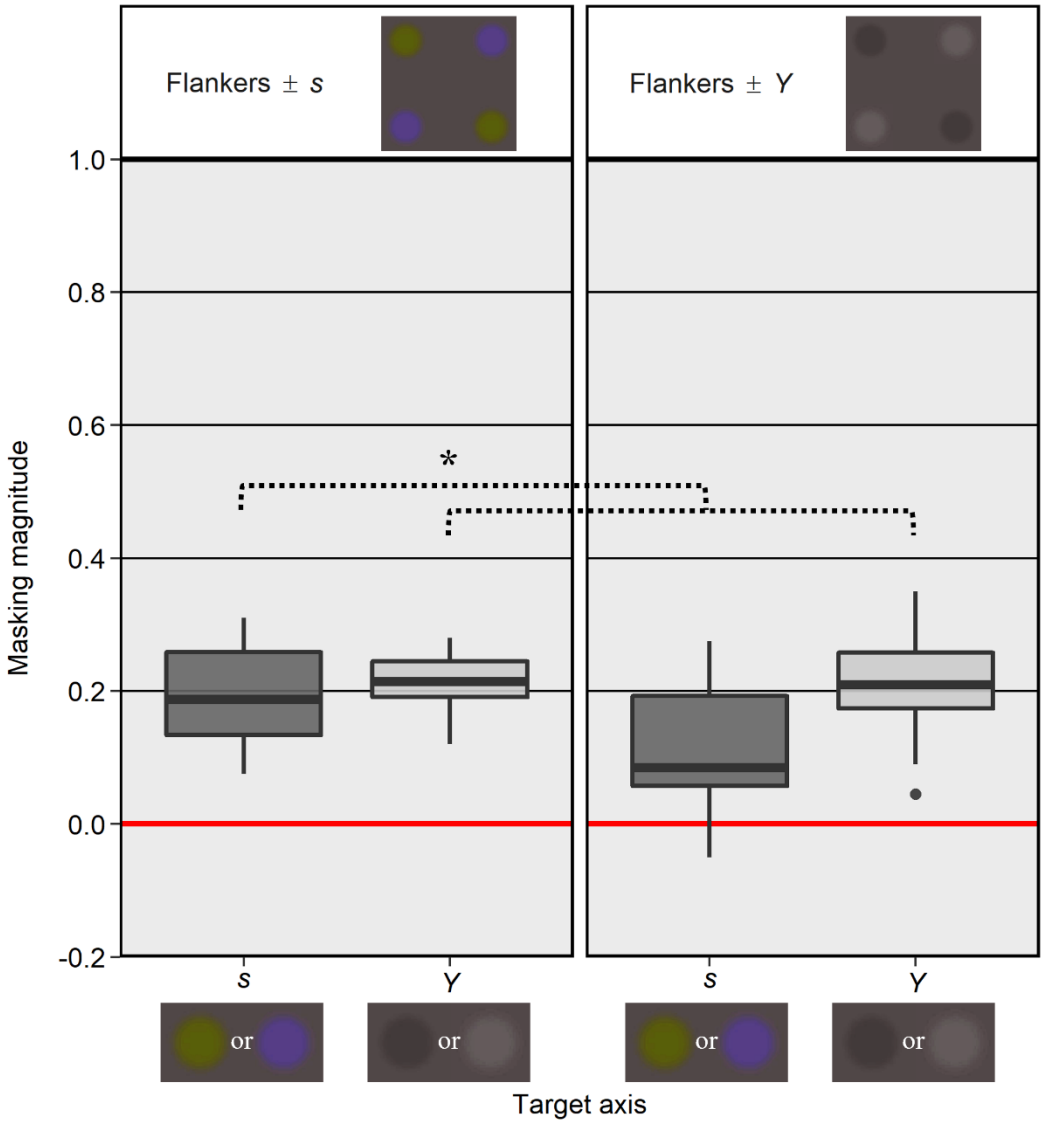

Figure D-6. Masking by flanker and target axes in Exp. 3C. Dots represent outlier values for masking magnitudes. Significant contrasts are indicated by groups of brackets as follows: Bracket group with dotted lines: Main effect of target axis. *p<0.05. The flanker axis × target axis interaction was not significant (p=0.323).

D.3 Details of supplemental analyses for Exps. 3A-3C

Supplemental analyses of the data from Exps. 3A-3C used masking magnitudes for each condition of either target color, or flanker axis × target axis. Masking magnitudes by target color and target axis were analyzed separately.

For the analyses of masking by target color, separate analyses were run for each flanker axis. The four-level `[target color]` served as the within-subject factor for four planned, non-orthogonal contrasts. Each of the 1×4 cells of the design contained `n=10` masking magnitude values. Each of these 10 values in turn represented a single subject's masking magnitude for that target color within that flanker axis, with masking magnitude defined as the overall proportion of correct responses for "flanker offset simultaneous" trials minus the overall proportion of correct responses for "flanker offset delayed" trials. The four contrasts were performed using the repeated-measures, nonparametric contrasts `R` function `mctp.rm()` in the `nparcomp` package (Konietschke et al., 2019). The non-parametric contrasts used "global pseudo-rank" estimation algorithms, and multivariate t-distributions with Satterthwaite's approximation for degrees of freedom. Each contrast compared masking for that target color to grand-mean masking across the four target colors; cells were weighted equally and sum-to-zero contrast coding was used. See Table D-1 for ANOVA table weights for these contrasts for each color versus the grand mean, within each flanker axis, for Exps. 3A-3C.

Exp. 3: Contrasts to grand mean masking (within a flanker axis)		Color #			
		1	2	3	4
Contrast (color # vs grand mean)	1	0.75	–0.25	–0.25	–0.25
	2	–0.25	0.75	–0.25	–0.25
	3	–0.25	–0.25	0.75	–0.25
	4	–0.25	–0.25	–0.25	0.75

Table D-1. ANOVA table weights for target-color contrasts in Exps. 3A-3C.

For the analyses of flanker axis × target axis, the two-level `[flanker axis]` and `[target axis]` served as within-subject factors for the 2×2 repeated-measures ANOVA. Each of the 2×2 cells of the design contained `n=10` masking magnitude values. Each of these 10 values in turn represented a single subject's masking magnitude for that flanker axis × target axis combination, with masking magnitude defined as the overall proportion of correct responses for "flanker offset simultaneous" trials minus the overall proportion of correct responses for "flanker offset delayed" trials. Note that this averaged across + and – modulations of targets. The 2×2 repeated-measures ANOVA was performed using the `R` function `aov_car()` in the `afex` package (Singmann et al., 2022). Each ANOVA test used equal cell weights and sum-to-zero contrast coding. If an ANOVA test gave a significant ($p<0.05$) flanker axis × target axis interaction effect, four planned contrasts were performed to test for simple effects of flanker axis at each level of target axis, and vice-versa. These four contrasts were performed using the `R`

functions `emmeans()` and `contrast()`, in the `emmeans` package (Lenth et al., 2022). used equal cell weights and sum-to-zero contrast coding, and p-values were corrected with the Holm procedure for four comparisons. See Table D-2 for ANOVA table weights for the contrasts used to test simple effects of flanker and target axis in Exps. 3A-3C.

Exp. 3: Simple-effects contrasts for masking by flanker axis × target axis		Flanker axis × target axis condition ($F_i \times T_j$)			
		$F_1 \times T_1$	$F_1 \times T_2$	$F_2 \times T_1$	$F_2 \times T_2$
Simple effect contrast	Target axis (Flanker axis=1)	1	–1	0	0
	Target axis (Flanker axis=2)	0	0	1	–1
	Flanker axis (Target axis=1)	1	0	–1	0
	Flanker axis (Target axis=2)	0	1	0	–1

Table D-2. ANOVA table weights for simple-effects contrasts in Exps. 3A-3C.